TKI Dotter-project

Towards coupled risk-based aquatic vegetation management and EU-WFD-targets

Report - Final

April, 2017

Editors: Gé van den Eertwegh/KnowH2O

Ellis Penning/Deltares

TKI-project 2016

In cooperation with partners Water Boards Rivierenland and Aa en Maas

www.knowh2o.nl Watertorenweg 12 6571 CB BERG EN DAL t +31 (0)6 23 22 49 68
e info@knowh2o.nl Bank NL83 INGB 0006 2713 22 KvK 59020229

KnowH2O
Advies, Innovatie en Verbinding in Water

www.knowh2o.nl Watertorenweg 12 6571 CB BERG EN DAL t +31 (0)6 23 22 49 68
e info@knowh2o.nl Bank NL83 INGB 0006 2713 22 KvK 59020229

KnowH2O
Advies, Innovatie en Verbinding in Water

Deltares

Title
TKI Dotter-project Towards coupled risk-based aquatic vegetation management and EU-WFD-targets

Pagina's

Keywords
Vegetation management, Remote Sensing, drones, full spectrum camera's, vegetation roughness, Water Framework Directive

Summary
The Dotter project was initiated in order to provide the first steps in the development of a new method for spatially explicit information on the presence of vegetation in and along water ways, using a full spectrum camera in combination with an Unmanned Aerial Vehicle (UAV/drone). When merged, images from this camera provide information on the amount and location of vegetation along the waterways. This information can be used to define when and where vegetation management through mowing might be necessary in order to provide sufficient conveyance capacity. At the same time the images can provide information about locations with ecologically valuable vegetation. This can help selecting an efficient and ecologically friendly mowing method.

During the project field visits to 2 Dutch locations (Lage Raam and Linge) were made to collect data for the development of this method. A detailed set of images was recorded at the River Experiment Center of the Korean Institute of Civil Engineering and Building Technology in Andong, South Korea, in order to assess the sensitivity of the method for changes in water depth and turbidity, and to compare recordings from the camera in combination with the UAV to recordings taken by the camera from a fixed position. Images were analysed using indices from literature and first steps towards clustering were made. Data was collected to relate these results to the biomass at the locations and the potential for linking this information to assessments in line with the requirements for the Water Framework Directive.

The results show that the method is promising and that the use of the camera in combination with the UAV is providing valuable insight in the location and amount of vegetation. The UAV provides the suitable height from which the most usable images were collected. Images from the fixed pole were generally too close to the water surface and were more difficult to stitch together due to a lack of reference points.

Referenties

Versie	Datum	Auteur	Paraaf	Review	Paraaf	Goedkeuring	Paraaf
	mrt. 2017	W.E. Penning (Deltares)	[signature]	S. Groot		S. de Rijk	[signature]
		G. van den Eertwegh (KnowH2O)				[signature]	

Status
definitief

KnowH2O
Advies, Innovatie en Verbinding in Water

CONTENT

KnowH2O
Advies, Innovatie en Verbinding in Water

SUMMARY

The Dotter project was initiated in order to provide the first steps in the development of a new method for spatially explicit information on the presence of vegetation in and along water ways, using a full spectrum camera in combination with an Unmanned Aerial Vehicle (UAV/drone). When merged, images from this camera provide information on the amount and location of vegetation along the waterways. This information can be used to define when and where vegetation management through mowing might be necessary in order to provide sufficient conveyance capacity. At the same time the images can provide information about locations with ecologically valuable vegetation. This can help selecting an efficient and ecologically friendly mowing method.

During the project field visits to 2 Dutch locations (Lage Raam and Linge) were made to collect data for the development of this method. A detailed set of images was recorded at the River Experiment Center of the Korean Institute of Civil Engineering and Building Technology in Andong, South Korea, in order to assess the sensitivity of the method for changes in water depth and turbidity, and to compare recordings from the camera in combination with the UAV to recordings taken by the camera from a fixed position. Images were analysed using indices from literature and first steps towards clustering were made. Data was collected to relate these results to the biomass at the locations and the potential for linking this information to assessments in line with the requirements for the Water Framework Directive.

The results show that the method is promising and that the use of the camera in combination with the UAV is providing valuable insight in the location and amount of vegetation. The UAV provides the suitable height from which the most usable images were collected. Images from the fixed pole were generally too close to the water surface and were more difficult to stitch together due to a lack of reference points.

www.knowh2o.nl Watertorenweg 12 6571 CB BERG EN DAL t +31 (0)6 23 22 49 68
e info@knowh2o.nl Bank NL83 INGB 0006 2713 22 KvK 59020229

NEDERLANDSE SAMENVATTING

Seizoensmatige ontwikkeling van vegetatie in kleine stromende wateren kan leiden tot een verhoogd overstromingsrisico vanuit watergangen bovenstrooms van deze vegetatie. Tegelijkertijd is deze vegetatie een belangrijk onderdeel van een gezond functionerend ecosysteem, zoals ook door de KRW wordt beoogd. Te veel vegetatie moet echter wel tijdig verwijderd worden om voldoende aanvoer en afvoer van water te garanderen. Daarnaast geldt in KRW-verband dat er niet te weinig, maar ook niet teveel vegetatie aanwezig moet zijn. Waterschappen maaien veelal meerdere keren per seizoen hun watergangen. Maaien en ook baggeren gebeurt voor het verminderen van het risico op wateroverlast door opstuwing en voor het verbeteren van de ecologische waarden. Voor verbetering van de ecologische waarde van de vegetatie is het uitvoeren van een representatieve monitoring en afstemming met onderhoud van watergangen een wezenlijke rol. Deze monitoring is niet vlakdekkend.

Het ontbreekt de beheerders vaak aan overzichtelijke, snelle methoden om objectief inzichtelijk te maken waar en hoe het maaien doelmatig en efficiënt uitgevoerd kan worden. Innovatieve meetmethoden en bijbehorende software leiden tot vlakdekkende informatie om meer effectieve en beter gerichte beheerkeuzes te maken. Deze informatie wordt aangewend om in eenvoudig te gebruiken visuele tools weer te geven *waar* in het watersysteem *welke* mogelijke significante weerstanden en verstoppingen zitten, en of deze door vegetatie worden veroorzaakt. Zo kan men gericht in tijd en ruimte en met het juiste beheer ingrijpen, vóórdat eventuele calamiteiten zich voordoen tijdens veel neerslag.

Zoals een vaatchirurg een Dotter-operatie uitvoert en kijkt welke verstoppingen waar moeten worden weggehaald, zo kunnen de verstoppingen in watersystemen in kaart gebracht worden. Zo zetten waterbeheerders gericht hun beheermiddelen in, zoals maaien, baggeren en stuwen, om alleen probleemlocaties aan te pakken daar waar nodig. Zo wordt de vegetatie gespaard op andere plekken en wordt ook menskracht en geld effectiever ingezet. Tenslotte verbetert zo de communicatie tussen verschillende beheeronderdelen binnen het waterschap én onderbouwt men het werk ten behoeve van externe communicatie naar hun ingelanden.

Met het Dotter-project zijn we gestart met de ontwikkeling van een snelle techniek om te bepalen waar de daadwerkelijke hydraulische obstakels in een watergang zich bevinden en tegelijkertijd de ecologische waarde van de vegetatie te karteren. Door 'patches' van vegetatie direct om te zetten in ruwheden en tegelijkertijd de verschillende typen vegetatie te identificeren, bepalen we waar de echte knelpunten in de beek zitten. Door alleen deze 'knelpunten' te schonen (te dotteren), kunnen andere waardevolle patches blijven bestaan, wat ten gunste komt aan het bereiken van KRW-doelen.

Het Dotter-project is in 2016 als TKI-project vormgegeven (Topconsortia in Kennis en Innovatie). Projectpartners uit Nederland en Zuid-Korea hebben extra bijdragen geleverd en een toeslag gegenereerd uit fondsen van de Topsector Water. De waterschappen Rivierenland en Aa en Maas hebben financiële middelen ter beschikking gesteld voor deze innovatie.

Doel van het project

Nieuwe UAV- (drone) technieken maken het mogelijk om grote trajecten snel en geautomatiseerd in kaart te brengen. Het doel is om een vlakdekkend beeld te krijgen van de watervegetatie en mogelijk ook soortensamenstelling (experimenteel). De eigenschappen van vegetatiesoorten bepalen welke stromingsweerstand kan optreden. Ook is dit belangrijk om de biomassa ontwikkeling (en daarmee weerstand-ontwikkeling) te bepalen. Door gebruik te maken van specifieke full spectrum camera's en een geautomatiseerd vliegtraject van de UAV/drone, via een koppeling van de leggerwatergangen met GPS-sturing van de UAV/drone, kan deze informatie snel worden ingewonnen en verwerkt. Via een gekalibreerd en gevalideerd algoritme worden de beelden in één keer verwerkt tot een vlakdekkende kaart van het gemonitorde traject, waarin kansen en knelpunten oplichten. We maken bij de kalibratie en validatie van deze techniek niet alleen gebruik van Nederlandse locaties maar ook van een unieke proeflocatie in Zuid-Korea (via het River Experiment Center-KICT). Het doel is om met deze techniek snelle en betrouwbare beslissingen te kunnen nemen over de mate en locatie van ingrijpen.

Resultaten 2016

Aquatische vegetatie reflecteert zonlicht. Die reflectie heeft een bepaald frequentiebereik. De uitgekozen full spectrum camera is geschikt om dit waar te nemen, in het zichtbare en deels onzichtbare deel van het spectrum (450-998 nm). Deze bandbreedte is geschikt bevonden, alsmede de ruimtelijke resolutie van de opnames. De camera is getest via een vaste opstelling op een boot, aan een brug, aan een ladder boven het wateroppervlak, aan een telescopische paal (op 6 m hoogte) en onder een UAV/drone op 10 à 20 m vlieghoogte. De toepassing onder een UAV/drone was inclusief het gebruik van een stabilisatie-systeem, om de camera steeds in dezelfde positie te houden. Het gebruik van de boot leverde problemen op met de positie van de camera, die onder een schuine hoek stond ten opzichte van de waterspiegel. Het gebruik van de brug, ladder en de paal resulteerde in een te lage waarnemingshoogte, waardoor de resolutie te hoog werd en beelden te gedetailleerd waren met te weinig variatie per beeld. De opnames met de UAV/drone bleken prima te verwerken, op een geschikte afstand en loodrecht op de waterspiegel.

De opnames met de camera moeten verwerkt worden tot bruikbare informatie. Hiervoor is een aantal proces-stappen nodig. De ortho-rectificatie en de geo-referentie wordt uitgevoerd met behulp van dGPS-informatie. Normalisatie van de opnames is nodig, waarbij inkomend zonlicht, de verandering hiervan tijdens het maken van opnames en de lichtgevoeligheid van de camera een rol spelen. Dit vereist aandacht in de praktijk van het maken van opnames. Daarnaast is het belangrijk om opeenvolgende beelden aan elkaar te kunnen koppelen ('stitching') voor een volledig vlakdekkend beeld. Als op deze manier verwerkte beelden gereed zijn, kunnen diverse spectrale banden met elkaar gecombineerd worden via indices, bijvoorbeeld een specifieke groenindex (NDVI). Verschillende indices die bedacht zijn voor vegetatie-opnames geven verschillende informatie over de vegetatie.

Het is door tijdgebrek nog niet gelukt om vegetatiesoorten te herkennen op basis van de hyperspectrale opnames. Wellicht is herkenning van soortgroepen, via typische eigenschappen van deze groepen, mogelijk. Nader onderzoek hiernaar is nodig, wellicht gebruik makend van software die vormen en patronen kan herkennen.

De waterdiepte en de troebelheid van het water beïnvloeden de kwaliteit van het opgenomen beeldmateriaal. Naarmate de waterdiepte groter wordt, neemt de reflectie van de (ondergedoken) waterplanten af, en deze afname is groter bij grotere golflengtes. Zo zijn planten met reflecties bij grotere golflengtes moeilijker op te sporen naarmate ze dieper onder water staan. De troebelheid speelt daarbij ook een rol. Een grotere 'turbidity' maakt waterplanten slechter zichtbaar. Er zijn indices die meer of minder gevoelig zijn voor troebelheid, maar nader onderzoek hiernaar is gewenst.

Als we via de spectrale analyse vlakdekkende informatie kunnen genereren over de aquatische vegetatie in termen van vóórkomen en dichtheid, dan kunnen we hieruit de hydraulische weerstand schatten van de aanwezige vegetatie. Hiervoor zijn kentallen en soortkennis nodig. De hydraulische weerstand, die via de vegetatiekartering na bewerking vlakdekkend beschikbaar is, kan in een hydraulisch model als ruimtelijke variabele ingevoerd worden. Zo kan voor iedere watergang uitgerekend worden welke vegetatie waar tot welke opstuwing leidt. Daarmee kan ingezet worden op tijd- en ruimte-specifiek maaibeheer. Er is al een hydraulisch model ontwikkeld dat vlakdekkend werkt. Het kan informatie verwerken over aanwezige weerstanden in de vorm van vegetatie en baggerslib. Het kan uitgebreid worden met een vegetatie-groeimodel, om zo meer voorspellend te kunnen rekenen nádat een vegetatieopname is gemaakt.

De resultaten uit 2016 laten zien dat de ontwikkelde methode werkt. De combinatie van de full spectrum camera met de UAV/drone is waardevol, omdat daarmee de gewenste grote(re) opnamehoogte bereikt kan worden. Opnames van geringe(re) hoogte blijken moeilijk te verwerken. Diverse beeld-verwerkende software is succesvol toegepast. Er zijn indices berekend op basis van de spectrale banden die daadwerkelijk informatie bevatten over de aanwezige watervegetatie.

Doorkijk naar toepassingen in de nabije toekomst

De door ons voorgestelde werkwijze, gebruik makend van nieuwe technologie, levert een vlakdekkend en hoge resolutie (ordegrootte cm) informatieproduct op over de toestand (biomassa, dichtheid) en aanwezigheid (locatie) van waterplanten in de watergangen, met een bepaalde/gewenste frequentie in de tijd. Waterplanten die aan de oppervlakte zichtbaar zijn zullen sowieso onderdeel van de informatie zijn. In een bepaalde mate zullen we in staat zijn ondergedoken waterplanten te herkennen en te karteren. Patroonherkenning kan op termijn leiden tot benoeming van vegetatiesoorten. Naar verwachting kunnen we de nu genomen eerste stappen binnen enkele jaren omvormen tot een in de praktijk bruikbaar product (2018-2019).

ACKNOWLEDGEMENTS

The Dotter Project was carried out with financial support from the Dutch TKI subsidy fund, the Korean KAIA subsidy fund, and in-kind contributions from Water Board Rivierenland, Water Board Aa en Maas, Deltares, KnowH2O, University of Twente, the Korean Institute of Civil Engineering and Building Technology and the KICT-Joint Venture.

The following people contributed to this research: Gé van den Eertwegh (KnowH2O), Ellis Penning (Deltares), Rik Noorlandt (Deltares), Mike van der Werf (Deltares), Koen Berends (Deltares/University of Twente), Remi van der Wijk (Deltares), Gerben van Geest (Deltares), Yong-Uk Ryu (KICT), Un Ji (KICT), Chanjoo Lee (KICT), JoonGu Kang (KICT-Joint Venture), SangHwa Jung (KICT), Eun-Jin Park (KICT-Joint Venture), Florian Laurens (TU-Delft), Anke Wetser (TU-Delft), Pim van Santen (Waterschap Aa en Maas), Mirja Kits (Waterschap Aa en Maas), Jappe Beekman (Waterschap Aa en Maas), Sante Dorigo (Waterschap Rivierenland), Ronald Gylstra (Waterschap Rivierenland), Judith van Tol (Waterschap Rivierenland), and Vincent Struik (Waterschap Rivierenland).

1 INTRODUCTION

1.1 GENERAL

Seasonal development of vegetation in streams and rivers can introduce enlarged flow obstruction, and increased flood risk upstream of dense vegetation patches. At the same time vegetation is a natural aspect of flowing waters and valued for its ecological services and provision of habitat for other organisms. Therefore, aquatic vegetation is an explicit part of the EU-Water Framework Directive (EU-WFD), aiming to meet the water quality targets by 2015, 2021, and 2027.

When vegetation obstructs flow it must be removed by mowing, cutting down trees etc. Methods to determine the threshold of acceptable levels of biomass in streams are for example relationships between discharge and water levels: when water levels upstream increase beyond a given point with a given discharge the overall roughness in the channel has increased too much as a result of vegetation development and mowing must be carried out. When discharge capacity is becoming too small, field assessments must be carried out to identify where and how much vegetation must be removed. Currently this is often done based on expert judgement by individual persons, while objective quantifying methods are lacking.

Regional water authorities usually have limited information and knowledge on stream vegetation. Generally, point or section (typically 100 m long) measurements are available at a small number of moments in time and space. This hampers the connection of EU-WFD field monitoring achievements to hydraulic aspects and has negative feedback on policy aspects and measures taken to enhance the presence and quality of aquatic vegetation.

1.2 SHORT DESCRIPTION OF PROJECT

We used an innovative full spectrum camera to make images of the (semi)aquatic vegetation in and around a number of pilot water bodies. Emergent (shoreline) vegetation as well as submersed aquatic vegetation (SAV) were monitored, taking into account the effects turbidity of the water and water levels. We used both a fixed position for obtaining the imaging at specific spots, as well as attaching the camera to an Unmanned Aerial Vehicle (UAV) or Remotely Piloted Aircraft System (RPAS) to enable aerial mapping from the sky. We developed an algorithm to process the full spectrum images into maps of aquatic vegetation, in terms of type, size, shape, and % aerial coverage. This information can be translated into hydraulic flow resistance to be used in modelling water flow dynamics in water systems. Also, the information can be used to determine EU-WFD-targets. The combination of the hydraulic consequences and observed vegetation types with an ecological added value, will enhance the management strategies that water authorities can apply regarding operational water course maintenance.

Field work was carried out in both The Netherlands at sites provided by the end users involved, as well as in Korea at the KICT-River Experiment Center (REC). At the REC, a controlled setup of emergent vegetation is present in the 1:1 scale open air laboratory for surface water systems.

The project team includes experts of research institutes (Deltares, KICT), combined with SME (KICT-Joint Venture, KnowH2O) and end users (Water Board Rivierenland and Water Board Aa en Maas). The techniques developed in this project can be applied both for the Dutch Water Management, as well as for water managers elsewhere in the world. We have been communicating about the project in Dutch and in English, to provide present and future water managers and users with information and updates about ongoing research and developments.

1.3 Operational maintenance of regional water systems

Regional Water Management Authorities in The Netherlands (Water Boards) face operational maintenance challenges with respect to aquatic vegetation and sludge removal from in and around surface waters. Maintenance needs to be planned, implemented, checked, and financed every year. The water system is divided into various types of water courses. The three most common types are main channels, tributaries, and farm-scale ditches. Each type has its own management rules and targets with respect to the discharge of rainfall excess and to the intake of water. During winter time the vegetation presence in the water system is usually low and as such does not significantly contribute to risk of flooding during and shortly after heavy rainfall. However, climate change effects on rainfall and evaporation during the growing season seem to lead to more frequent and more intense rainfall events. This causes more pressure on the operational hydraulic functioning of the water system and on the management of the aquatic vegetation. Therefore, the Dotter-project aims to provide an improved toolbox for Regional Water Management authorities to meet these new and increased challenges.

The current maintenance strategy is such that the vegetation in water and on both shores should not hamper the hydraulic functioning of the water course. In practice, this means that the water levels should not exceed certain threshold levels for a given discharge rate needed to transport water through the system. As a result of this maintenance strategy, the vegetation in and around water courses is removed once or several times each growing season.

The EU-Water Framework Directive (EU-WFD) focuses on healthy and ecological sound groundwater and surface water systems. Within the biological part of the EU-WFD policy targets, the aquatic vegetation plays a significant role. There needs to be a balance between hydraulic and ecological needs and policy targets set. Also national legislation in The Netherlands on the protection of fauna and flora leads to restrictions on water system maintenance. However, removal of all aquatic vegetation in and around surface water systems, puts EU-WFD targets at risk.

Regional Water Management Authorities in The Netherlands are using calculation tools to couple field measurements on water levels with model calculations on water flow, hydraulic resistance, and resulting water levels in sections of the surface water system. From a physical point of view, flow is hampered by vegetation, causing so-called resistance to flow (Figure 1.1). Higher flow resistance leads to higher surface water levels in the water system. These tools relate vegetation to flow resistance, to give direction to reduce possible flooding risk during the growing season. Here we give two examples of such tools.

The first example is the so-called MaaiBOS tool, a decision support system to facilitate operational maintenance (Water Board Aa en Maas). With a 1D hydraulic SOBEK model, water flow in sections of the water system is calculated, without any vegetation being present. Using a 25 year return period discharge rate event, a critical Manning roughness parameter *n* is calibrated to field data. This discharge rate and parameter value lead to a set of surface water levels across the section under consideration. After this, a range of discharge rates is used to calculate different sets of water levels. In daily operation, field data are available on discharge rates at weirs and water levels (better: hydraulic heads) in sections between weirs. These are compared to the calculated water levels, given the discharge rates measured. As soon as measured water levels in the field exceed the calculated water levels with the critical *n*-value, the conclusion is drawn that aquatic vegetation present in the section is causing too much resistance to water flow. Removal of this vegetation in the section under consideration is a way to solve the hydraulic problem, decreasing flood risk after a possible rainfall event in the near future on one hand, and increasing the irrigation water supply capacity on the other.

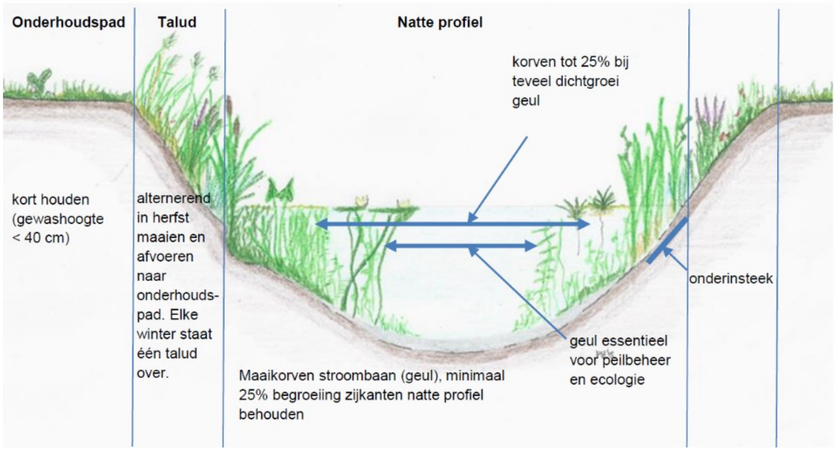

Figure 1.1. Cross section of a water course with an aquatic vegetation pattern (Hendriks et al., 2016).

KnowH2O
Advies, Innovatie en Verbinding in Water

The second example is the Water Board Rivierenland MS Excel tool that is to some extent comparable to the MaaiBOS tool. The tool uses the actual measured water levels and discharge rates, the calculated slope of the hydraulic head in a section, and the theoretical and targeted section water level in the summer period/growing season. The thickness of a sludge layer present is taken into account to decrease the cross-section depth. The wet cross-sectional profile of the water course combined with the targeted water level in summer is used to calculate the cross-sectional average flow velocity. With this, the hydraulic radius can be calculated and the Manning roughness n-parameter can be derived. Using this calculated n-parameter, the % vegetation coverage of the 2D cross section is calculated in the tool according to a linear relationship:

$$\%\, coverage = -3.28\, n + 97.56$$

If this coverage exceeds the threshold value of 50%, the MS Excel tool of Water Board Rivierenland suggests to remove part of the aquatic vegetation in the specific section.

In the Dotter-project, attention has been paid to these and similar tools. Based on knowledge, references and expert judgment, recommendations are given to improve existing tools and to feed future tools with new type of information regarding presence of aquatic vegetation, as collected by spectral imaging of water systems.

1.4 PROJECT ORGANIZATION

The project includes the following five partners. Two water authorities are cooperating with the project team as end-users. The following organizations and specialists were involved:

Deltares:

Ellis Penning – project leader, eco-hydraulics, vegetation parameters
Mike van der Werf – UAV/RPAS and camera expert
Rick Noorlandt – software development for the interpretation of camera images

KnowH2O:

Gé van den Eertwegh – hydrologist and water quality expert – experience and link with water management practices and ecological interpretation according to EU-WFD standards

University of Twente:

Koen Berends – hydraulic modelling tool development

KICT:

Jong Uk Ryu – project leader for REC-experimental setup and data interpretation
Un Ji – senior fluvial expert – coupling of data to flow parameters and analytical interpretation
Sang Hwa Jung – eco-hydraulics

Eun Jin – UAV/RPAS expert

KICT Joint Venture:

Joongu Kang – CEO of KICT Joint Venture, responsible for the personnel management of the REC-experiment

Regional water authorities NL:

Ronald Gylstra, Judith van Tol, Sante Dorigo, Vincent Struik – Water Board Rivierenland
Mirja Kits, Pim van Santen, Jappe Beekman – Water Board Aa en Maas

2 CURRENT KNOWLEDGE, RESEARCH QUESTIONS AND PROJECT TARGETS

2.1 INTRODUCTION

In case of operational water management, water system maintenance aiming at a sufficient hydraulically as well as ecologically functioning, is not an easy task. Climate change effects, like an increased chance on high rainfall events during the growing season, call for a balance between flood risk-management and measures to meet EU-WFD-targets, in which aquatic vegetation is an important factor. Water authorities therefore need information on the actual status of the aquatic vegetation, on water levels as a result of hydraulic resistance due to vegetation, and on the %coverage and vegetation types present.

2.2 CURRENT KNOWLEDGE

2.2.1 Hydraulics and flow resistance by plants

Resistance to water flow may have several causes, all resulting into drag forces, like bottom and wall roughness, sludge present, and vegetation in and around the water course. Vegetation comes in all different kinds of sizes, shapes, and strengths, which partly or completely prevent bending. Also, vegetation can be emergent, submersed, floating, or attached to the bottom or side of the water course. Besides this, aquatic vegetation can have an effect on retention of sediments. Also, dissolved particles may deposit after entering a vegetation patch.

Effect of vegetation type on hydraulics of stream

Vegetation in streams changes the total roughness and conveyance capacity of a stream. Changes in biomass during the growth season affect this roughness. Not every vegetation type will change in the same manner and to the same extent over the season. The roughness of vegetation depends on the flexural rigidity of the plants and on their biomass per unit of surface area. A common way to classify the roughness of vegetation, is to quantify the number of stems per m^2, the diameter and rigidity of these stems and their height in relation to the water depth (Baptist, 2007; Van Velzen et al., 2003). Additionally, a distinction must be made between species that are present in winter and summer time, versus those which will die back in winter time. Perennial species that stay also during the winter season are often emergent and rigid shoreline vegetation species such as reeds and tall grasses (riet, lisdodde en liesgras). Other species will develop yearly from seeds or root systems and are often less firm, submersed or floating and found in the true aquatic part of the stream (o.a. hoornblad, fonteinkruiden, gele plomp, sterrenkroos, kleine egelskop etc.).

Vegetation may cause eddy's on top or on the side of the vegetation, causing (3D!) mixture of water, leading to extra loss of energy of flow (e.g., Zong and Nepf, 2010; Figure 2.1). In different ways, vegetation directly and/or indirectly may cause extra resistance to water flow. Huthoff (2012) studied the influence of wake turbulence on flow resistance in channels.

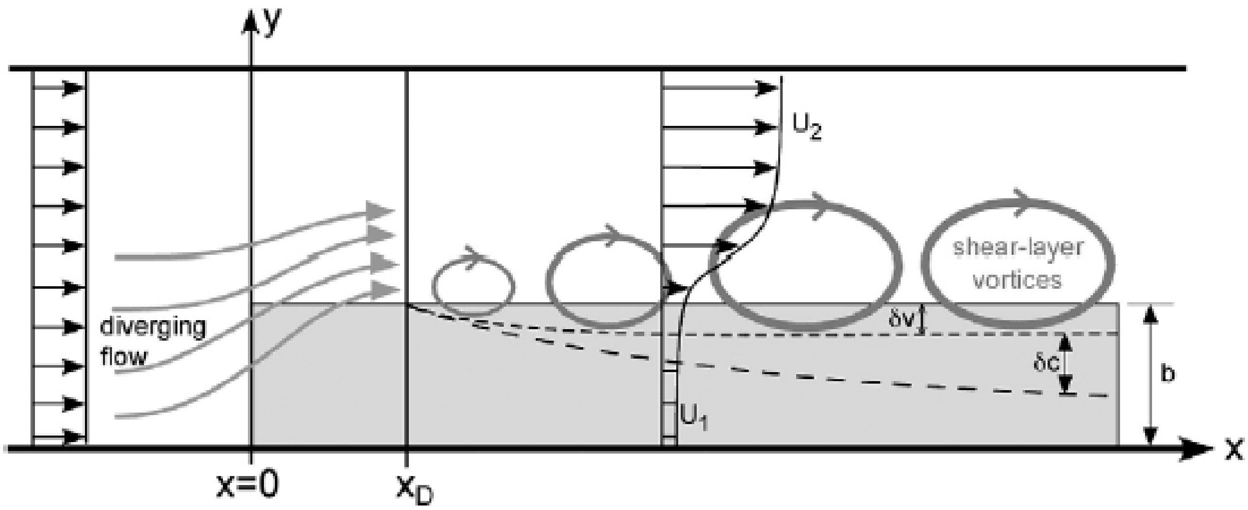

Figure 2.1. 2D flow pattern around a finite vegetation patch (after: Zong and Nepf, 2010).

Vargas-Luna et al. (2014) (Figure 2.2) summarize an extensive dataset of experiments on artificial and real plants and flow resistance. They distinguish in their analysis submersed and emergent conditions. They show and compare different approaches by different authors to calculate flow resistance by vegetation, using identical datasets. Their analysis shows that Klopstra et al., 2007, Baptist, 2005 (see: Baptist et al., 2007), and Cheng, 2011, come up with relatively well calculated resistance factors, as compared to other authors, both for emergent and submersed plants. The equations by Baptist et al., 2007, are implemented in the Delft3D open source software package (http://www.oss.deltares.nl).

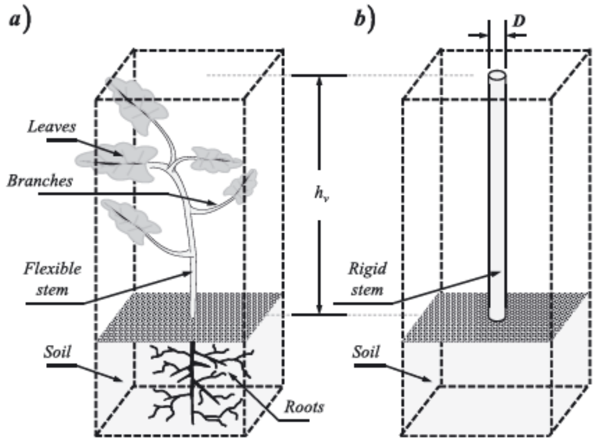

Figure 2.2. Geometric properties scheme of real (left) and artificial rigid plants (right) (after: Vargas-Luna et al., 2014).

Effects of aquatic vegetation on water level

The amount and location of vegetation in the cross section of a stream will influence the water levels upstream. Below figure illustrates the effect of location and aquatic vegetation density in a fictive 'model stream' modelled in Delft3D using the trachytopes approach (Baptist 2007) to assess the effect of vegetation on flow dynamics and water levels. The model stream is 500 m long, and vegetation was added in a variety of manners (Figure 2.3). For example, by adding vegetation to the full stream, only at the shores, only on one side of the stream or with a changed density. The dark blue cells are 'dry' cells. In the left hand side figures, the calculated flow velocities are presented and in the right hand figure the resulting water levels over the section. This shows that location and density of the vegetation are important for the upstream water level.

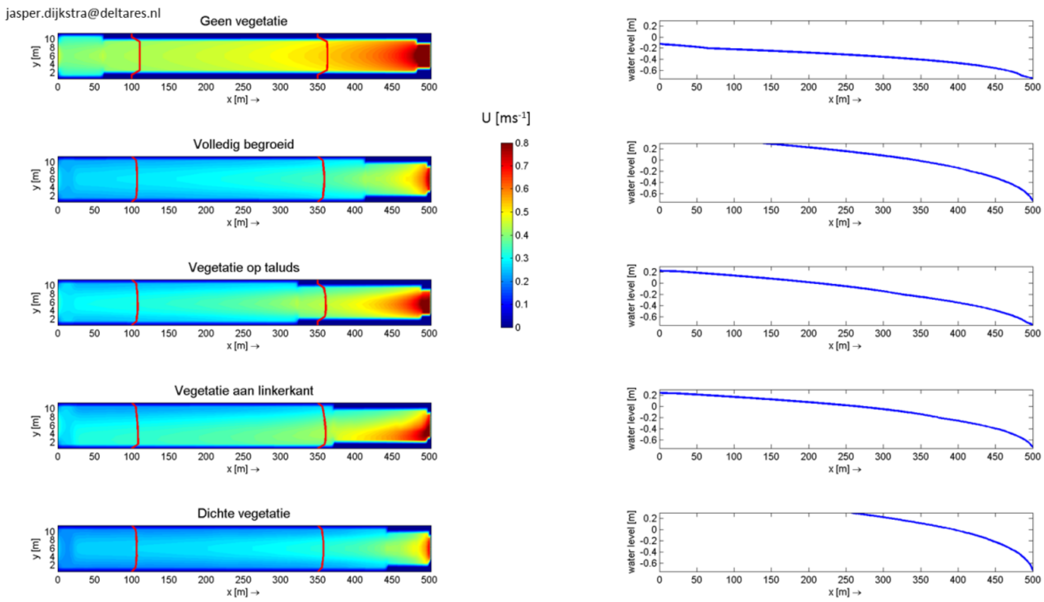

Figure 2.3. Effect of location and density of aquatic vegetation on water level and flow patterns in a fictive stream of 500 m long (source: Jasper Dijkstra, Deltares).

The effects of vegetation on water level can be both positive and negative: In dry periods, the aquatic vegetation will retain water upstream, while in wet periods the same vegetation blocks discharge and increases the risk of local flooding. This calls for a good understanding of the pro's and cons' of vegetation. Due to the increasing intensity of summer showers, local downpours are becoming more likely to cause sudden discharge problems during otherwise dry periods. This increases the complexity of proper vegetation management. Current tools do give overviews based on the assessment of a full stream section, but cannot predict yet where in the section true problems will arise during a rainfall event.

Effect of aquatic vegetation on flow velocities and flow dynamics

Under good ecological conditions, aquatic vegetation does not cover the full width of a channel but exists in patches of different species. This results in a varied flow dynamics and sedimentation patterns (Schoelynck et al., 2012; Figure 2.4). Water will choose the path of least resistance and meanders around the patches. Higher flow speeds outside the patches will create local scour and thus larger water depths than inside the patch. The low flow velocities in the patch will result in additional sedimentation inside the patch, resulting in a diverse stream bed. These dynamics may result in a higher habitat diversity, which is beneficial for the biodiversity of the macro invertebrate and fish community.

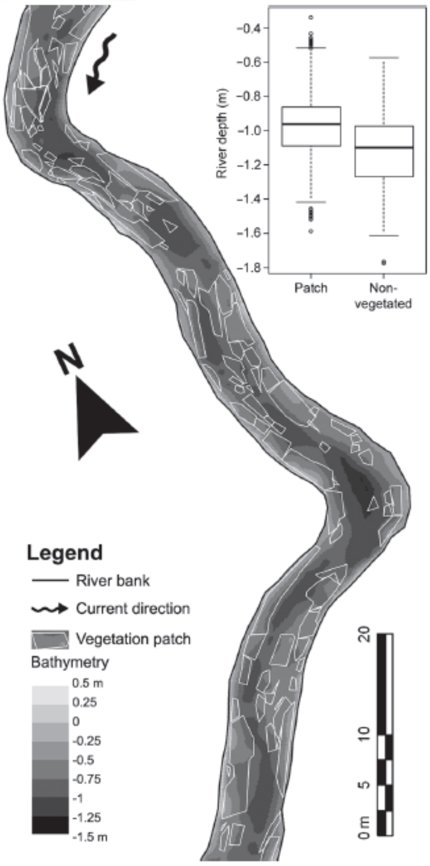

Figure 2.4. Vegetation patch distributions in a stream stretch and related water depth (source Schoelynck et al., 2012).

2.2.2 Ecological targets and plants

The EU-Water Framework Directive (WFD; 2000/60/EC), requires an integrated approach to the monitoring and assessment of the quality of surface water bodies in the European Union. The assessment of ecological status takes into account the effects at the population and community levels, quantified by the use of specific indices and ecological quality ratios. The chemical status assessment is based on compliance with legally binding Environmental Quality Standards (EQSs) for 53 selected chemical pollutants (priority substances) of EU-wide concern.

For macrophytes, the presence of different species and their abundance are important factors. The abundance is split into emergent, submersed, floating, flab, and duck weed, within the area of presence. Also the %coverage and total coverage is important, given the conditions of the monitoring location like water depth and length/width. The width and length of the water course shore line, in which specific vegetation is present, is relevant.

Surface water bodies are categorized into different types, into salt/brackish and freshwater, into lakes and rivers, into man-made channels and natural small streams. They can be either stagnant or freely flowing. Different water types have different ecological standards and targets. In The Netherlands, we distinguish between 'ecologically sound status' (GET in Dutch) for natural water systems, and in 'ecologically good potential' (GEP in Dutch) for artificial and heavily modified water systems.

The Dotter-project introduces innovative monitoring, using spectral images, which should be capable to deliver monitoring information, comparable to the current monitoring methods. Two relevant elements appear to be important, the recognition of specific plant species, and their abundancy. The recognition of specific plants will be based on shape, size, and pattern on one hand, and on specific spectral reflection of sunlight onto the (submersed) plants. Once specific plants can be 'recognized' and detected by the spectral image, ecological knowledge about the plants' geometry on and under water can be added to obtain hydraulic resistance characteristics. Secondly, EU-WFD monitoring can profit from the results of the spectral observations. The innovative monitoring will obtain continuous aerial observations of the vegetation present, not only at a 100 m stretch or 10x10m² grid, according to the current monitoring methods.

2.3 Research questions

We have different groups of research questions within the TKI Dotter-project.

Full spectrum camera and vegetation recognition

- To what extent can we detect and map the presence of floating, emergent and submersed aquatic vegetation by use of a full spectrum camera? (450-988 nm band width, divided into 125 sections)
- Can we determine the type of aquatic vegetation by pattern recognition or other method(s)?
- What circumstances and conditions can we derive from our experiments to estimate the potential successful application of the full spectrum camera?
- What is the added value of mapping vegetation with a full spectrum camera to the current mapping methods?
- How is the performance of the full spectrum camera mounted on an Unmanned Aerial Vehicle (UAV, 'drone')?
- What is the best protocol for image processing from the full spectrum camera

Translation into hydraulics

- How can we translate observations regarding the vegetation presence into flow resistance for model applications?
- How can we deal with the dimensionality issues with respect to vegetation and flow resistance? Can we translate 3D-flow resistance caused by vegetation into 1D model parameters?
- How does this technique help to define a time- and space-specific maintenance program for aquatic vegetation, based on our innovative measurement method, in order to maintain water courses hydraulically functioning well?
- How can we use this data in line with existing and potentially newly developed tools for quantifying the water levels in relation to vegetation presence?

To serve EU-WFD targets

- To what extent can we distinguish vegetation types that are of importance to biological essays of water systems, relevant for EU-WFD?
- How can we define a time- and space-specific maintenance program for vegetation, based on our innovative measurement method, to serve ecological targets for water courses?
- How can we combine and integrate maintenance for hydraulic and ecologic purposes?
- Is the technique sufficiently capable of dealing with less abundant species?

Application to practice

- How can we cooperate with regional water authorities to facilitate them to optimize water course maintenance and define less expensive and more effective (hydraulics and ecology) maintenance programs?
- What are the next steps in upscaling this technique to larger areas?
- Can these monitoring activities with the UAV be combined with other instruments attached to the drone following a 'one-sweep-for-all' idea.

2.4 PROJECT TARGETS

The Dotter-project aims to develop new techniques to determine where the true hydrological obstacle points in a stream are located, by which vegetation types these are caused, and at the same time identify the ecological values that the vegetation represents, all in a uniform and quantified manner. By transforming data on vegetation patches into a hydraulic roughness coefficient like the Manning roughness parameter (n in dimension $(T/[L^{1/3}])$, based on bio volume and species characteristics, we define the true obstructions in the stream. By only removing these true obstructions, as if 'removing obstructions from a vein', other valuable patches can remain unharmed. The determination of ecological values of the stream vegetation in this project aims at aerial mapping of the occurrence of vegetation and recognition of vegetation patterns. We look at the feasibility of recognition of vegetation species.

New UAV and camera techniques, e.g. a full spectrum camera (450-998 nm), enable to automatically map larger stretches of brooks, channels, and rivers and translate these images into spatial maps of vegetation cover, biomass and species composition. By using a full spectrum camera and an automated flight path, this information can be obtained quickly and processed objectively. By means of a validation experiment in the River Experiment Center (REC) of the Korean Institute for Civil Engineering and Building Technology (KICT) in Andong, South Korea, the developed technique has been further improved.

We demonstrate the use of UAV/RPAS and cameras involved in The Netherlands by demo flights across selected streams in management areas of regional water authorities taking part in the project.

3 Methods and Field Experiments

3.1 Project Activities

The project consisted of the following activities:

1. Definition phase for UAV/RPAS-camera combination and for field experiment

During the definition phase the appropriate equipment needed for the project was selected and acquired. A full spectrum camera (UHD 185 - 'Firefly'; Figure 3.1) from the firm Cubert was selected for further testing in this project (technical details of the camera can be found in Appendix A). This camera has the advantage that it takes both a high resolution (1000*1000 pixels) black and white image and 138 low resolution (50*50) spectral images from 450 nm to 998 nm in steps of 4 nm bandwidth. These two types of data can be overlaid to get more details.

Figure 3.1. The Cubert UHD 185 - 'Firefly' full spectrum camera.

2. Construction of UAV/RPAS-camera combination

The various parts were assembled and tested for initial camera settings, calibration parameters, flight capabilities and adjoining technical aspects, both in The Netherlands as well as in Korea. In the Netherlands the tests were carried out from either a fixed point in a boat, a bridge or from a high pole (6 m high), and in Korea the camera was used both from a fixed point as in combination with the KICT-REC drone.

3. Software set-up and first testing

The software needed for management of the camera was available from Cubert. First testing of both the set-up of the camera itself and the software was carried out in the Netherlands, specifically for the settings used to obtain appropriate images in the field cases of both the Linge (Water Board Rivierenland) and the Lage Raam (Water Board Aa en Maas) in August 2016 and September 2016 (see paragraph 3.2). After these field visits calibration data was gathered at the KICT-REC (see point 5.)

4. Demonstration flights at regional streams in The Netherlands
Although it was planned to make demonstration flights with the full spectrum camera – drone combination in The Netherlands, we only had a demonstration flight with a regular drone camera combination at the Linge. This was both due to timing and to drone flight regulations, which did not allow us to fly in the Lage Raam as a result of a nearby military airport.

5. Start-up of the REC-experiment
The REC experimental set-up in the A1 channel consisting of four dense patches and three sparse patches, was prepared by KICT and KICT-Joint Venture in the summer season. Detailed flow measurements were carried out for this year's (2016) set-up using ADVs and ADCP equipment for a setting with 1 m^3/s discharge and a maximum water level (downstream weir at maximum height). This set-up was used to test (Figure 3.2):

- The ability of the camera to distinguish between densities and vegetation types: One vegetation type consisting of young willows, with two densities, covering a set of patches in the channel. At the same time, naturally growing vegetation along the sides and on the bed of the channel was also photographed.
- The effect of varying water levels on resulting images. Water levels were adjusted from empty bed to bankfull. During these water level changes pictures were made and the water height was recorded. This procedure was repeated.
- The ability of the camera to deal with turbidity: images were obtained while changing the turbidity of the water by manually adding a sand mixture to the stream. Suspended sediment samples and PAR measurements using a LiCOR underwater light meter were recorded to link the images to related turbidity equivalents.

Figure 3.2. The REC experimental set up with a. camera on fixed ladders, and b. on the UAV

6. Testing UAV-camera combination at REC
The camera was both attached to a fixed point at the tip of a ladder construction on the movable bride over the A1 Channel and attached to the drone, in order to compare the difference arising from changes in height and the movement of the drone.

7. Data processing and interpretation
After completing all series of tests at the Dutch field sites and the KICT-REC data interpretation and analysis was carried out by all partners. The processing of the spectral images consists of three main steps. First, the images taken need to be normalized for camera sensitivity and the incoming light spectrum. Second, the reflectance values are used to determine indices or clusters enabling the separation of the vegetation and other objects photographed. Third, because one image is typically not enough to cover the area of interest with enough resolution, multiple overlapping images are made that need to be stitched together to form one image that covers the whole area.

8. Translation to hydraulic and ecological water management practices
The results of the testing and validation of the measurement data from the UAV-camera combination were evaluated in line with ideas considering new management practices possibilities for flexible management and aerial mapping and possibly recognition of vegetation in streams. Dissemination of the results was carried out by various presentations at stakeholder symposia and (popular) scientific articles (see appendix F for the full list of dissemination activities).

3.2 FIELD EXPERIMENTS IN THE NETHERLANDS AND KOREA

Two field locations in the Netherlands, Linge and Lage Raam water systems, were visited, and combined with measurements in the KICT-REC. A summary of all measurements and types of measurements is given in table 3.1.

Table 3.1. Overview of measured parameters per case study site

Measurement	Linge	2. Lage Raam	3. Korea - REC
Spectral photos from boat	x (incl. GPS)	x	
Spectral photos from fixed point (bridge/ladder/pole)		x	x
Spectral photos from drone			x
Photos from drone	x		
Vegetation biomass		x	x
Vegetation species distribution	X(aquon)	x	x
Water quality parameters		X (Aquon)	
Depth		x	x
Turbidity measurements		x	x
Flow measurements		x	x

3.2.1 Linge

On September 1, 2016 we performed field observations at a site on the 'Linge', near Echteld in the Betuwe district of Water Board Rivierenland. This end-user also organized a vegetation mapping activity on the stretch observed at the time of our visit, divided into four parts/sections. The work focused on uniform vegetation parts, on %coverage per vegetation type, and on growing forms (emergent, submersed, floating). Also, the dominant vegetation was determined. Pictures were taken with the spectral camera every 5 seconds, mounted on a mowing boat. The observations were combined with dGPS-measurements and digital photographs.

This visit was the first time we deployed the full spectrum camera in the field. The main emphasis of the visit was to experiment with the camera settings, use of additional polaroid filters and understanding the software used to manage the camera (Figure 3.3).

Next to using the camera on the mowing boat provided by the Water Board we also deployed a standard drone (DJI Phantom 3 Pro) with standard camera to get a first impression of airborne images for better view of the vegetation.

Figure 3.3. Test site De Linge, near Echteld in the Betuwe district of Water Board Rivierenland.

3.2.2 Lage Raam

On September 15 and November 15, 2016, we performed field observations at a site on 'Lage Raam', near Mill in the Raam district of Water Board Aa en Maas. The section between the upstream weir IJzerbroek (108IJZ), weir 108HOL, and downstream weir 108TDE (tributary) was subject to the field observations. As reported by the water board, Q_{max} @weir 108IJZ equals 2.2 m^3/s.

Three locations were selected for sampling (Figures 3.4 and 3.5):

- Location 1 Ziepweg bridge
- Location 2 IJzerbroekseweg bridge with weir 108IJZ
- Location 3 Kwekerijweg

At all these locations fixed-position observations were performed using the spectral camera.

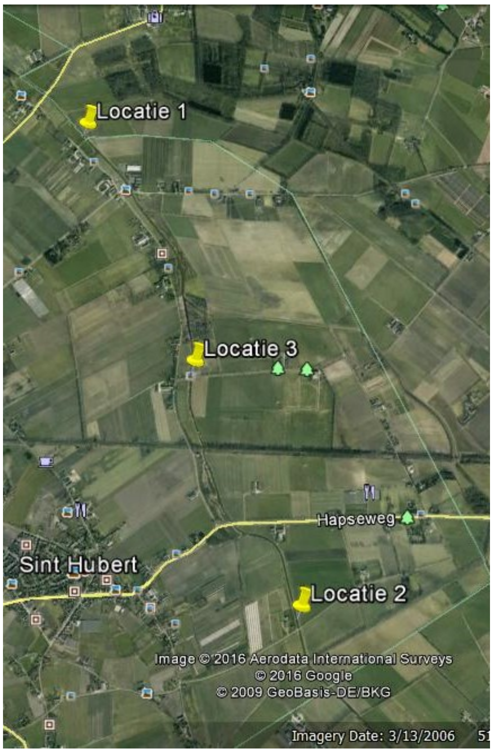

Figure 3.4. Locations at the Lage Raam (left) and ADCP flow measurements at location 3 (right).

A EU-WFD-proof vegetation mapping was carried out as well (Figure 3.6). Due to the absence of sufficient discharge on September 15, 2016, stream flow velocity was delayed to the 15th of November (ADCP, StreamPro).

3.2.2.1 Flow measurements

ADCP measurements were carried out at location 2 and location 3 using the StreamPro. Vegetation was cleared out of the transects in order to get a good overview of the full cross channel flow. The shoreline edge of the transects were recorded at the point where recordings did not longer function. The distance to the real bank was recorded in the software. At each location the width of the stream was also recorded by hand. For each transect 6 measurements were carried out in order to obtain a valid average. Starting at one shore with a 10 second measurement the StreamPro was slowly pulled across to the other side of the stream with a constant speed. At various locations in the transect a more accurate flow measurement was carried out in which the StreamPro was not moving.

3.2.2.2 Vegetation parameters

The hydraulic consequences of the vegetation were measured in terms of type, density, stem width, leaf surface, and height.

Vegetation biomass parameters were both measured on September 15th and November 15th for the most dominant species in the section. The biomass and parameter recording procedures were the same for both visits, and this procedure was also implemented at KICT-REC for the dominant species there.

Biomechanical properties of plants are used to define their total effect on the resistance of a patch.

Vegetation characteristics were measured for dominant species in the stretch, being *Callitriche palustris, Glyceria maxima, Sparganium erectum* and *Potamogeton natans*. For each species a plot of 0.5*0.6 m^2 was harvested, in which emergent and submersed parts were treated separately. Water depth and organic layer depth were recorded using a handheld measuring stick and sediment thickness disc. Vegetation was laid out on a cloth with a printed grid of 0.1*0.1 m to define average height, and biomass distribution over the water column. Where necessary the vegetation was separated in distinct length layers. For instance, for *P. natans* the stems branches at a given length, and leaves are present at the tip of the vegetation. These layers were than separately counted. For each sample the approximate length of the stems, the average diameter of the stems (n=12), number of stems per m^2, number of leaves and average leave dimensions (n=12) were measured. Wet weight and wet volume were determined for the full sample in order to define the total Plant Infested Volume and plant rigidity. Wet weight was measured using a normal kitchen weighing scale and wet volume was defined by assessing the volume of a 1 litre beaker being taken by the vegetation when submersed fully. Subsamples of the wet vegetation were air dried for 3 days and measured again to define approximate wet-weight/dry weight ratios as a measure of plant rigidity. (Field recording protocol is found in Appendix E).

3.2.2.3 *Light measurements*

In September also, optical measurements were carried out on the local surface water by means of a PAR-sensor and a Secchi disc. Water samples were taken, to be analysed on chlorophyll-A, suspended matter, and humic acids. The water depth in cross sections was determined, to the sludge depth present and to the sandy bottom of the Lage Raam water course.

Light attenuation was measured using a LiCOR underwater PAR sensor and additionally with a Secchi-disk for reference to the regular monitoring values of the water management authority at both locations where vegetation measurements were done, and at a third location where upward seepage through iron-rich sediments caused red colouring of the water. Additionally water samples were taken at each location in the middle of the stream and analysed at the AQUON lab for Chlorophyll-a content, Suspended matter and humic acid concentrations following the standard NEN-protocols. The resulting data were used to determine the total underwater light climate for better assessment of the taken photographic images.

Figure 3.5. Location 2 IJzerbroek weir (108IJZ; main water course, left) and 108TDE weir (tributary, right) in Lage Raam water system, Aa en Maas, near Mill. Red arrow points at measurement location of upstream water level.

Figure 3.6. Field observations in Lage Raam water system, Aa en Maas, near Mill location 1. Date: September 15, 2016.

3.2.3 Experiments at KICT-REC Korea

The River Experiment Center (REC) of KICT in Andong, South Korea, is an excellent site to test and calibrate/validate vegetation mapping under controlled conditions (Figure 3.8). Established in 2009, the Center is capable of scale 1:1 tests in three prototype channels of 600 m length and 11 m width at maximum. Its pump capacity leads to stream discharge rates up to maximal 10 m^3/s. Two test channels are straight water courses, while the third channel is meandering with different sinusoidal levels.

From September 22 to 29, 2016, we used the straight A1 channel including its patches of vegetation to test the spectral camera. We started with a fixed position on the railing bridge across the test channel. At the end of the field work, we used a Korean UAV/RPAS with the spectral camera mounted to take pictures from the same section during flight (Figure 3.7).

Figure 3.7. River Experiment Center (REC) of KICT at Andong, Korea.

Figure 3.8. Aerial image of the full River Experiment Center, with the Nakdong River next to it.

The REC experiment was prepared by KICT and KICT-Joint Venture colleagues. The setup was such that we looked at one vegetation type, partly with patches of young willows, and two different water level heights, controlled by a downstream weir, creating emergent and submersed situations for the same patches. We used a standard discharge rate of 1 m^3/s, and for most photos the maximum obtainable water level by raising the weir at the end of the channel.

Additional images were shot to test the impact of fluctuating water levels by reducing the water input to the channel and recording images every approx. 5 cm water level change. Also, we tested the impact of turbidity on the resulting images by manually adding a suspended sediment load to the water, and recording the images together with measurements on turbidity and suspended sediment concentrations.

After the images were taken from the fixed positions the camera was mounted on a Korean UAV. After initial test flights to balance the weight and to familiarize with the new set up we carried out a set of operational flights under the same discharge conditions and the highest possible water level setting that was also used for most of the fixed camera photos.

4 METHODS FOR VEGETATION IMAGING AND IMAGE ANALYSIS

4.1 Mapping vegetation using spectral imaging

The full spectrum camera is provided with a dedicated software suite (see screenshot in Figure 4.1). This software provides some basic methods of analysing the spectral images, but it is not suited for advanced analysis. Therefore we further analysed the images using custom made Matlab functions and scripts, making use of the source code provided by Cubert. Healthy vegetation absorbs most of the visible light that hits it, and reflects a large portion of the near-infrared light. Unhealthy or sparse vegetation reflects more visible light and less near-infrared light. This index is available within the Cubert Software package. The NDVI (normalized difference vegetation index) is calculated from the visible and near-infrared light reflected by vegetation NDVI = (NIR — VIS)/(NIR + VIS (Tucker, 1979).

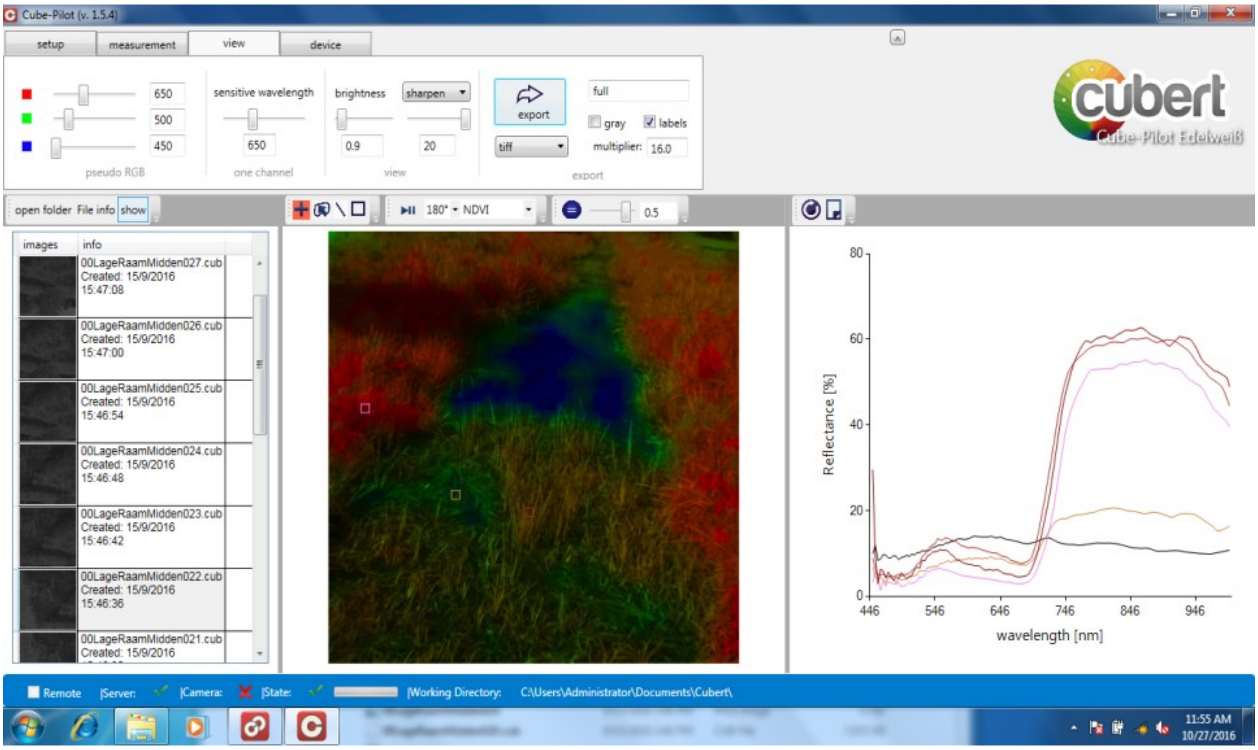

Figure 4.1. An overview of the main software window of the Cubert software, in which one picture of the Lage Raam in NDVI colours (Normalized Difference Vegetation Index) indicating the vegetation biomass,

and with several pixels showing reflectance spectrum per pixel (black line represents a water reflectance, the other lines are curves representative for vegetation.

The currently applied workflow of processing consists of the following steps:

1. Copy the images from the field laptop to network location
2. Export the CUB files (raw camera file format, proprietary of Cubert) to CUE files (raw camera file format, well described binary files) using Cube-Pilot
3. Make a digital logbook in excel describing the files, settings, field observations etc.
4. Read the raw images in Matlab and normalize with respect to incoming light spectrum and camera sensitivity
5. Apply different indices to visualize the vegetation and export images of the different index rules.
6. Stitch multiple images together using Pix4D, Hugin, Manual Picking and/or Autostitch.

As the method has been developed throughout this project, not all steps could be completed successfully for all field locations. Steps 1 to 3 are self-explaining.

Step 4, Image normalization is needed to obtain the reflection of the object in the image, without having too much imprint of the acquisition setup. The raw images must be corrected for the camera sensitivity and the varying amount of incoming light. Three steps are taken to normalize the images. First, the camera sensitivity has been determined and images are corrected for that. Second, the incoming light spectrum was determined in the field using a grey/white check card. The check card used in the field is relative cheap and robust, but does not reflect all wavelengths equally. The reflectance of the check card was calibrated using a perfect reflectance material, which is too delicate to be used in the field directly. Third, for the REC experiments only, the change of light intensity over time was recorded and used to correct the images. The resulting images after normalization represent the reflectance of the materials photographed and were used for further processing.

The information extraction in step 5 was mainly done using indexing. With indexing the wavelength, information is transformed to a domain that can be used to interpret different classes (vegetation, water, ground etc.). We selected various indices from literature. Typically, these indices are based on calculating the relative difference of two wavelengths, NIR/green for vegetation (Mitchell et al., 2015), in order to get an idea of which might be suitable for future use in the foreseen application.

Instead of transforming the data to index domain using a few wavelengths at a time, clustering is done based on the full 138 wavelengths. The so produced indices/cluster images can be used stand-alone or can be feed into a stitching program to generate an aerial coverage.

4.1.1 Stitching

As described before, the spatial resolution of the spectral image is poor (50x50 pixels). Therefore to get both a good spatial coverage and enough resolution multiple images need to be made and stitched together. Stitching images can basically be done in two different ways. In the simplistic way the images are just overlapped and shifted until the pixels within the images line up nicely. Typically this is done using some sort of correlation of the images to find pixels present in multiple images. This method works best if the camera is rotated and images are corrected for lens distortions. There are several panoramic software packages available on the commercial market at this moment (see e.g. https://en.wikipedia.org/wiki/Comparison_of_photo_stitching_software for an overview). Within this project we used both Hugin and Autostitch software programs. The other method of combining the different images is by building point clouds of the objects imaged. In principle this method is more suited for our case where the camera is translated instead of rotated. Where parallax (difference in the apparent position of an object viewed along two different lines of sight) can be minimized when the camera is rotated, it is always present in case the camera is translated. This parallax makes generating a panoramic image difficult, but assists in generating a 3D model of the objects imaged. For this project we made use of Pix4D. The Pix4D software can handle multiband images and can generate a point cloud, 3D mesh, digital terrain model, ortho-mosaic and index images. During this project it was found that the program has great difficulty in combining images with many moving objects (water surface and vegetation).

4.2 MEASUREMENTS LINGE

The Linge measurements were the first set of measurements carried out with the spectral camera. The camera was mounted on a tripod that was installed in a mowing boat provided by Water Board Rivierenland. The boat was slowly moving along the shore lines of the selected site within the Linge while the first images were captured.

4.2.1 Cubert camera settings

In the Linge case we used the spectral camera in time lapse mode. In this mode the camera automatically takes images at a predefined interval. Although this is an optimal setting on a moving platform, it was found that this option has not been correctly implemented by the camera manufacturing company Cubert. The high resolution grey images and low resolution spectral images are out-of-sync, which results in different output images from the black and white image with the same time stamp. This could only partially be recovered. Together with the fact that the spectral images were recorded close to the water surface, this made it difficult to stitch and interpret these images for a larger area.

Although the spectral images do not provide a good coverage, the field work contributed a lot in the development of the method. It was found that under sunny conditions with small clouds it is very hard to visualize vegetation below the water surface due to the strong reflections caused by the sun and clouds. Figure 4.2 shows a picture taken with a regular camera to illustrate this effect.

Figure 4.2. Illustration of strong reflections by the water surface.

Part of the reflections could be removed with the help of a polarization filter, but these conditions made it very difficult to look into the water column, especially given the oblique orientation of the camera with respect to the water surface. Figure 4.3 shows some examples of the spectral results, compared to the black and white images. The difficult light situations are also clearly visible in these images.

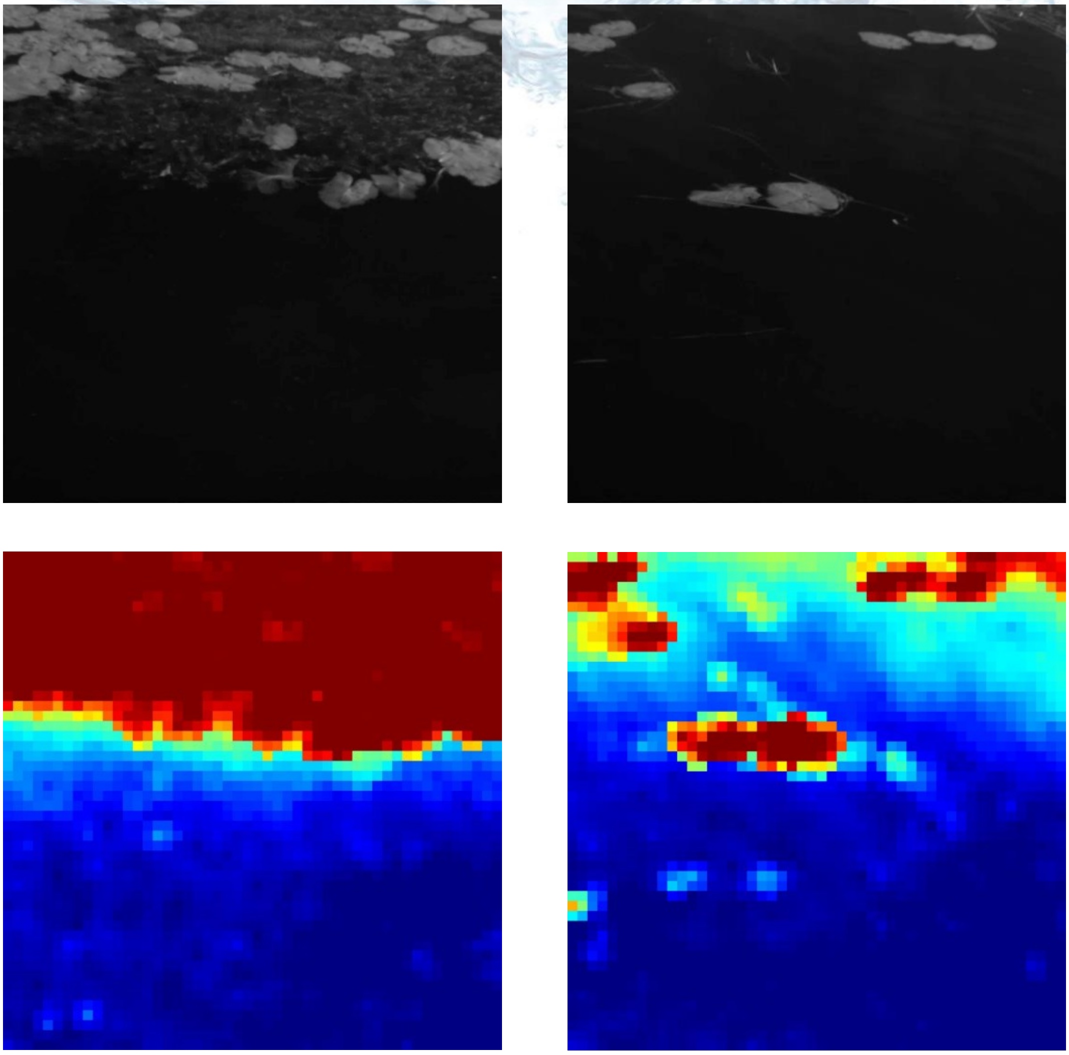

Figure 4.3. Top row shows black and white image, Bottom Row shows NDVI indexes. Top image has a resolution of 1000x1000 pixels, while lower image has a resolution of 50x50 pixels.

4.2.2 Drone images

At the Linge we also flew with a normal camera to observe the value of a 'birds eye view' using a DJI Phantom 3 Pro with a 12 megapixel visual camera. The drone was programmed to fly a predefined flypath and some of the images taken were also stitched using the Hugin software (Figure 4.4). The images give a good overview of the location and the type of vegetation. Glare from the sunlight reflecting on the water is clearly visible.

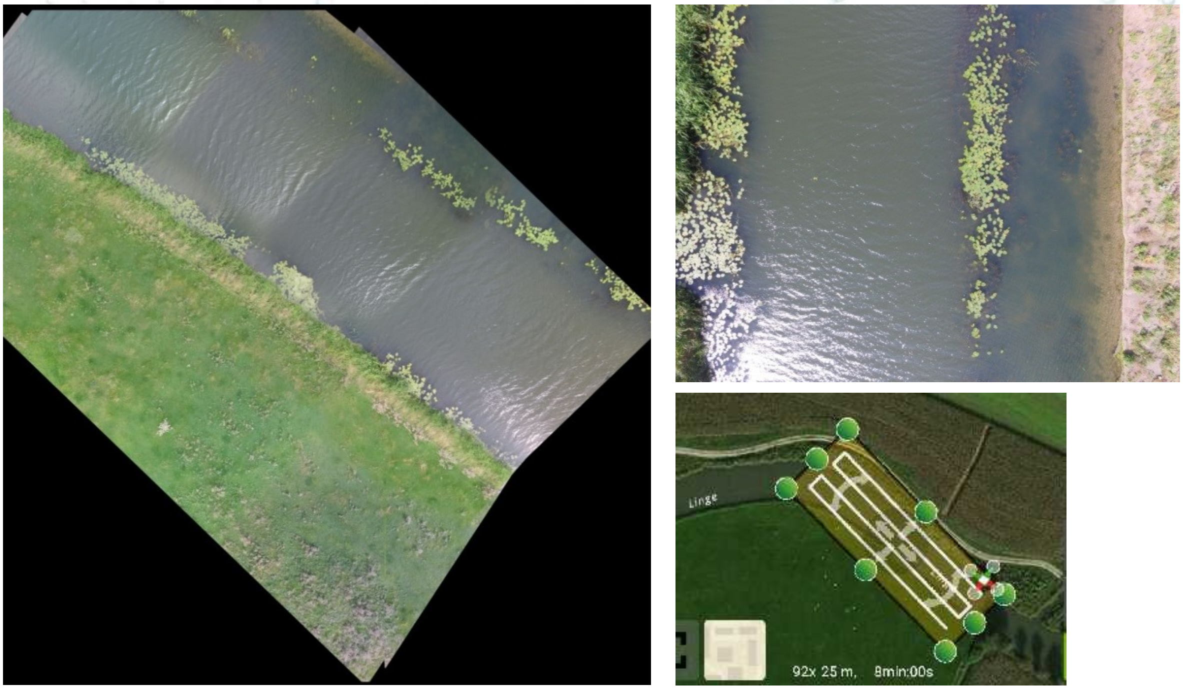

Figure 4.4. Drone images from the Linge, and the flight path of the total flight.

4.3 Measurements Lage Raam

In the Lage Raam we took images from the bridges at location 1 and 3 and images from a tripod on the shore line along location 2 on the 15th of September, 2016. We also used a boat provided by Water Board Aa en Maas to take images while sailing on location 1. During the November 2016 visit the camera was mounted on a Gimble fixed to a 6 m high pole and moved along approx. 100 m of shoreline at locations 2 and 3.

4.3.1 Cubert camera images

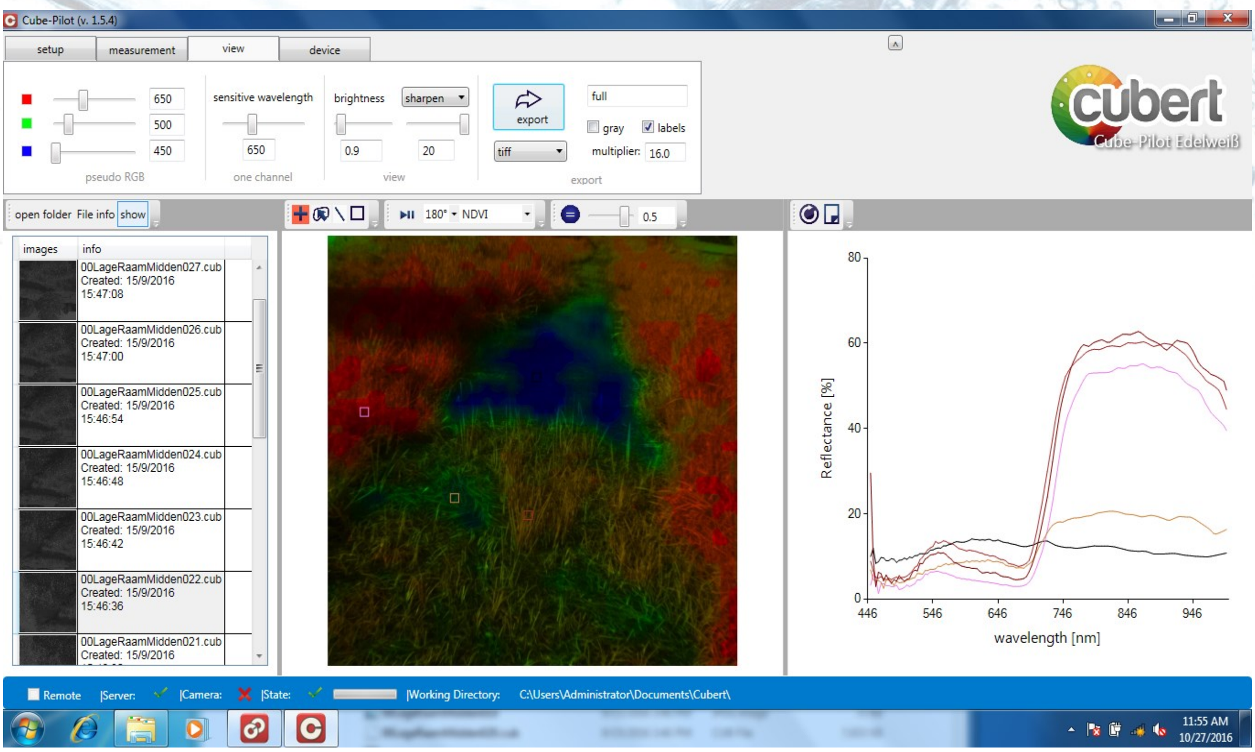

Figure 4.5. An overview of the main software window of the Cubert software, in which one picture of the Lage Raam in NDVI colours, and for several pixels the reflectance spectrum per pixel (right hand section).

Figure 4.5 shows one of the images taken at the Lage Raam location 3 during the September visit. This image is represented in NDVI –index settings. In Figure 4.5 a few individual pixels are selected and the right hand panel of the figure gives an overview of the spectral characteristics of these pixels. Reflectance over the different wave lengths is given. Pixels from the ‘open water’ have a general low reflectance over the full wave length scale (the black line), while vegetation has a small peak around 550 nm and a high peak above 700 nm.

Figure 4.6a shows a number of black and white images stitched together (using Autostitch) at the bridge at location 1. In Figure 4.6b these same images are represented using the NDVI index. Note that best results are obtained looking down (lower part of the panorama), while the vegetation further away from the bridge is becoming blurry. This vegetation was having the same density as the vegetation closer to the bridge based on visual interpretation in the field. The angle of the camera and the difference in distance thus affect the overall interpretation of the vegetation further away.

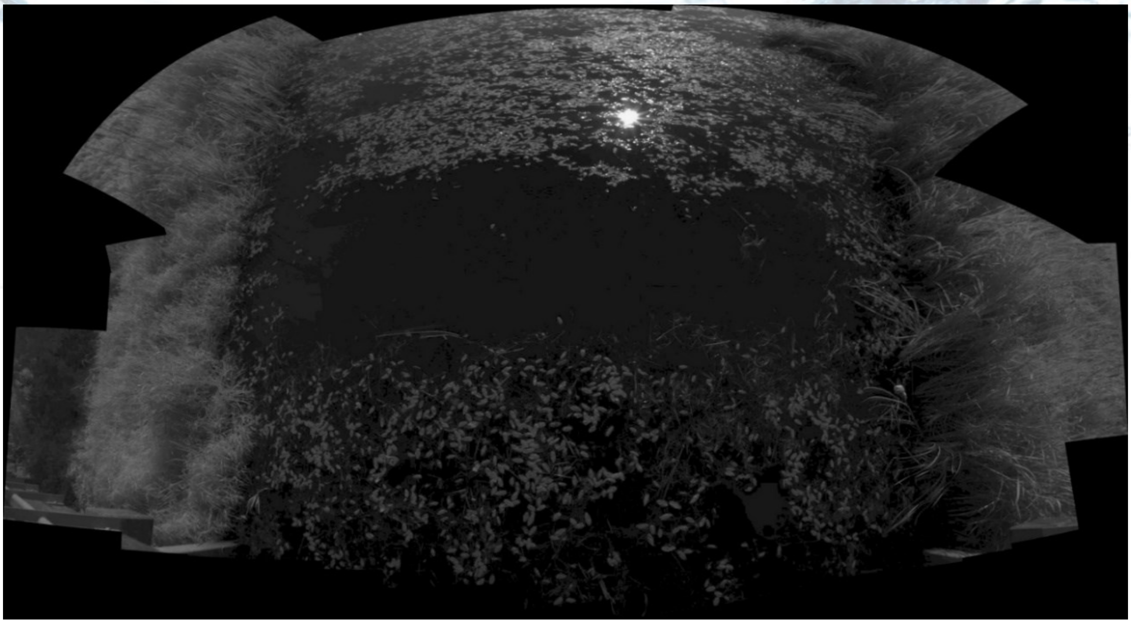

Figure 4.6a. Stitched black and white image of the vegetation close to the bridge at location 1 Lage Raam,

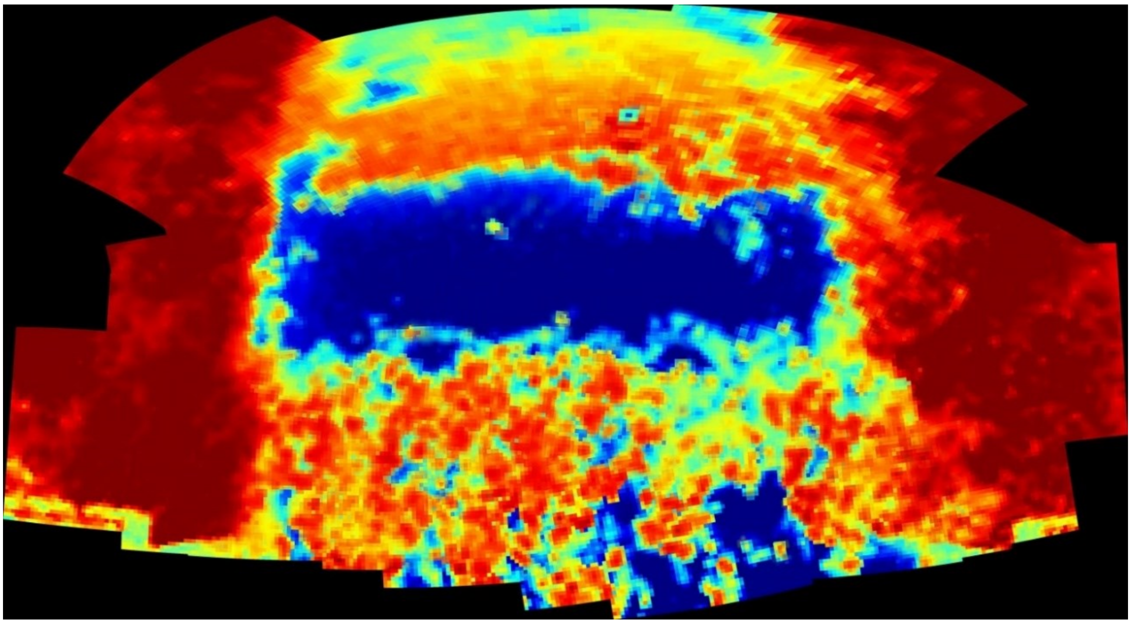

Figure 4.6b.The calculated NDVI values of the same images taken from bridge at location 1 looking upstream.

4.3.2 Individual images normalization and analysis

The individual images are sometimes 'stripy' in nature, due to the incoming light and camera position. Therefore images need to be normalized before further analysis. From discussions with the manufacturer 'Cubert' it appeared there is a strong need to correct for the incoming light spectrum and for the sensitivity of the camera pixels. It has different intensity for different pixels. The grey reference plate gives wavy pattern at different wave lengths. This is a result of some of the properties of the camera hardware. In order to correct for this, several grey images must be combined. The waviness does not change from image to image, but effects from shade on partially shaded images can be seen. Pixel sensitivity of the camera might have to do with exposure time of the camera.

The spectral cube normalization procedure consists of three steps:

1) Correct for camera sensitivity
2) Correct for incoming light spectrum
3) Correct for light intensity changes over time

Due to the construction of the spectral camera, the sensitivity of the pixels of the camera is far from homogenous. Even if the light source and reflection material/angle etc. is constant, the recorded spectrum differs depending on which pixel is used to record it. This is clearly seen in the image of the grey check card below in Figure 4.7.

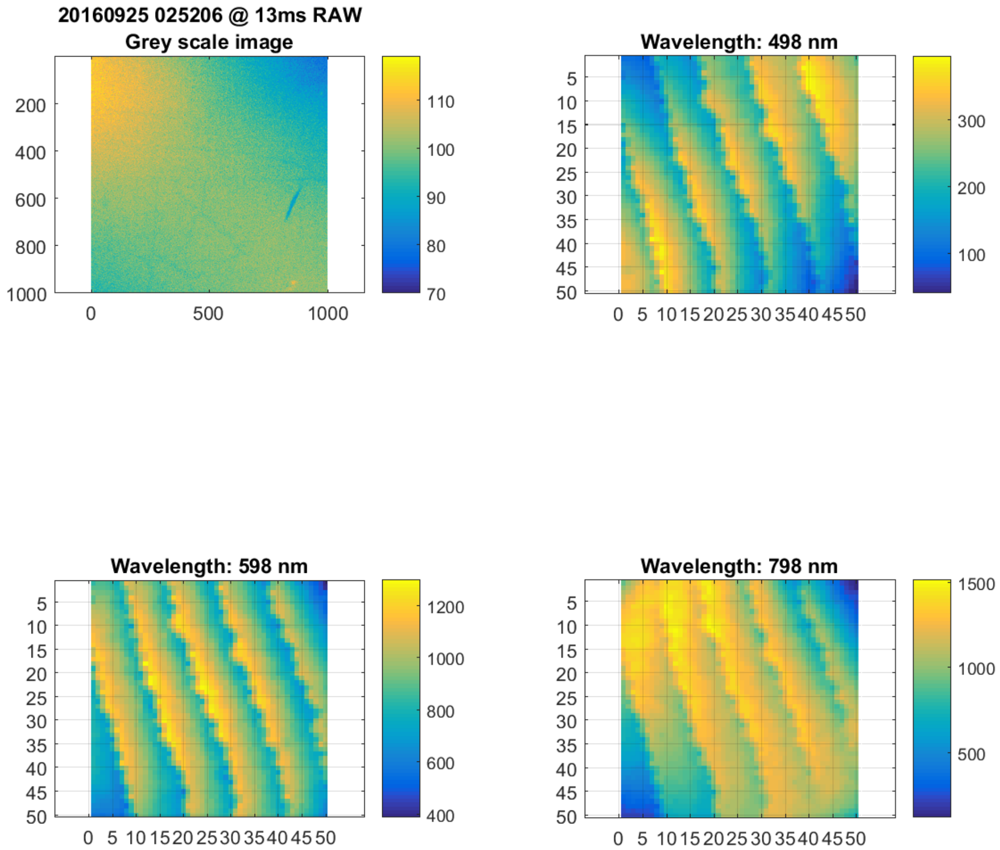

Figure 4.7. Waviness in the non-normalized images.

The images need to be corrected for changes of the light during the day. This is done by taking one reference grey image at the start of each measurement set. During the measurements on 15th of November in the Lage Raam, the very precise (yet very delicate) reference tile was used. This reference tile is made of a special material and has a perfect white reflectance. A small difference between the normalization results from the reference tile and the reference photo paper plate was found. Unfortunately, the use of the reference tile is very impractical because it is easily damaged, and damages hinder the normalization procedure. We therefore recommend to continue using the reference photo paper for normalization purposes, as it is cheaper and potential damages are of less concern. The reference tile can be used in lab-set ups but is better not used in the field.

4.4 Measurements River Experiment Center REC

At the River Experiment Center a large set of images was made in order to test various aspects of image quality and responsiveness of the camera to altering positions and changes in the general settings in the experimental setup, such as the effect of water level, turbidity and whether or not the camera was positioned on a fixed or flying platform.

4.4.1 Effect of water level on image quality

In order to test for the effects of water level on the image quality a set of images was taken from a fixed position while water levels were varied. At approx. each five cm of water level change a picture was taken. A steel reference plate was placed at the bottom of the dry bed and pixels were selected for further analysis that were located on different areas of vegetation, the steel plate, the bare sediment and on some very light bottom vegetation. Figure 4.8 shows a few of the black and white images taken during these measurements.

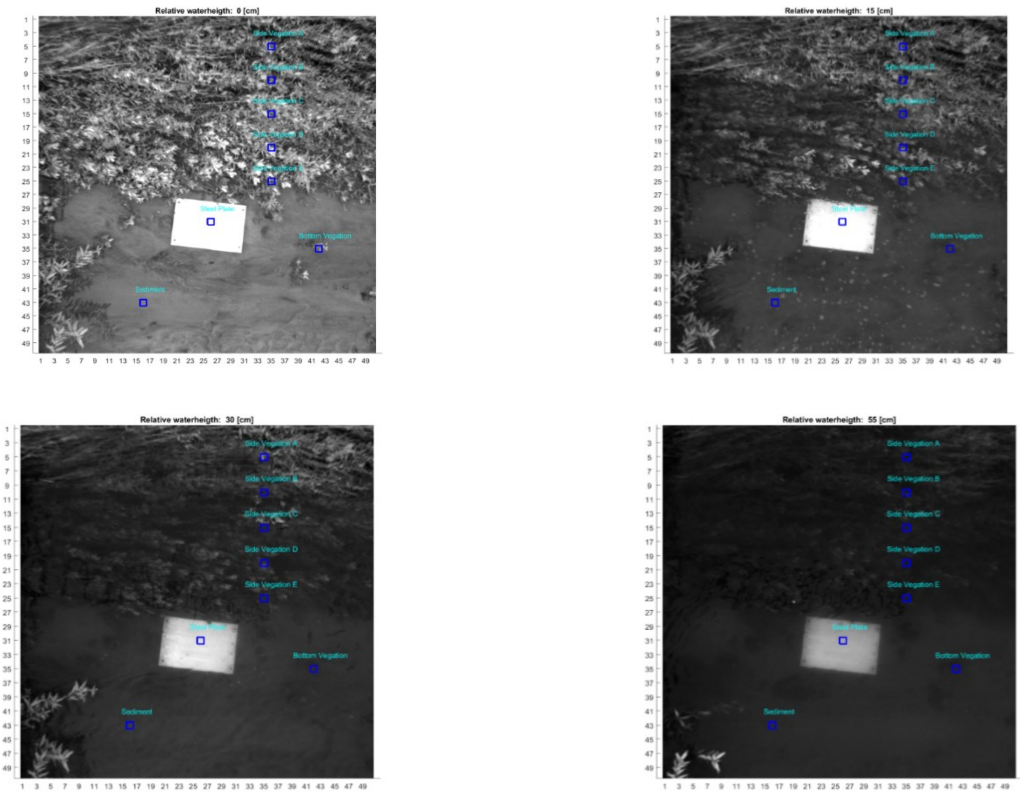

Figure 4.8. Effect of water level on black and white image 0 cm, 15 cm 30 cm and 55 cm of water level depth, with indications of the pixels used for further analyses.

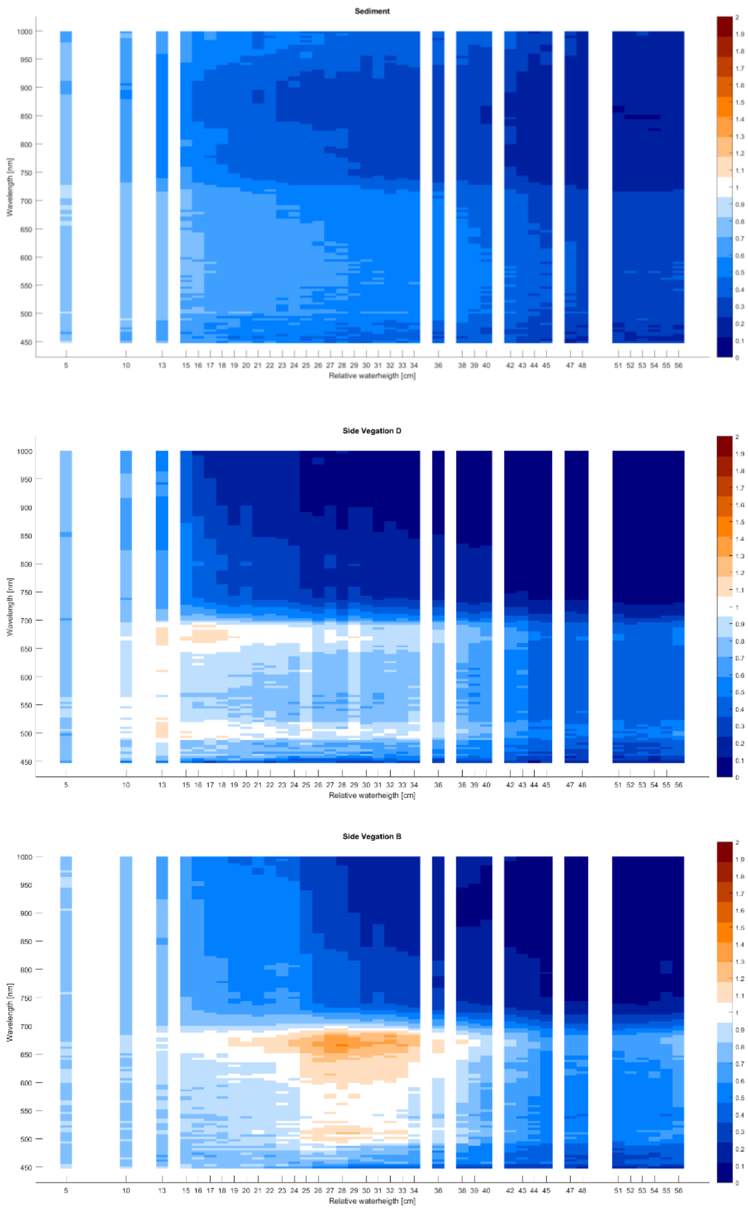

Figure 4.9. ABC, reflectance spectrum per wave length (y axis) of 3 pixels over the full amount of vegetation depths (x axis): sediment, side vegetation B (halfway up the slope) and side vegetation d (down edge of the slope).

The effect of water level on the resulting spectrum is clearly visible when comparing bare sediment and vegetation located either on de deepest part of the slope (side vegetation D) or in the middle part of the slope (side vegetation B; Figure 4.9). There is a general trend in reduction of the reflectance with increasing water depth, especially in the higher wavelengths (as can be seen specifically from the sediment pixel). The vegetation reflectance is also affected by the water, which reduces the reflectance along the full spectrum with increasing depth. The full set of pictures can be seen in Appendix D.

4.4.2 Effect of turbidity on image quality

In order to test the effects of turbidity on the image quality a set of images was taken from a fixed position while turbidity levels were varied by adding inorganic suspended load to the water (Figures 4.10 and 4.11).

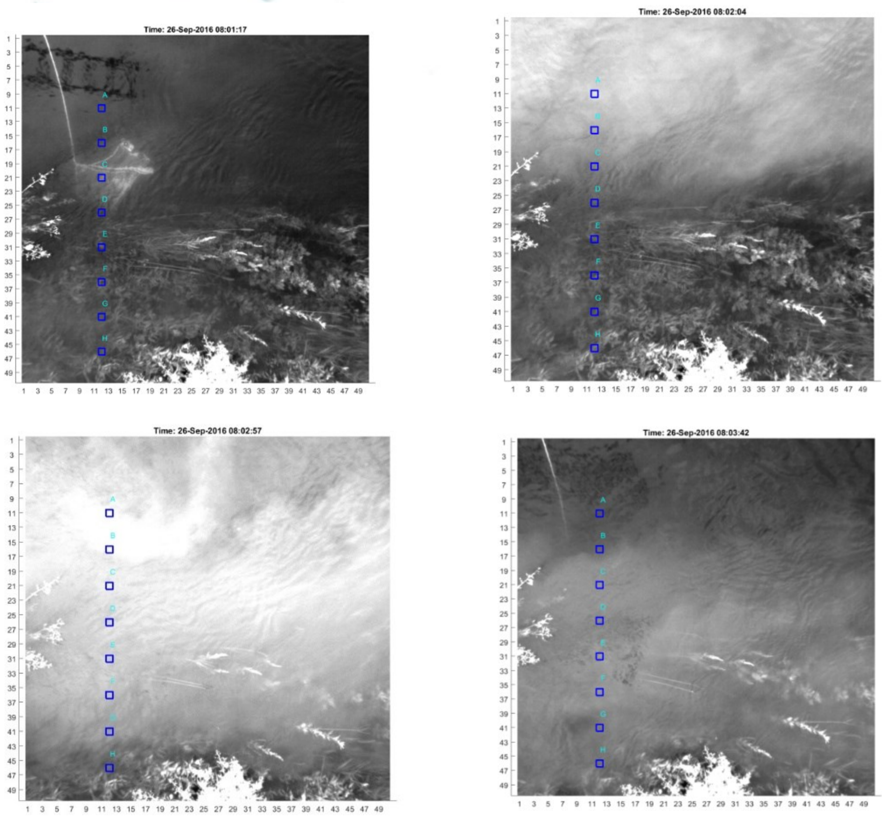

Figure 4.10. A-D4 photos of different levels of turbidity from the black and white image over time. Blue pixels a–h show the selected pixels for interpretation of the full spectrum images.

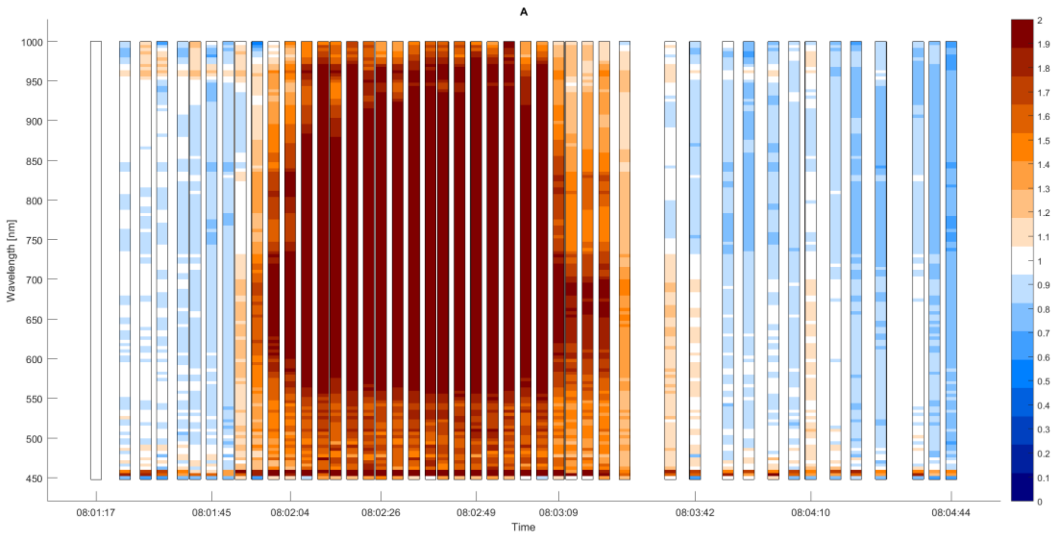
A
Wavelength [nm]
1000
950
900
850
800
750
700
650
600
550
500
450
08:01:17
08:01:45
08:02:04
08:02:26
08:02:49
08:03:09
08:03:42
08:04:10
08:04:44
Time
2
1.9
1.8
1.7
1.6
1.5
1.4
1.3
1.2
1.1
1
0.9
0.8
0.7
0.6
0.5
0.4
0.3
0.2
0.1
0

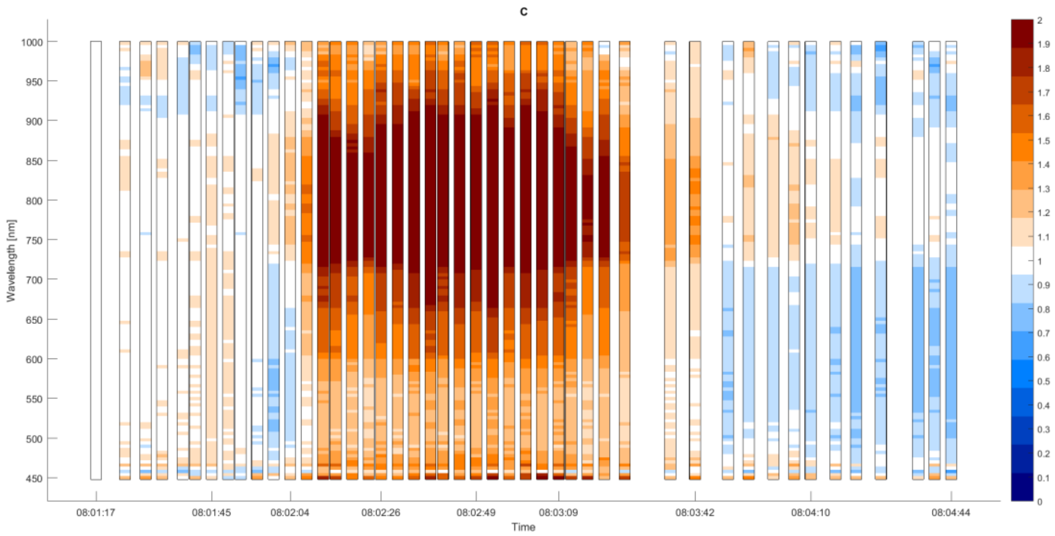
C
Wavelength [nm]
1000
950
900
850
800
750
700
650
600
550
500
450
08:01:17
08:01:45
08:02:04
08:02:26
08:02:49
08:03:09
08:03:42
08:04:10
08:04:44
Time
2
1.9
1.8
1.7
1.6
1.5
1.4
1.3
1.2
1.1
1
0.9
0.8
0.7
0.6
0.5
0.4
0.3
0.2
0.1
0

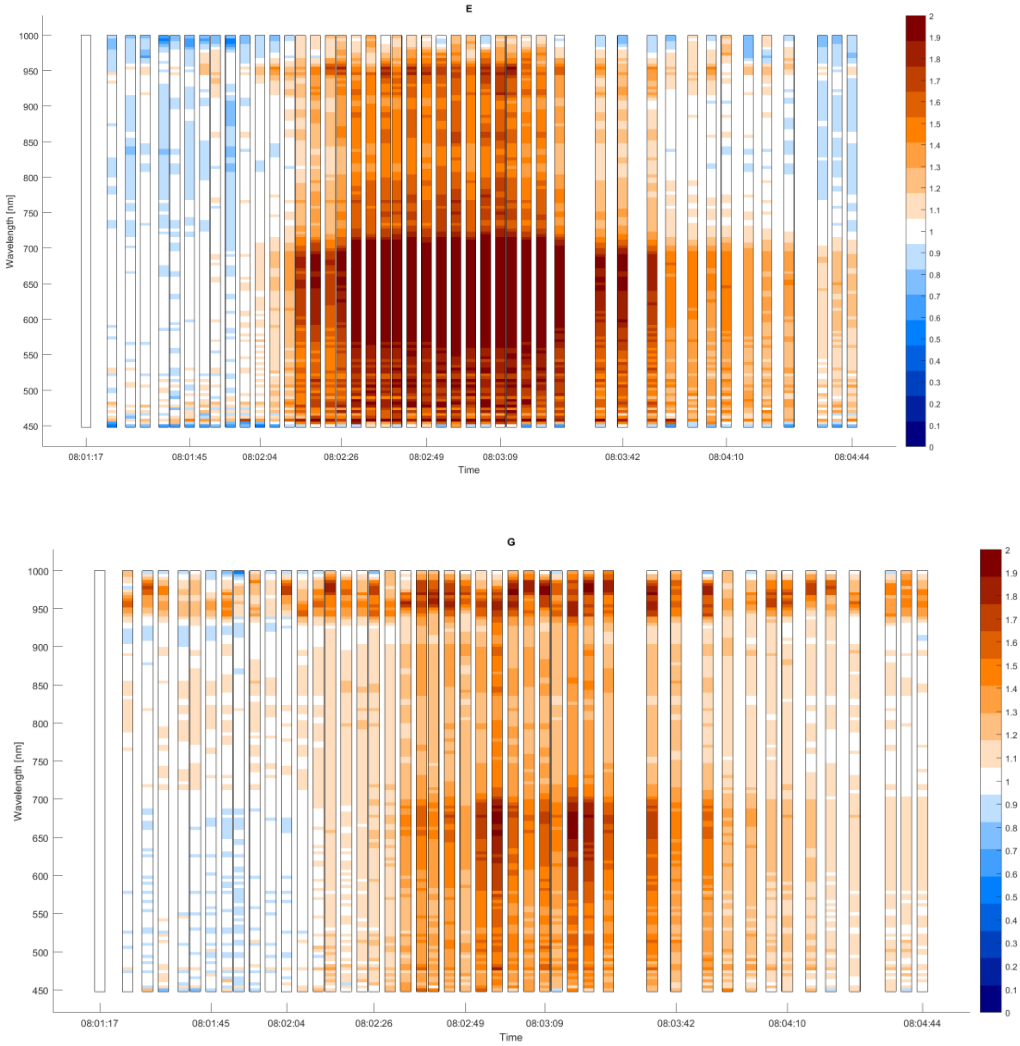

Figure 4.11. A-D turbidity effects ever time (x axis) on the reflectance spectrum of all wave lengths (y axis) for 4 different pixels from the deeper section A to the shallow near shore section G. A full set of images can be found in Appendix D.

4.4.3 Stitching full spectrum images from fixed position

Stitching the full spectrum camera images was tried for various data sets and with various software programmes. Stitching proved more difficult than expected because the images do not contain many clear reference points, comparable to images from e.g. buildings. Moving vegetation, flowing water and

3D effects cannot be fully accounted for. Also, as we have been moving the camera along the flume, the point of reference from the camera standpoint was not fixed (compared to stitching images all taken from one fixed point of reference). Most stitching software assumes the camera remains at a fixed point. The Hugin software is able to deal with moving cameras to some extent.

The software package Pix4D can make a real 3D visualization of your stitching and was designed for 3D images of buildings with xyz-data. Pix4D assumes that static objects can be behind each other. However, moving vegetation makes it very complicated to stitch images in Pix4D.

During the Linge case it was discovered that there is a time lag in the Cubert camera between taking the black and white image and the full spectrum image. With the camera mounted on the sailing boat, the time difference between the black and white image and the full spectrum image appeared too large to accurately correlate the images. Therefore it was not possible for that case to stitch the black and white images and to relate them to the full spectrum images.

Similarly the initial images from the Lage Raam were taken very close to the water surface, on a boat. These images were also taken too close to the surface to stitch. Individual images taken from a bridge under an angle were able to give more information from different vegetation species reflection, yet the angle was skewing this information (see paragraph 4.3.1). Only the KICT-REC images were taken from a sufficiently high and fixed position to allow proper stitching. This was carried out with both the Pix4D and the Hugin software (Figure 4.12).

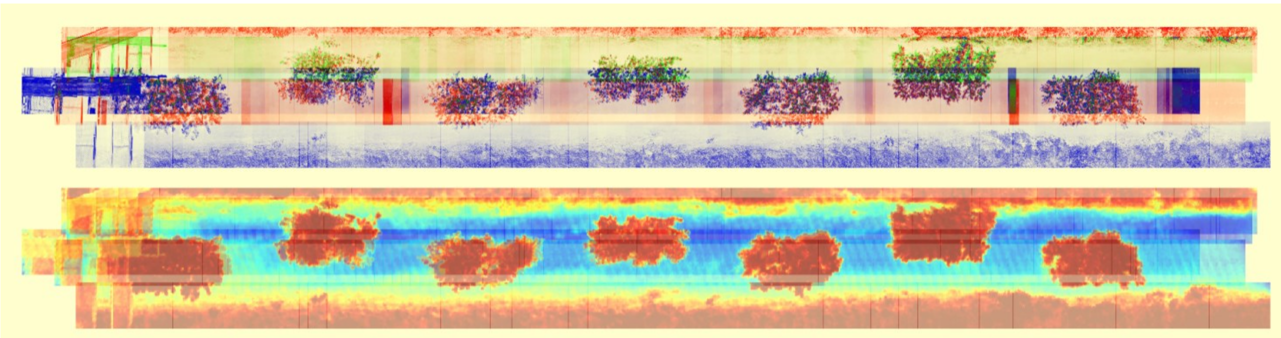

Figure 4.12. Stitching the images taken from the fixed ladder position for both black and white images and the NDVI-version of the images using the Hugin software.

In the ladder configuration we shifted the camera manually, and in a controlled manner. For the stitching only the center of a photo was used and not the edges to avoid 3D-effects.

For the Lage Raam data it appeared the camera is not easily positioned in a fully controlled manner and not always facing the exact same position as a focal point. The practical solution to avoid stitching problems is to have a bigger distance to the surface water, but this results in a lower resolution. Fortunately, for the cases that the camera is intended to be used (e.g. small streams with vegetation), the 50*50 pixel resolution in the spectral cube is more than enough on the drone height. More pixels would look nicer, but will not result in more information.

The main conclusion of stitching of images from a fixed position is that moving objects with diffuse colours such as vegetation make it difficult to use Pix4d, (despite good experiences in other projects) and panoramic stitching (e.g. with Hugin) works easier. By giving (fake) coordinates per image relative to the other images, the ladder images could be stitched. We recommend to apply all spectrum analyses at individual images, that are stitched afterwards for the full spatial overview. dGPS info of the drone can be partially used for giving coordinates, but it needs to be taken into account that the camera position is not exactly the same as the drone position.

4.4.4 Stitching drone – full spectrum images for REC set-up

The REC-drone images were easily and quickly (few hours) stitched using an automated stitching procedure in the Hugin panorama software (Figure 4.13). Because this programme is not georeferencing the images, the channel is not straight after stitching. Being at a higher position, the stitching of drone images is easier than the stitching of the ladder images (manual input required a few days extra work). The more pronounced differences/contrast of the drone images helped for easy stitching. The ladder photos do not have enough contrast for easy stitching, especially of water surfaces stitching.

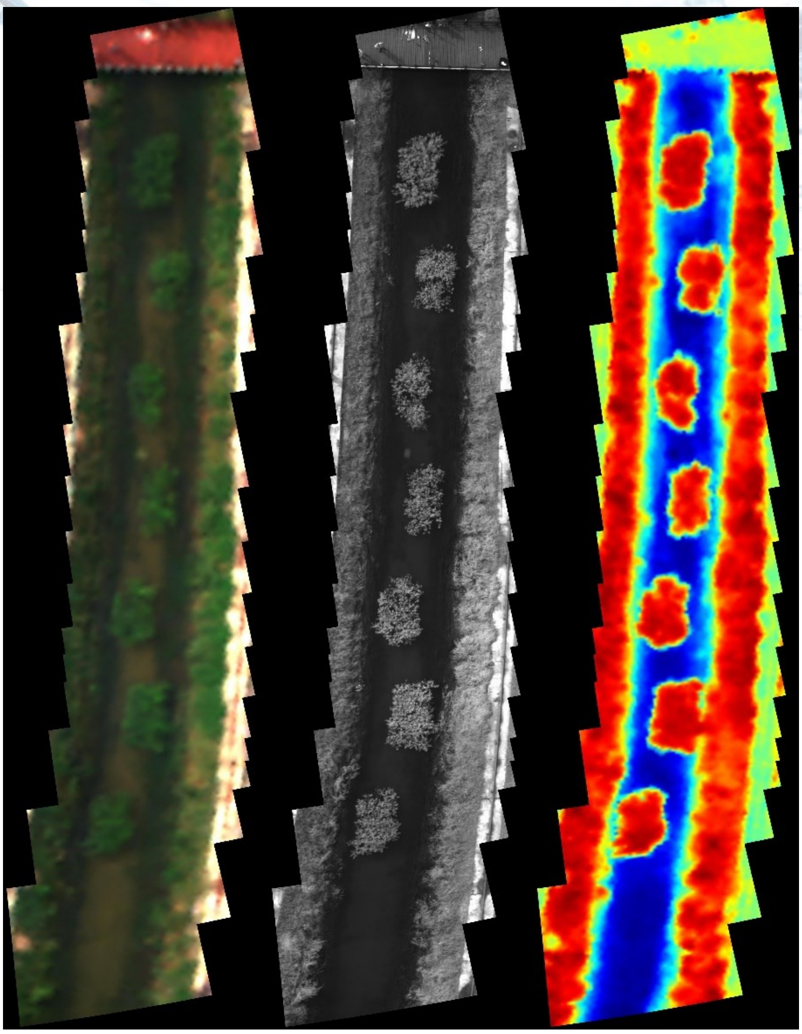

Figure 4.13. Stitched images from drone flight at REC over A1 channel patches setup Left: RGB = pseudo colour image made from spectral reflectance cube (50x50 base resolution), Middle: GRAY = grey scale image (1000x1000 base resolution). Right: NDVI =NDVI calculated from spectral reflectance cube (50x50 base resolution).

The drone images acquired at the REC were the only images that Pix4D could use to generate a 3D model. Some results are presented in Figure 4.14.

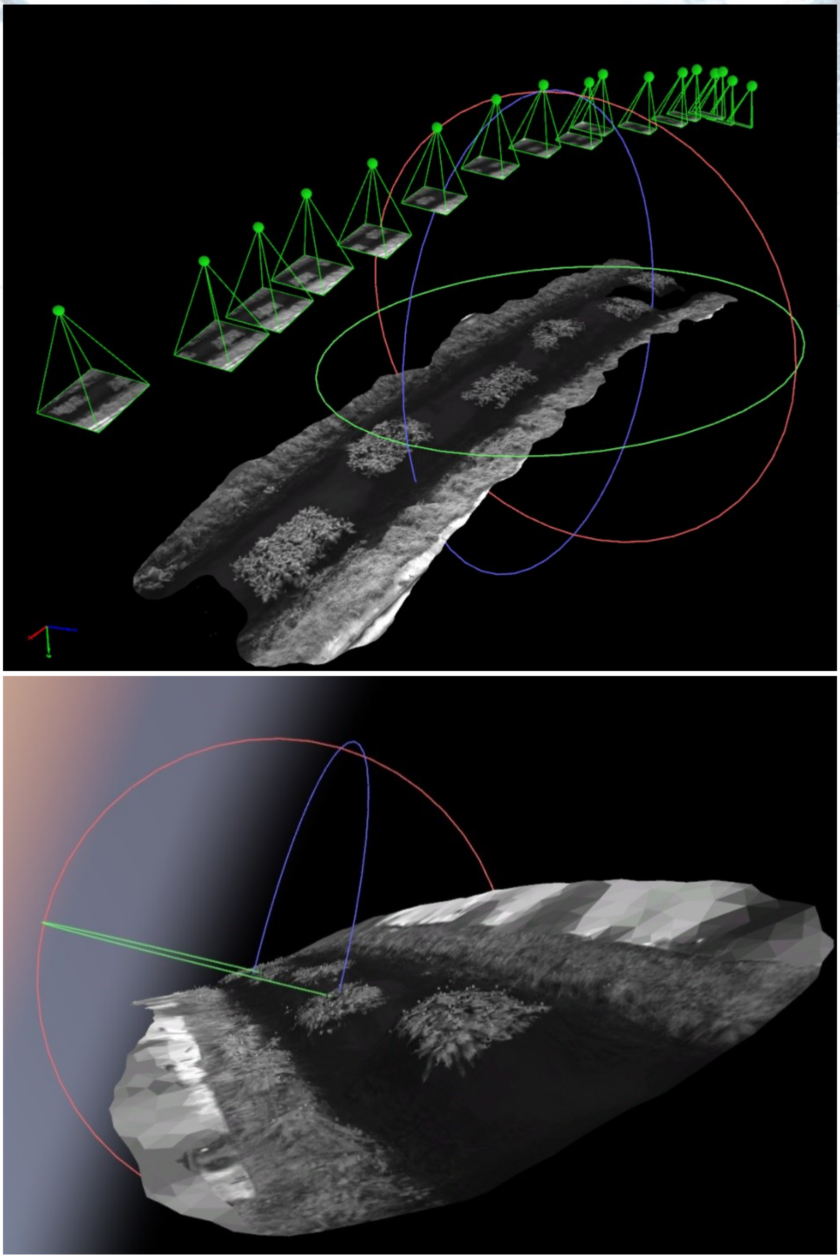

Figure 4.14. Two examples of Pix4D results for a 3D model of the UAV images @REC.

5 TRANSLATION OF DATA TO INFORMATION

5.1 SPECTRAL INDICES FOR BIOMASS

In order to assess the effect of vegetation biomass on roughness, a series of steps is taken to translate the vegetation information in the field from both the full spectrum camera and the samples taken from the most prominent plant species to a model input such as a 3D or 1D roughness.

The NDVI and additional used indices can be related to measured biomass. For the drone data we corrected this in the field. The drone started from a white plate and was corrected for incoming light.

After normalizing the raw spectrum data, NDVI and other clustering algorithms can be applied. The spectral images can be processed individually, which gives results as presented in Figure 5.1: a pseudo-colour image based on RGB colour bands, or individual spectrum lines (e.g. the red image line below). Also, Cubert software allows for some automated calculations of common indices such as the NDVI index (bottom right).

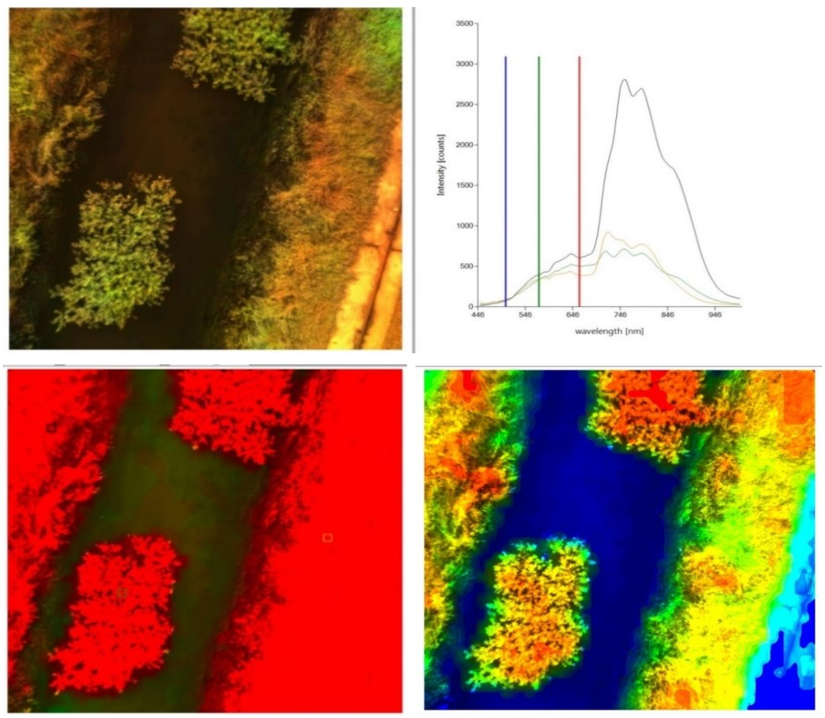

Figure 5.1. Pseudo full colour image from one UAV picture, a spectral image of the picture for 1 nm band and the resulting NDVI index.

Various types of indices can be used to assess the type and amount of vegetation present in the picture. These indices result in a series of different pictures. Different types of vegetation indices were selected from literature. From these, the indices that best related to the measured biomass were selected for our research (Table 5.1 and Figure 5.2 – images A to P).

Table 5.1: Tested indices (source: Mitchell et al., 2015).

Index	Formulation (R = reflectance, wavelengths in nm)	Reference
Normalized difference vegetation index	$NDVI = (R_{NIR} - R_{Red}) / (R_{NIR} + R_{Red})$	Rouse, Haas, Schell, and Deering (1973)
Green normalized difference vegetation index	$GNDVI = (R_{NIR} - R_{GREEN}) / (R_{NIR} + R_{GREEN})$	Gitelson and Merzlyak (1996)
Red edge normalized vegetation index	$NDVI_{705} = (R_{750} - R_{705}) / (R_{750} + R_{705})$	Gitelson and Merzlyak (1994)
Simple ratio index	$SRI = R_{NIR} / R_{RED}$	Tucker (1979)
Enhanced vegetation index	$EVI = 2.5(R_{NIR} - R_{RED}) / (R_{NIR}^{6} R_{RED}^{-1.5} R_{BLUE})$	Huete, Liu, Batchily, and van Leeuwen (1997)
Red edge position index	REPI = Maximum value[a] from 690 to 740 nm region	Curran, Windham, and Gholz (1995)
Normalized difference lignin index	$NDLI = (\log R_{1510} - \log R_{1680}) / (\log R_{1510} + \log R_{1680})$	Serrano, Penuelas, and Ustin (2002)
The plant senescence reflectance index	$PSRI = (R_{680} - R_{500}) / R_{750}$	Merzlyak, Gitelson, Chivkunova, and Rakitin (1999)
Water band index	$WBI = R_{900} / R_{970}$	Peñuelas, Pinol, Ogaya, and Filella (1997)
Normalized difference infrared index	$NDII = (R_{819} - R_{1649}) / (R_{819} + B_{1649})$	Hardisky, Klemas, and Smart (1983)
Moisture stress index	$MSI = R_{1599} / R_{819}$	Hunt and Rock (1989); Ceccato, Flasse, Tarantola, Jacquemoud, and Gregoire (2001)
Vogelmann red edge index 1	$VOG1 = R_{740} / R_{720}$	Vogelmann et al. (1993)
Vogelmann red edge index 2	$VOG2 = (R_{734} - R_{747}) / (R_{715} - R_{726})$	Vogelmann et al. (1993)
Vogelmann red edge index 3	$VOG3 = (R_{734} - R_{747}) / (R_{715} - R_{720})$	Vogelmann et al. (1993)
Red green ratio	$RG\ ratio = R_{RED} / R_{GREEN}$	Gamon and Surfus (1999)
Photochemical reflectance index	$PRI = (R_{531} - R_{570}) / (R_{531} + R_{570})$	Gamon, Serrano, and Surfus (1997)
Sum green index	SGI = normalized mean reflectance from 500 to 600 nm	Lobell and Asner (2003)
Carotenoid reflectance index 1	$CRI1 = (1/R_{510}) - (1/R_{550})$	Gitelson, Zur, Chivkunova, and Merzlyak (2002)
Carotenoid reflectance index 2	$CRI2 = (1/R_{510}) - (1/R_{700})$	Gitelson et al. (2002)
Anthocyanin reflectance index 1	$ARI1 = (1/R_{550}) - (1/R_{700})$	Gitelson, Merzlyak, and Chivkunova (2001)
Anthocyanin reflectance index 2	$ARI2 = (800^{a}(1/R_{510}) - (1/R_{700})$	Gitelson et al. (2001)

[a] Derivative reflectance (Dixit & Ram, 1985).

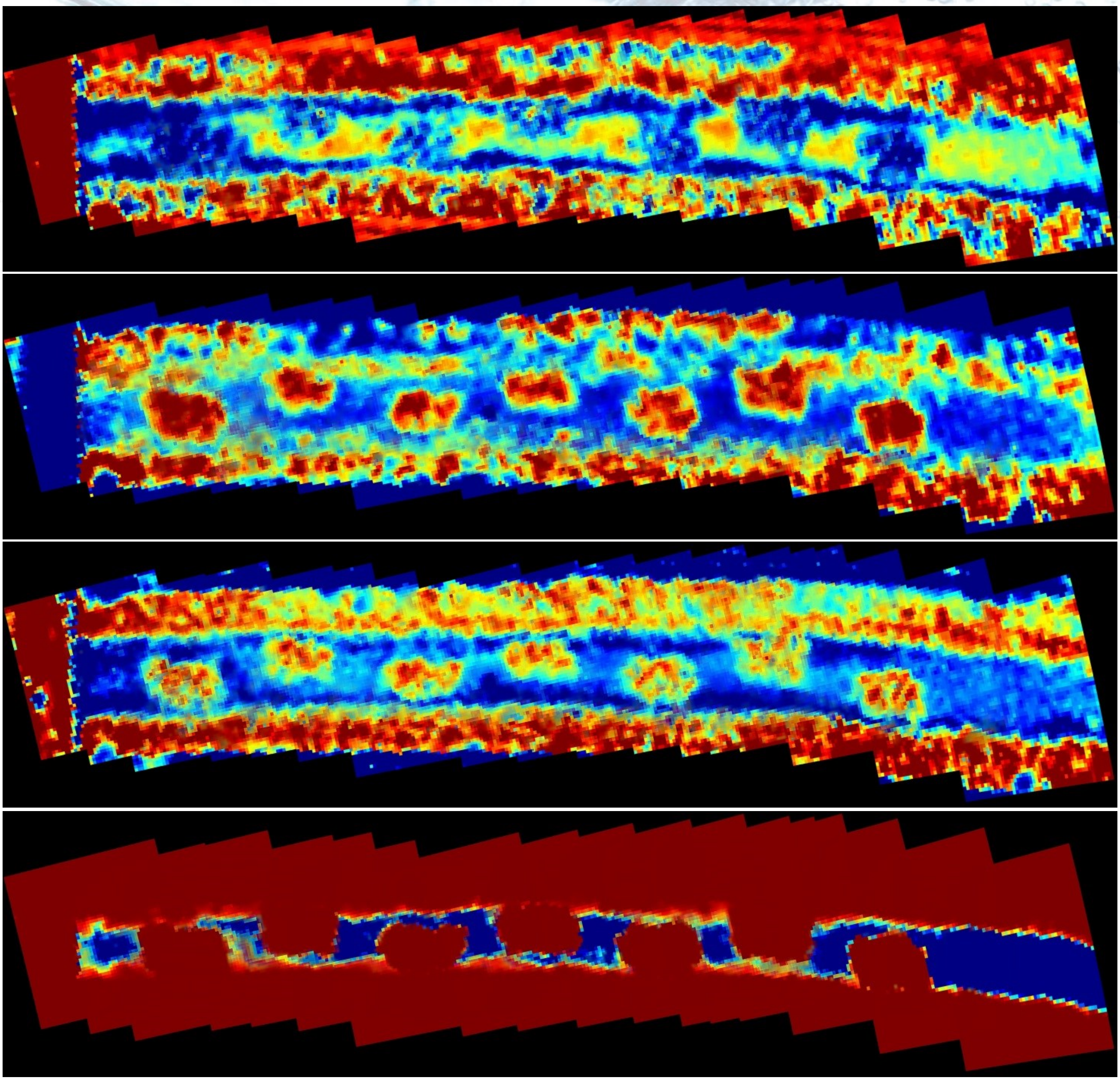

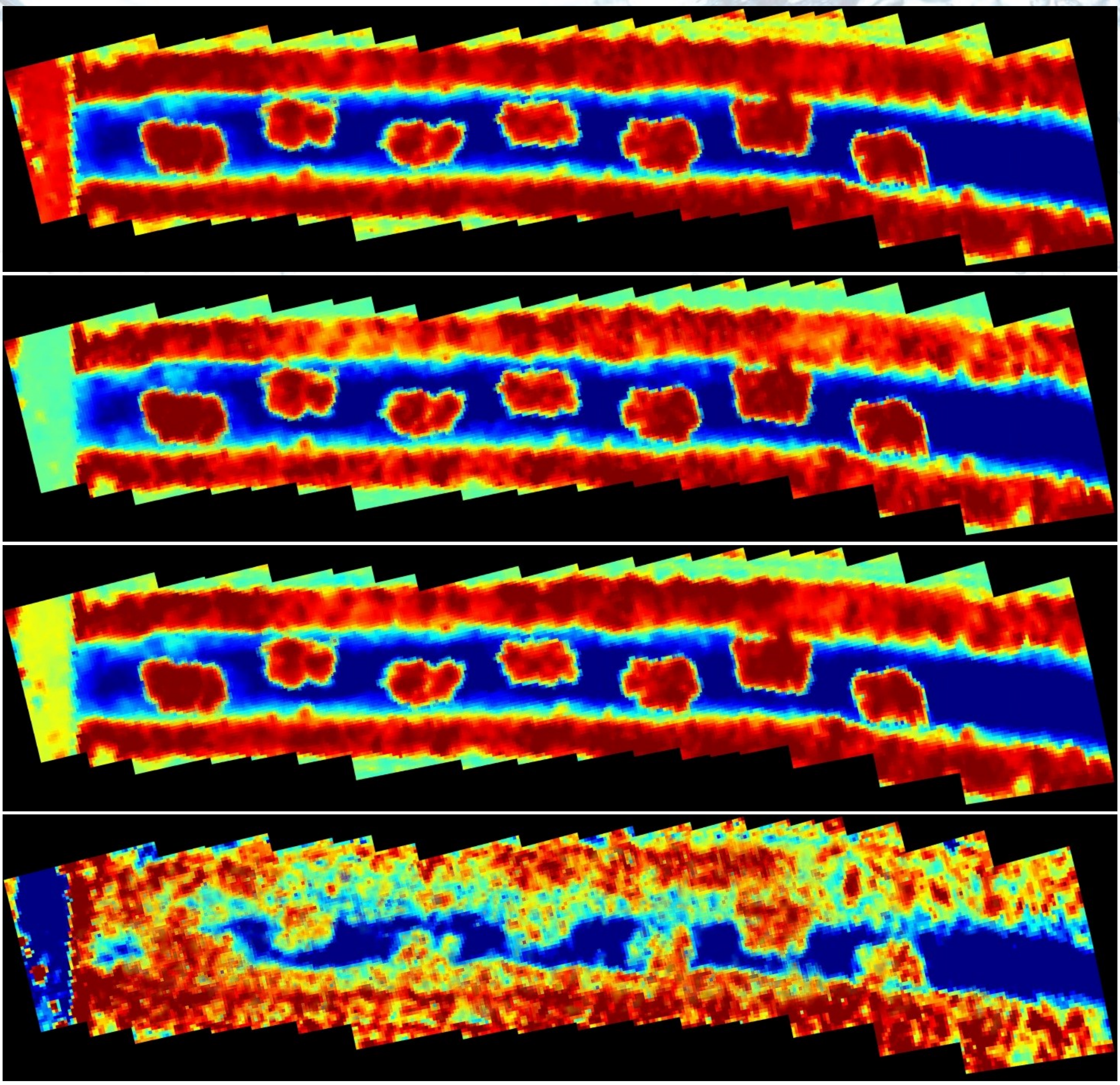

Advies, Innovatie en Verbinding in Water

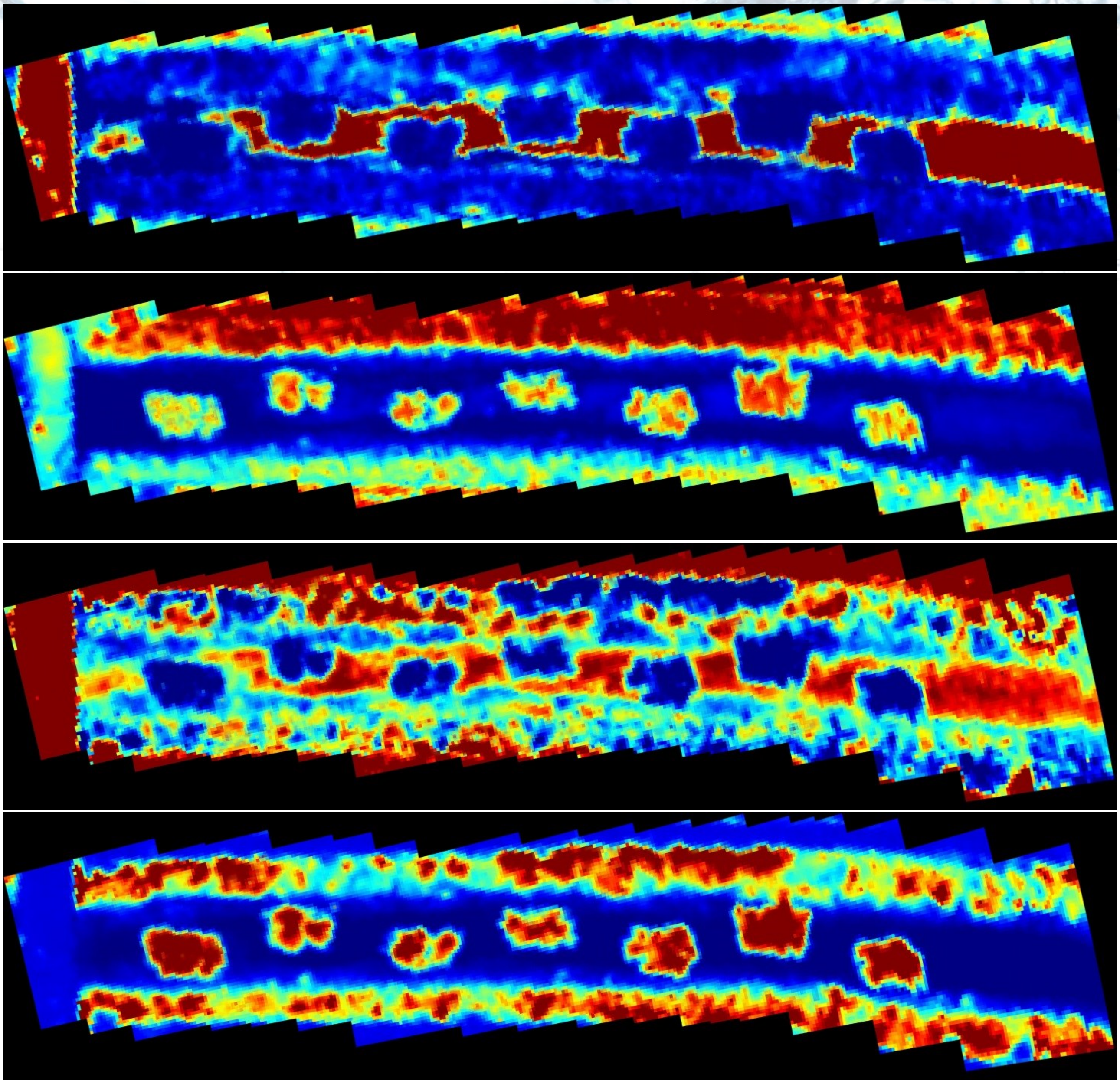

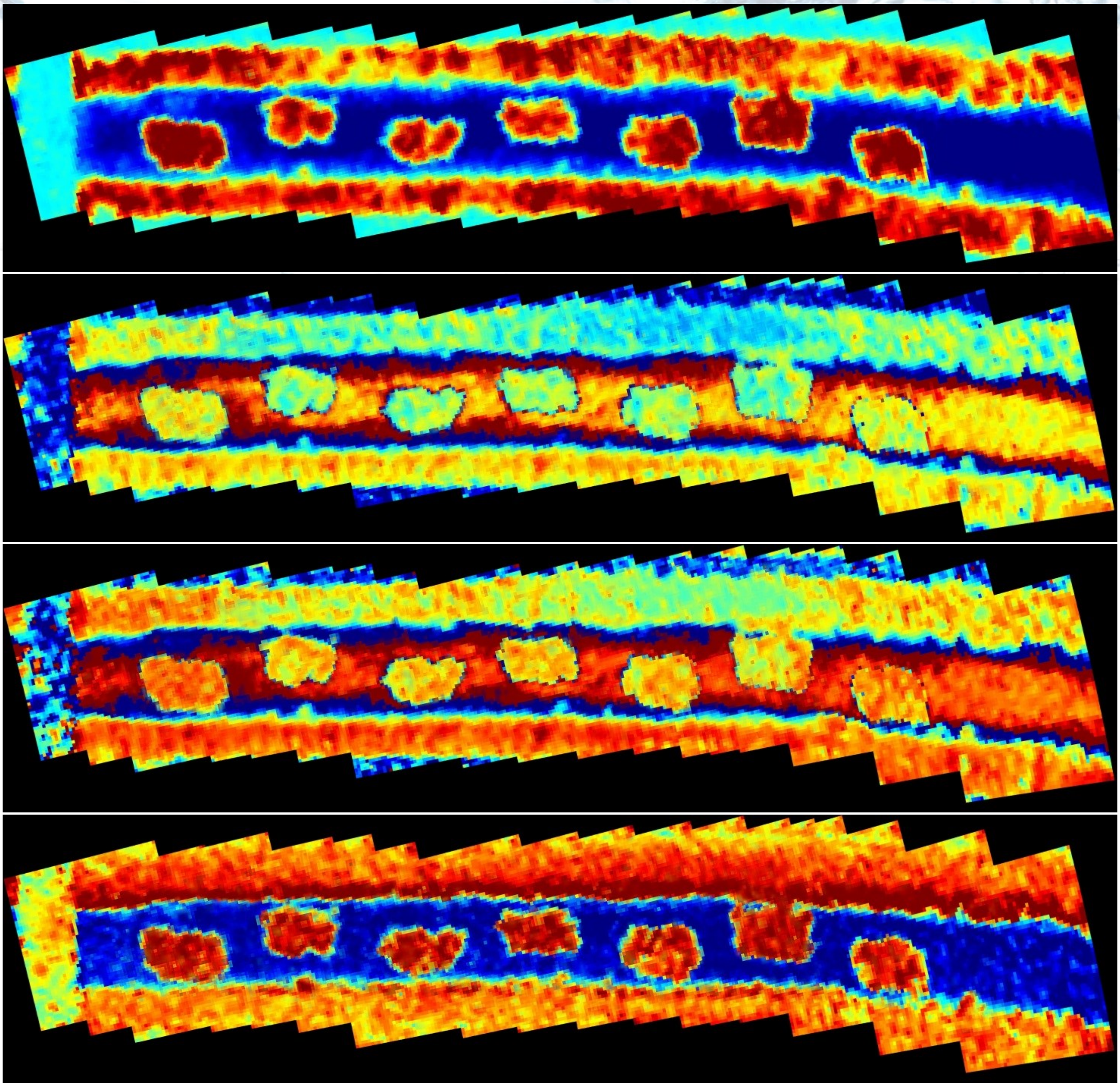

Figure 5.2 (images A-P). Calculated indices (16) ARI1, CRI1, CRI2, EVI (A-D), GNDVI, NDVI705, NDVI, PRI (E-H), PSRI, REPI, RGratio, SRI (I-L), VOG1, VOG2, VOG3, WBI (M-P).

Response of these indices on changes in water level and turbidity were assessed (all results are included in Appendix D). It was observed that some indices respond stronger to these changes than others. In Figure 5.3 (three images) a clear difference was observed between the vegetation and the group of pixels representing 'steel plate, bottom vegetation and sand', with the GNDVI decreasing for both groups with an increasing water level, and the PSRI increasing with an increasing water level, while the ARI1 did not make a good distinction between the vegetation and other materials nor responded well to changes in water level.

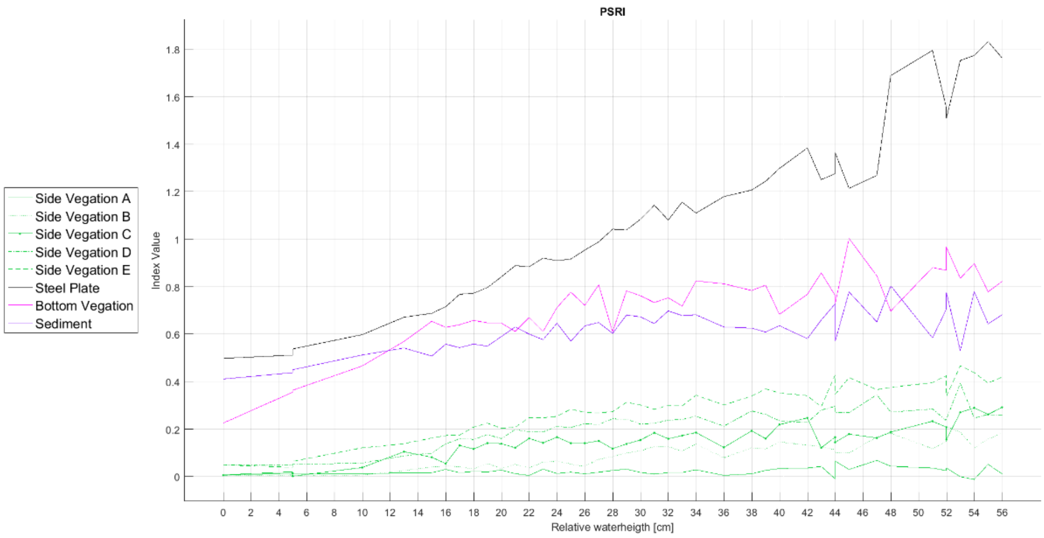

Figure 5.3. Response of different indices to changes in water level.

For the response of these indices to changes in turbidity it was also observed that different indices respond in different manners with the GNDVI, showing a very strong response in the increased turbidity for the deeper sections, but not for the shallow sections, where the signal remained more or less constant, while the WBI index did not give a clear change in signal with an increasing turbidity (Figure 5.4, two images).

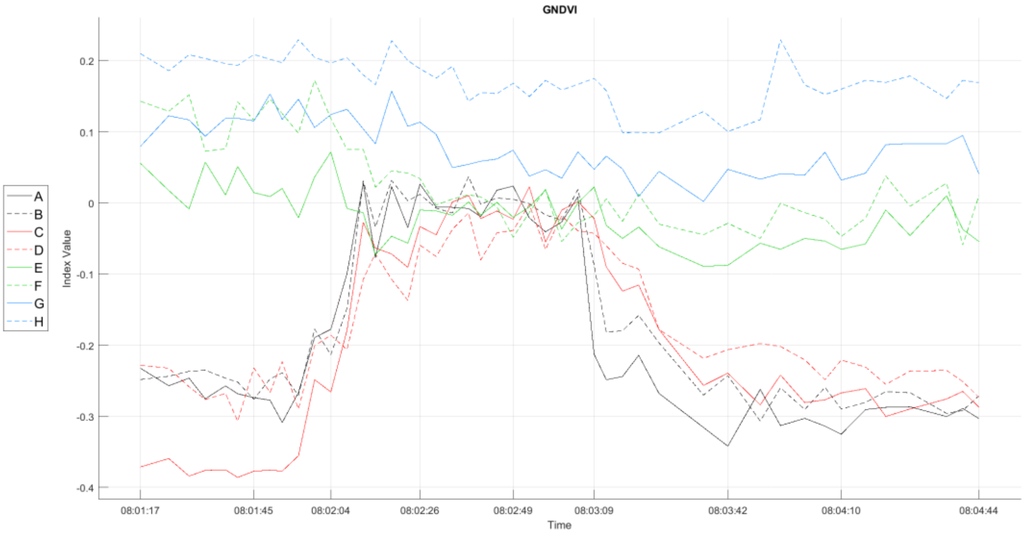

Figure 5.4. Response of different indices to changes in turbidity.

During the turbidity experiment, measurements were taken of the changes in suspended sediment concentration and light attenuation changes. As expected, there is a clear relation between the light attenuation and suspended sediment concentrations (Figure 5.5). The timing of the photos can thus be related to the timing of the suspended load sampling, in order to link the visual image results to the suspended loads. This way, we can define a maximum suspended load where the image is still sufficiently representing the submersed vegetation, based on a comparison of different indices.

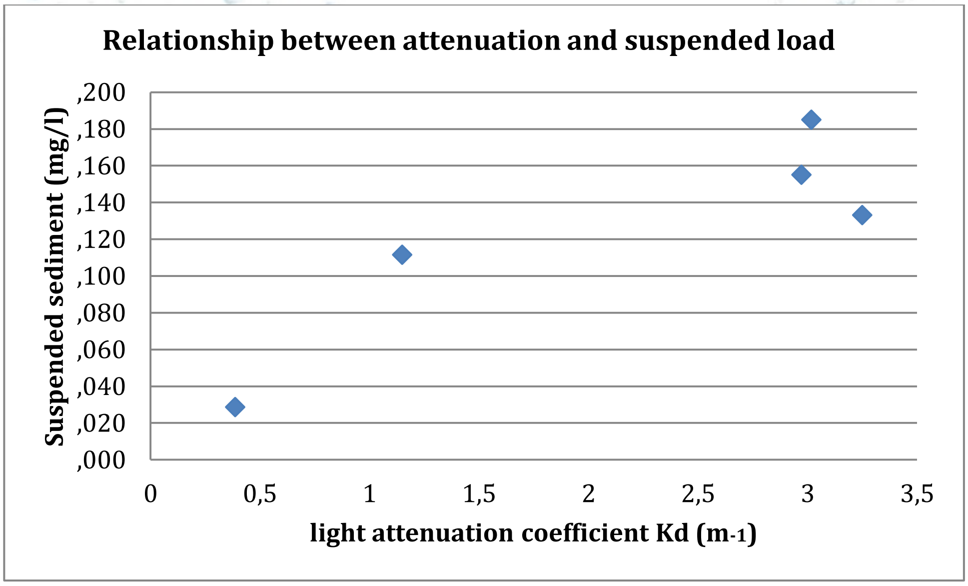

Figure 5.5. Relation between light attenuation and suspended sediments during turbidity testing @REC.

5.1.1 Image Clustering

Clustering the images also shows promising results, but this has not yet been furthered beyond a few first trials with 5 different classes (Figure 5.6).

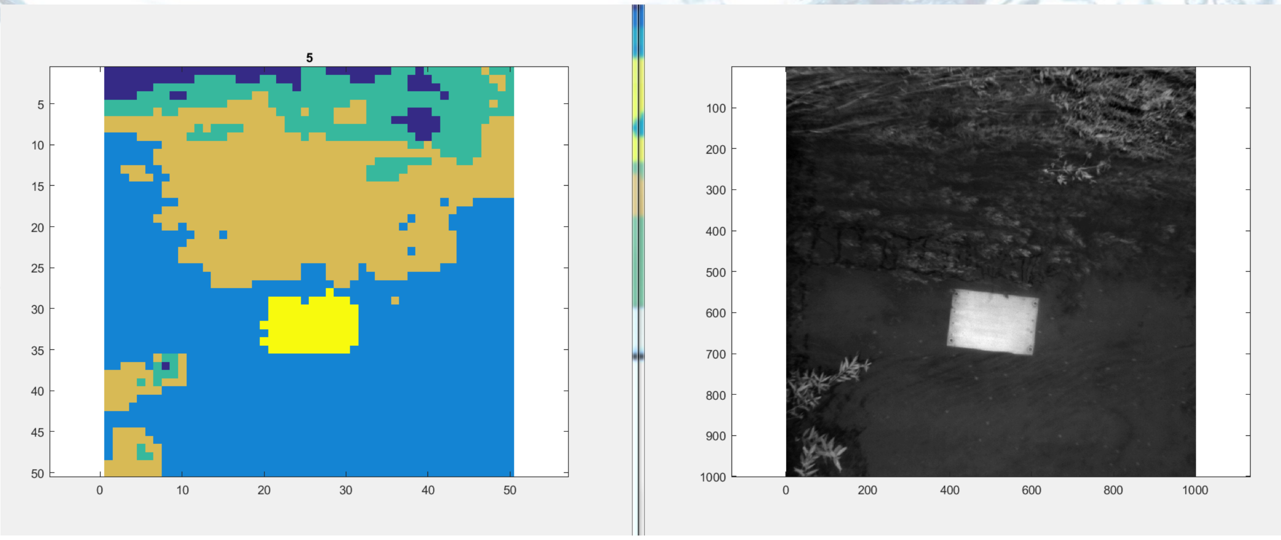

Figure 5.6. Clustering in five classes of one image at the REC/Korea.

5.2 VEGETATION ANALYSIS IN THE LAGE RAAM

Vegetation samples were taken at the Lage Raam at location 1 and 2 during the September 15, 2016 visit and at location 2 and 3 during the November 15, 2016 visit. Biomass was weighed, both for wet and dry biomass, and parameters relevant for modelling were measured (Tables 5.2 and 5.3). By determining the percentage dry biomass we can estimate a measure for the stiffness of the plants, and relate this to an estimated drag coefficient Cd for the biomechanical properties (Table 5.4). It also indicates how well the plant will bend under higher flow conditions. In general the biomasses collected in November were higher than in September for all species. Despite that we expected that in November biomass might have decreased for almost all species this was not the case. It should be noted that at location 1 the *P. natans* was reducing in biomass due to decomposition, and that the remaining biomass of that was getting very brown. Given that we did not sample for flow nor camera images at location 1, this species was not sampled during the field visit of November 2016.

From this analysis we concluded that *Callitriche platycarpa* represents the highest biomass per m^2, with a maximum of more than 7 kg/m^2 when covering the full water column in September, and approx. 14 kg in the November visit. This species at the same time has the lowest % dry biomass, making it more flexible. However, if the total wet biomass becomes very high, the ability of the species to bend becomes less due to the restrictions in bending based on the excessive presence of biomass in general.

Also the emergent shoreline species *Glyceria maxima* and *Typha latifolia* have a high biomass per m^2. (*Typha latifolia* was only sampled at location 3 in November). These species specifically have a strong submersed root system that fills the full water column with rigid stems and catches a lot of sediments in between these stems. As a result the water column at the location of the *G. maxima* can be considered fully obstructed (see also the flow analysis section) and that of *T. latifolia* also is relatively strongly obstructed. Given its high % dry biomass and related strong rigidity it has a high estimated drag force coefficient.

Sparganium erectum is another dominant shoreline plant in location 2, also colonizing shallow parts of the middle section of the stream. Its biomechanical properties are comparable with *G. maxima*. It is also often intermingling with this species.

The floating aquatic species *Potamogeton natans* was covering the full width of the open water area in location 1. However, the total biomass was low, and also the low drag coefficient makes that this plant appears to be the least obstructing of the three dominant species.

Table 5.2. Biomass of the dominant species present in the Lage Raam on September 15, 2016.

		Species name	Dutch name	Sample wet biomass (g)	total wet biomass (g /m²)	total dry weights (g/m²)	% dry mass
1		*Potamogeton natans*	Drijvend fonteinkruid	363	1210	105	29
1		*Callitriche platycarpa*	Gewoon sterrenkroos	1118	3727	152	14
1	submersed parts	*Glyceria maxima*	Liesgras	1406	4687	446	32
	emersed parts	*Glyceria maxima*	Liesgras	563	1877	240	43
2	total	*Glyceria maxima*	Liesgras	1427	4757	261	18
2		*Sparganium erectum*	Grote egelskop	1320	4400	349	26
2	full water column covered	*Callitriche platycarpa*	Gewoon sterrenkroos	2167	7223	354	16
2	half water column covered	*Callitriche platycarpa*	Gewoon sterrenkroos	598	1993	54	9

Table 5.3. Biomass of the dominant species present in the Lage Raam November 15, 2016 visit.

Location	depth	mud layer	Dutch name		Sample wet biomass (g)	total wet biomass (g /m²)	total dry weight (g/m²)	% dry mass
2	0.9		liesgras	layer 1 (from bottom - submersed)	2281	7603	333	15
			liesgras	layer 2 -emergent	821	2737	303	37
2	0.7		egelskop	layer 1 (from bottom - submersed)	2102	7007	676	32
			egelskop	layer 2 -emergent	200	667	46	23
2	0.65	0.2	sterrekroos	layer 1 (from bottom - submersed)	1450	4833	108	7
2	1.2	0.6	liesgras	layer 1 (from bottom - submersed)	2714	9047	564	21
			liesgras	layer 2 -emergent	1100	3667	584	53
3	0.8	0.4	sterrekroos	layer 1 (from bottom - submersed)	4098	13660	348	8
			sterrekroos	roots	2310	7700	861	37
3	0.75	0.4	liesgras	layer 1 (from bottom - submersed)	4332	14440	1217	28
			liesgras	layer 2 -emergent	833	2777	266	32
3	0.75	0.3	lisdodde	layer 1 (from bottom - submersed)	3236	10787	539	17
			lisdodde	layer 2 -emergent	899	2997	338	38

Table 5.4a. Biomechanical properties of dominant plants at Lage Raam and estimated Cd during the September 15, 2016 visit.

location	**water depth (m)**	**species name**		**length (m)**	**average diameter (m)**	**nr of stems/m²**	**d*#**	**Cd estimate**	**d*#*Cd**
1	0.65	*Potamogeton natans*	layer 1 (from bottom)	0.5	0.0021	303	0.62	0.40	0.25
			layer 2	0.8	0.0024	187	0.44	0.40	0.18
			layer 3 - leaves properties						
1	0.45	*Callitriche platycarpa*	layer 1 (from bottom)	0.5	0.0007	1947	1.40	0.30	0.42
1	0.4	*Glyceria maxima*	layer 1 submersed	0.2	0.0094	86	0.81	1.00	0.81
			layer 2 emergent stems	0.55	0.0063	225	1.43	0.80	**1.14**
			layer 2 emergent leaves	0.55	0.0115	185	2.13	0.80	**1.70**
2	0.8	*Sparganium erectum*	layer 1 (from bottom)	0.6	0.0112	247	2.75	1.00	**2.75**
			layer 2 - emergent	1.1	0.0161	200	3.22	0.80	**2.58**
2	0.81	*Callitriche platycarpa*	layer 1 (up to half way the water column)	0.6	0.0007	1233	0.91	0.30	0.27
2	0.99	*Callitriche platycarpa*	layer 1 full water column	0.9	0.0008	5000	3.79	0.30	1.14
2	0.8	*Glyceria maxima*	layer 1	0.6	0.0091	300	2.73	1.00	**2.73**
			layer 2	0.7	0.0126	563	7.09	0.80	**5.67**

Table 5.4b. Biomechanical properties of dominant plants at Lage Raam and estimated Cd during the November, 2016 visit.

location	water depth	mud	common name	layer	length (m)	average diameter (m)	nr of stems/m^2	d*#	Cd estimate	d*#* Cd
2	0.9		liesgras	layer 1 (from bottom - submersed)	0.6	0.01000	47.0	0.470	1	0.47
				layer 2 -emergent	0.6	0.01795	76.7	1.376	0.8	1.10
2	0.7		egelskop	layer 1 (from bottom - submersed)	0.7	0.02190	23.3	0.511	1	0.51
				layer 2 -emergent	0.4	0.02300	45.0	1.035	0.8	0.83
2	0.65	0.2	sterrekroos	layer 1 (from bottom - submersed)	0.65	0.00090	283.3	0.255	0.3	0.08
2	1.2	0.6	liesgras	layer 1 (from bottom - submersed)	0.6	0.00920	41.7	0.383	1	0.38
				layer 2 -emergent	0.7	0.01580	75.0	1.185	0.8	0.95
3	0.8	0.4	sterrekroos	layer 1 (from bottom - submersed)	0.8	0.00125	385.0	0.481	0.3	0.14
3	0.75	0.4	liesgras	layer 1 (from bottom - submersed)	0.8	0.00840	65.0	0.546	1	0.55
				layer 2 -emergent	0.5	0.01565	83.3	1.304	0.8	1.04
3	0.75	0.3	lisdodde	layer 1 (from bottom - submersed)	0.75	0.05710	3.3	0.190	1	0.19
				layer 2 -emergent	1.5	0.03510	3.3	0.117	0.8	0.09

5.3 VEGETATION ANALYSIS IN THE REC

Samples were taken to quantify the vegetation in the A1 channel at various locations. Removing the organic material from five different locations with a size of 50 by 50 cm made it possible to get some more understanding of the type and characteristics of the vegetation.

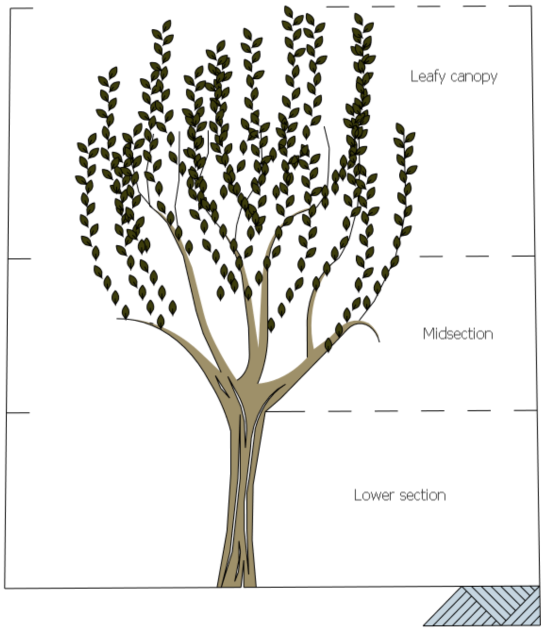

Figure 5.7: Dividing the vegetation into different layers

Location 1 and 2 were both situated within the willow vegetation patches. Location 1 was taken in a representative part of the most upstream patch of sparse willows. For location 2 a representative part of the most downstream dense patch of willows was chosen. The willows were then roughly divided into three different layers (in accordance with Figure 5.7) and analysed.

The willows could not be removed from the soil to conduct a full analysis because that would influence future research. Only the top layer could be removed and completely analysed and therefore some of the information in the table is missing.

Table 5.5. Vegetation analysis of vegetation patches in the A1 channel, carried out on September 28, 2016.

	Location: 1 (Willows) (sparse)			Location: 2 (Willows) (dense)		
	Lower section	Midsection	Leafy canopy	Lower section	Midsection	Leafy canopy
Height (mm)	0 - 400	400 - 800	800 - 1400	0 - 400	400 - 800	800 - 1400
Number of stems (m^{-2})	20	56	136	44	80	172
Avg. stem diameter (mm)	10.68	6.78	2.20	10.94	4.50	2.23
Number of leaves (m^{-2})	-	-	1556	-	-	1704
Avg. leaf length (mm)	-	-	81.85	-	-	58.75
Avg. leaf width (mm)	-	-	8,5	-	-	13
Wet weight $(g * m^{-2})$	-	-	232	-	-	236
Dry weight $(g * m^{-2})$	-	-	132	-	-	103
Wet volume $(l * m^{-2})$	-	-	0.33	-	-	0.19

Locations 3, 4 and 5 are each representative for different types of vegetation that surround the patches. For each location an area of 50 by 50 centimetres was chosen and all vegetation within that area was then removed. For locations 3, 4 and 5 it was not possible to divide the vegetation into multiple layers and have therefore been analysed as just one layer, the results are presented in Table . In this chapter only a summary of the measurements is shown. Full analysis of all measurement locations is presented in Laurens (2016).

Table 5.6: Vegetation analysis of vegetation surrounding the patches, carried out on September 28, 2016.

	Location: 3 (Selenge Wormwood)	Location: 4 (Carex species)	Location: 5 (Mixed vegetation)
Height (mm)	45	40	65
Effective height (mm)	25	15	30
Number of stems (m^{-2})	428	3090	1484
Avg. stem diameter (mm)	3.12	2.39	2.31
Number of leaves (m^{-2})	4922	-	-
Avg. Leaf length (mm)	46.42	-	-
Avg. Leaf width (mm)	30.25	-	-
Wet weight $(g * m^{-2})$	2012	312	2372
Dry weight $(g * m^{-2})$	558	169	522
Wet volume $(l * m^{-2})$	2.14	0.64	2.31

Flow measurements Lage Raam

Flow measurements at the Lage Raam were carried out in November 2017. See Appendix E for the detailed report (in Dutch) regarding these measurements. Table 5.7 gives an overview of the main values recorded and proved useful for further data interpretation. During the measurements the total discharge through the Lage Raam was approx. 0.8 m^3/s, with a minimum flow through the vegetation patches along the shore line. The emergent vegetation along the shores is strongly limiting the flow in these areas.

Table 5.7. Average discharge and flow (n=6) for all profiles measured in location 2 (IJzerbroekseweg) and location 3 (Kwekerijweg). Kwekerijweg profile-2 is based on point measurements and IJzerbroekse Weir is based on water depth at the weir in combination with the width of the weir.

	Total Flow [m^3/s]	Flow through center [m^3/s]	Flow in vegetation [m^3/s]	Width [m]	Area [m^2]	Min. Flow velocity [m/s]	Max. Flow Velocity [m/s]	Channel velocity [m/s]
IJzerbroekseweg-1	0.87	0.87	0.01	10.85	5.53	0.15	0.75	0.28
Ijzerbroekseweg-2	0.76	0.76	0.00	11.30	6.46	0.11	0.72	0.25
Kwekerijweg-1	0.82	0.83	0.00	12.50	5.32	0.14	0.85	0.35
Kwekerijweg-2	0.79	0.80	-0.01	11.80	5.43	0.17	0.84	0.32
Weir	0.8							

It should be noted that the flow through the open channel at location 3 (Kwekerijweg) was high enough to leave a relatively hard bed with little deposits, while in the wider location 2 thicker layers of deposited soft material were present also in the non-vegetated zones. The vegetated areas all had a layer of relatively thick mud.

5.4 WATER QUALITY MEASUREMENTS LAGE RAAM

The water quality measured in the Lage Raam during the September visit were analysed by AQUON (Table 5.8), while Secchi disk and light attenuation was measured by Deltares. The measured values for suspended sediment and chlorophyll are very low and the water was relatively clear in location 1 and 2, while both locations had comparable transparency and attenuation coefficients. As location 2 is shallower than location 1, approximately 0.7 m depth at location 2 and 1.5 m depth at location 1, the transparency using a Secchi-disk could not be quantified (bottom view). Location 3 was characterized by a strong influence of upward seepage colouring the water visually red due to the chemical composition of the seepage water, resulting also in a very low transparency and high attenuation coefficient. This section also had a higher chlorophyll and suspended sediment concentration. DOC380 indicates the humic substances in the stream and this was highest at location 3.

Table 5.8. Measurements of water quality parameters.

Location	Chlorophyll-a (µg/l)	Suspended Sed. (mg/l)	DOC380	Transparency (m)	Attenuation coefficient (m^{-1})
Location 1	3	4	0.02	0.9	2.7
Location 2	3	4	0.032	Bottom view	2.7
Location 3	8.9	13	0.042	0.15	12

It was concluded that the water colour and transparency is less important than expected, because the reflectance of water as such is very different from vegetation as a general input. Of course, also in relation with the measurements of turbidity and water depth in the REC it can be concluded that when the water is too turbid or too deep the signal of submersed vegetation is lost, given the optical nature of the signal. In relativeshallow and transparent conditions the camera is still able to receive a signal, although depending on the water column depth above the vegetation.

5.5 Relating biomass to 3D model parameters and 1D roughness

5.5.1 Hydraulic parameters

In the most simple assumption open channel flow can be described with Manning's formula:

$$Q = \frac{A}{n} R^{\frac{2}{3}} i_b^{\frac{1}{2}}$$

with discharge Q (m^3s^{-1}), slope i_b (-), hydraulic radius R (m), wetted perimeter A (m^2) and Manning's parameter *n* ($m^{1/3}s^{-1}$). Manning's parameter describes the hydraulic roughness: the resistance against flow caused by bed material, bedforms, vegetation and other objects. Specifically in vegetated channels estimating a reliable Manning's *n* is not easy. Pitlo and Griffioen (1991) developed a model for stationary, uniform flow based on above formula to predict the roughness value based on the percentage open water (i.e. 'not covered by vegetation'). With this model a linear relationship was determined that directly links the percentage open water to Manning's *n*. The benefit of this model is its simplicity in use and the valuable insights it gives for the expected effectiveness of planned mowing actions. In this model it is assumed that flow through vegetation can be adequately described by Darcy's law for flow through porous media (vegetation being this porous medium), with a specific roughness value (w) per plant species. This roughness value will change over the season and along a transect depending on the plant growth, patch density, number of leaves, local sedimentation and patch-interactions. The model does not account for non-uniformity in flow or the presence of weirs that affect water levels.

Therefore we used a simple stationary non-uniform version of this model, based on Bélanger's formula (1828). This formula can be summarized with the following equation:

$$I_h = \frac{g i_b(x) + f(x)}{g - U(x,h)}$$

in which water depth change I_h is influenced by the bed slope $i_b(x)$, friction f(x), gravitational constant g and downstream hydraulic conditions U(x, h). Because this formula describes non-uniform flow, the water depth at a given location is also affected by the downstream water level. When the downstream water level is known (e.g. from measured data at a weir) the water depth at a given location along the channel can be calculated. As for complexity this model is a bit more advanced than the 'Pitlo & Griffioen' equation, but not yet a completely non-stationary model (such as e.g. SOBEK or Delft3D). As such, it can be used for communication and rapid operational assessment.

Vegetation patches are observable units of vegetation in the channel often dominated by a single species. The density, size and biomass of a patch develops over time, and thus affect the roughness at that given location along the channel. Locally the patch creates an increased upstream water level for a given length of channel. This can be illustrated by calculating the effect of such a patch in a fictive example channel. The example channel has a length of 10 km and a slope of 1 cm/km (0,01 ‰). The channel is controlled by a downstream weir with a set water depth of 1.2 m. Discharge is a constant 0,5 m^3s^{-1}. The channel has a trapezoidal cross sectional profile with a minimum depth of 3 m. In the example the channel is lightly overgrown (Manning's n=0,03), with an exemption of a locally occurring dense patch of 100 m length. This patch blocks flow substantially more than the vegetation in the rest of the channel (Manning's *n*=0,11) and the effect of this patch is noticeable in the upstream water levels (Figure 5.8).

When we then calculate two different mowing regimes, one for mowing the full stretch of 10 km and one for only the blocking patch, we can show that the blocking patch has a disproportional large influence on the water level of the channel. This is the key principle of 'Dottering': mow only where a maximum effect is expected to balance hydraulic gains and ecological loss. Similarly we can show that there might be areas where mowing is less useful and the problems with water levels may be the result of other factors (e.g. sediment deposition or a too narrow channel).

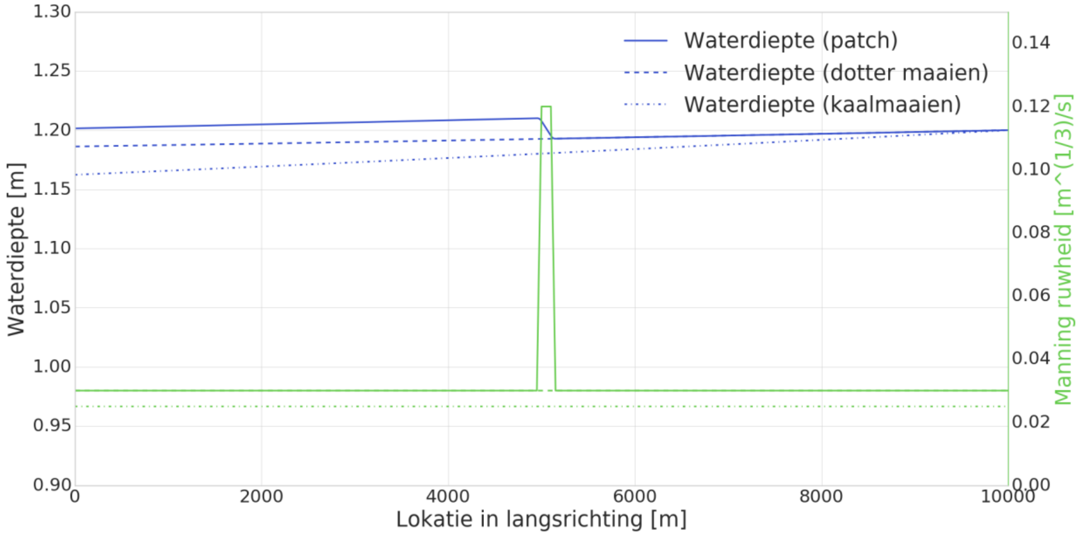

Figure 5.8. The effect of a local vegetation patch on water depth in a fictive channel and the results of two mowing strategies: large dashes – dotter mowing (i.e. only removing the blocking patch), small dashes mowing all vegetation of the full channel stretch.

However, to calculate the detailed effect of specific vegetation on resistance 2D or 3D models are necessary, for example, to assess the influence of vegetation patchiness. A 2D or 3D model allows for quantifying e.g. the effect of mowing only one side of the channel, or only the central bed of the channel. For this approach we use Delft3D that includes the possibility to represent vegetation in a detailed manner, following the Baptist formula (2) which describes vegetation based on number of stems, diameter of stems and drag coefficient of these stems. Figure 5.9 shows a fictive channel of 500 m long with a trapezoidal cross section. Dark blue lines at the top and bottom sides are dry cells (dry banks) and represented on the left is a top view of the channel. Water velocities are shown for various set-ups of vegetation presence: no vegetation, fully overgrown channel, vegetation only on the slopes, vegetation on the left hand side of the channel only, a higher density of the vegetation. The pictures on the right represent the same calculations as on the left, but show the water level changes over the length of the channel. This shows that removing the vegetation in the middle section of the stream and removing one side of all vegetation results in similar water level changes and that a change in density strongly affects that water level set up.

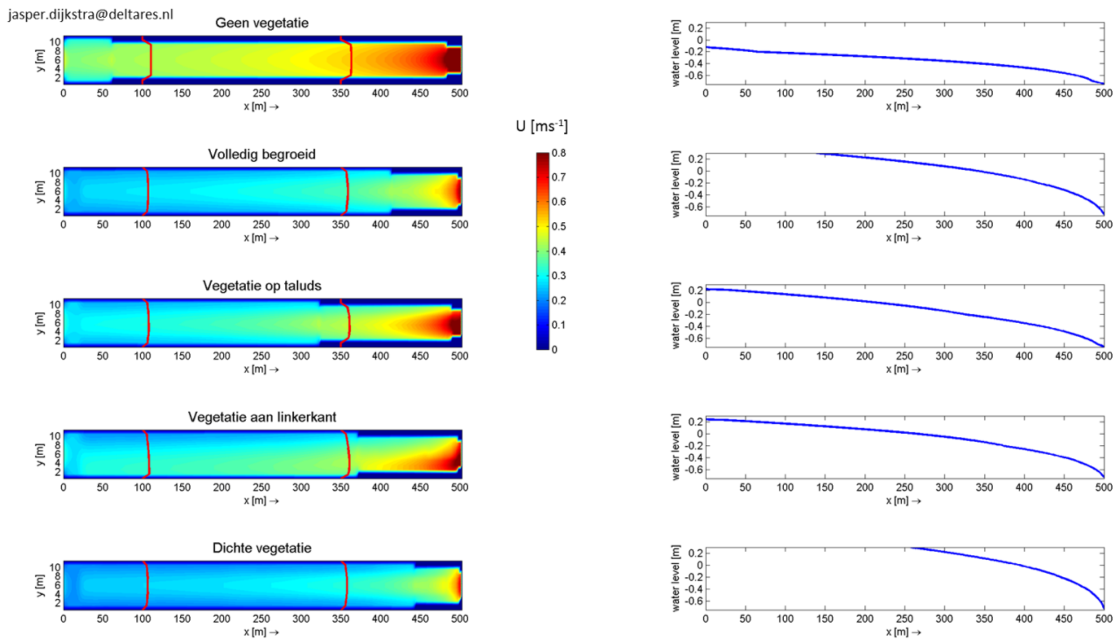

Figure 5.9. 3D calculations of a fictive stretch of stream with different vegetation settings. Left side panel: top view of flow velocity distributions. Right hand panel, related water levels.

5.6 EU-WFD AND VEGETATION

5.6.1 Linge results

The locations of the full vegetation recordings for the Linge (carried out by AQUON) can be found in Appendix B (Table 5.9). Unfortunately these recordings were not in line with the expected WFD requirements, yet they do give a feeling for the most important vegetation that is present at the site. In general the submersed vegetation has a high cover in most locations, with some floating leaves vegetation adjacent to it. *Nuphar lutea* is a prominent species, together with *Ceratophylum demersum*. None of the recorded species are positive indicators for an assessment in line with the Water Framework Directive requirements of the site, with most available indicator species referring to eutrophic stagnant situations.

Table 5.9. Vegetation recordings for the Linge water system, (source AQUON, 2016).

Opname door Tjeerd Dubois (Aquon)																								
WSRL Meetpunt	BETU0489				geen		BETU0487										BETU0488							
Locatie	Locatie 1				Locatie 2		Locatie 3										Locatie 4							
Traject	1-2			3-4	5-6	7-8	9-10			11-12							13-14			15-16				
Opnamevak	1	2	3	1	1	1	1	2	3	1	2	3	4	5	6	7	1	2	3	1	2	3	4	5
Bedekking groeivormen																								
Bedekking Emers	0	0	30	10	20	0	10	2	30	<1	0	0	0	0	0	90	0	<1	0	10	5	40	5	40
Bedekking Drijfblad	0	0	40	40	70	<1	60	40	0	0	0	0	0	0	0	10	0	0	0	1	80	20	60	30
Bedekking Submers	60	60	30	40	80	60	100	100	60	80	0	20	5	60	40	0	100	100	30	100	80	100	60	50
Bedekking kroos	2	20	5	5	3	1	2	2	2	3	3	3	3	3	3	3	10	80	2	10	15	20	20	20
Bedekking Flab/Darmwier	100	100	70	20	20	90	80	80	80	0	30	0	20	0	60	0	100	100	100	80	50	30	30	10
Totale bedekking	**100**	**100**	**70**	**80**	**80**	**90**	**100**	**100**	**80**	**80**	**30**	**20**	**20**	**60**	**60**	**90**	**100**	**100**	**100**	**100**	**100**	**100**	**60**	**90**
Dominante soorten per groeivorm																								
Emers																								
Gele waterkers							x											x						
Harig wilgenroosje								x																
Liesgras				x	x															x	x		x	
Moerasvergeetmenietje							x	x	x							x								
Riet			x						x	x						x					x	x		x
Rietgras				x																				
Drijfblad																								
Gele plomp			x	x	x		x	x													x	x	x	x
Kikkerbeet																x				x		x		x
Stomphoekig sterrenkroos						x																		
Submers																								
Smalle waterpest	x	x	x		x	x											x	x					x	
Grof hoornblad	x	x	x		x		x	x				x	x						x			x		x
Pijlkruid				x	x		x	x	x											x	x	x	x	
Gele plomp							x															x		x
Sterrenkroos										x				x	x					x				
Fonteinkruid																	x							
Kroos																								
Klein kroos	x	x	x	x	x	x	x	x	x	x	x	x	x	x	x	x	x	x	x	x	x	x	x	x

5.6.2 Lage Raam results

At location 1 and 2 vegetation recordings were carried out following standard WFD procedures. Due to time restrictions only a 'quick' recording was carried out at location 3 for the aquatic vegetation. The result is an overview (although incomplete) of the vegetation composition. Vegetation recordings were judged using the software programme QBWat (version with WFD-standards from 2012). In this programme the aquatic and shoreline vegetation are separately judged. The Lage Raam is classified as an 'R5'-type waterbody (slowly flowing middle reaches/downstream reaches on sand).

Reference description of the vegetation composition of an R5-type stream

Under reference conditions R5 streams are fed by clean, buffered upward seepage groundwater influx. A selection of aquatic species is characteristic for this type of streams being: Grote waterranonkel (*Ranunculus peltatus*), Haaksterrenkroos (*Callitriche brutia*), Dotterbloem (*Caltha palustris*), Bittere veldkers (*Cardamine armara*), Bronmos (*Fontinalis antipyretica*), Waterviolier (*Hottonia palustris*), Drijvende waterweegbree (*Luronium natans*), Teer vederkruid (*Myriophyllum alterniflorum*), Rossig fonteinkruid (*Potamogeton alpinus*) and Duizendknoopfonteinkruid (*P. polygonifolius*).

Results of the vegetation assessment in location 1 of Lage Raam

- Score aquatic growth forms: 0,62 (water)
- Score aquatic species composition: 0,11 (water)
- Score shoreline growth forms: 0,14 (shore)
- Score shoreline species composition: 0,00 (shore)

The score for the abundance of aquatic vegetation in location 1 is good (0,62), but aquatic species composition is judged poor (0,11). None of the above mentioned reference species was found during the sampling day. It should be noticed that Drijvend fonteinkruid (*Potamogeton natans*) and Schedefonteinkruid (*Potamogeton pectinatus, now Stuckenia pectinatus*) both are negative indicators for this type of stream and lower the total score. These species are more characteristic for stagnant situations with high trophic values, as is the case in the Lage Raam, which is not the case in a reference situation. In the reference situation, R5 is not subject to water level management by weirs and has a lower trophic state.

We note that in May 2016 Waterranonkels (most likely *Ranunculus peltatus*) were observed (pers. obs. M. Kits). This is a positive indicator species and would have improved the score of the aquatic species composition. Using a different timing of the year for WFD sampling (May/June) would probably increase the scores of the WFD assessment.

The shoreline vegetation score is low, while there is no forest on the shoreline and the coverage of helophytes is too high. The presence of Liesgras (*Glyceria maxima*) and Rietgras (*Phalaris arundinacea*) results in a low score, as these two dominant species are negative indicators of euthropic situations.

Results of the vegetation assessment in location 2 of Lage Raam

- Score aquatic growth forms: 0,72 (water)
- Score aquatic species composition: 0,53 (water)
- Score shoreline growth forms: 0,34 (shore)
- Score shoreline species composition: 0,55 (shore)

The bed of the stream at location 2 is more sandy than at location 1, and the vegetation has a more 'patchy' nature. This variation in structure also resulted in a more varied species composition, with a higher number of positive indicators for R5, such as Grote Waterranonkel (*Ranunculus peltatus*) The same was found for the shoreline vegetation.

Results of the vegetation assessment in location 3 of Lage Raam

- Score aquatic growth forms: 0,60 (water)
- Score aquatic species composition: 0,26 (water)

This location was very much influenced by iron: the water was strongly orange-brown coloured. The poor reachability of the location and the lack of time made that we might have missed some species.

5.6.3 General conclusions regarding translation to WFD-conform assessments

At present the spectral images cannot yet distinguish more than general vegetation type coverage, such as emersed, submersed and floating vegetation, which can be related to visual observations from the black and white images for further detailing of the dominant species. Rare species, that are often growing in between the dominant species, and seasonal species (e.g. only very visible in early spring) might be overlooked by this technique.

Still this technique gives a renewed view on how to deal with the vegetation cover index of the WFD, by allowing to calculate this for a larger section of a water body, rather than only representing a random point in a water body. (note that this is more elaborate than the standard assessment requirements)

6 CONCLUSIONS

Given the main research questions we can conclude that the full spectrum camera can detect and map the presence of floating, emersed and submersed aquatic vegetation.

We have not yet been able to determine the type of vegetation by pattern recognition, due to lack of time. The black and white images, together with the full spectrum images do give sufficient information to visually distinguish the dominant cover types.

The (lack of) transparency of the water does affect the capability of the camera to record the biomass of submersed vegetation, given the optical nature of the data. However, using predefined relationships between vegetation type and expected biomass, a reasonable estimate of the roughness can be made. For very turbid waters we expect that the high turbidity will hamper the development of submersed aquatic biomass, as lack of light will affect biomass development.

The full spectrum camera gives additional information on the biomass, which can be reflected in e.g. a standard NDVI analysis, representing the 'green-index' i.e. a measure for the amount of biomass for the vegetation. This cannot be done with normal cameras. Normal cameras give a good overview for visual inspection from a birds-eye view but do not allow for further translation of the image to e.g. NDVI type indices for biomass, and thus roughness estimates.

The performance of the full spectrum camera on a drone is classified as very good. The drone provides the desired height above the water surface to sample the full width of the channel, and provides more reference points for easy stitching than using the camera on a fixed position such as the ladder at KICT-REC or the hand-held telescope pole used in the Lage Raam. This makes stitching of images into a larger overview map much easier and quicker.

Image normalization and further processing is best done for individual images, followed by stitching of the resulting data.

At this moment we are able to distinguish vegetation cover types and through that the dominant vegetation species. However, timing of the recording might affect the foreseen use for assessment of ecological values. Some species are only prominently visible during specific periods during the year, making that they might be missed in other periods. This has a negative effect on the resulting assessment, specifically if these species have a strong ecological value. Also, rare and thus often valuable species that do not grow in large abundance, or submersed species that intermingle with dominant species types will not be easily spotted. This is also due to the distance at which the camera operates, making resolution too coarse for the fine details of these species.

The potential to survey a much larger area rather than a point sample, substantially increases the overall understanding of ecological potentially valuable sections within a water body. This can help to identify which areas might need specific, or more careful maintenance taking valuable areas into account, for both conserving or further improving the overall quality of the water body.

www.knowh2o.nl Watertorenweg 12 6571 CB BERG EN DAL t +31 (0)6 23 22 49 68
e info@knowh2o.nl Bank NL83 INGB 0006 2713 22 KvK 59020229

7 RECOMMENDATIONS

This first year, the Dotter-project has proved that there is a good potential for upscaling the full spectrum imaging using a drone. However, commercial drone flying in the Netherlands is restricted by legislation at some locations, including the field site 'Lage Raam' being a no-fly zone. Given that the drone does not need to fly very high (some 20 meter above the water surface is estimated to be enough for most applications), it is recommended to discuss with the authorities to get an exception for (helicopter) flights like we are intending to carry out for upscaling purposes.

In the Lage Raam we observed strong accumulation of soft sediments on the bed of the stream. This accumulation is substantial and hampers conveyance. We recommend to link the vegetation analysis with a mapping of the soft sediments to be able to judge if conveyance issues are more caused by the vegetation or by the soft sediments accumulated in the channels. This will require new techniques to be applied in combination with the full-spectrum camera on the drone. We recommend that this line of monitoring is further developed for an more holistic overview of the current status of the water ways.

In 2016 we used only a few different spectral image related indices, but many more are available or can be developed. We recommend an in-depth analysis of other available indices and potentially newly developed indices suitable for the specific data from the Cubert camera.

During our discussions with end-users it became apparent that the potential to supply them with maps covering a larger area with a good insight in critical spots for both hydraulic roughness and ecological sensitive areas can help them specify a better mowing regime. This year we have only assessed small representative sections. The project has not yet taken the step to translate the information of these images to larger areas, or stream length analysis of the roughness of the vegetation in the stretch and its influence on conveyance. We would like to upscale the technique in the coming year to fly a larger section to prepare and provide these maps.

The time-dependent growth and development of the aquatic vegetation can be incorporated into the available hydraulic models. This will generate an extra applicability of the model results in terms of prediction of the hydraulic resistance of the vegetation over time. This will serve the risk-based water management and reduce the potential risk taken.

We recommend that next year more attention is paid in this translation to roughness parameters. For this also other data sets, such as the one from Pitlo and Griffioen (1980's) and of the University of Antwerp might be very valuable, in combination with already available tools such as the MAAI-Bos, the WSRL-tool and the MS Excel-based analysis method provided by Chris Griffioen (2016-2017). At the same time we advocate that it would be beneficial to have one tool that is sufficiently tested, validated, user-friendly, properly maintained, and available for all water boards for future use.

8 REFERENCES

BAPTIST, M.J., V. BABOVIC, J. RODRÍGUEZ UTHURBURU, M. KEIJZER, R.E. UITTENBOGAARD, A. MYNETT, and A. VERWEY, 2007. On inducing equations for vegetation resistance. Journal of Hydraulic Research Vol. 45, No. 4 (2007), pp. 435–450.

Bélanger, J.-B. (1828). Essai sur la solution numérique de quelques problèmes relatifs au movement permanent des eaux courantes (red.: Traktaat over de numerieke oplossing van enkele problemen gerelateerd aan stationaire stroming). Carilian-Goeury: Parijs.

Cheng, Nian-Sheng, 2011. Representative roughness height of submersed vegetation. WRR Volume 47, Issue 8, August 2011.

Cho, Hyun Jung, Philemon Kirui, and Harene Natarajan, 2008. Test of Multi-spectral Vegetation Index for Floating and Canopy-forming Submersed Vegetation. Int. J. Environ. Res. Public Health 2008, 5(5) 477-483, 2008.

Curran, P.J. Windam, W.R. & Gholz, H.I. (1995). Exploring the relationship between reflectance red edge and chlorophyll concentration in slash pine leaves. Tree Physiology. 15, 203-206.

Everitt, James H., K. Rodney Summy, and Chenghai Yang, 2009. Spectral Reflectance and Digital Image Relations Among Five Aquatic Weeds. Subtropical Plant Science, 61:15-23, 2009.

Gitelson, A.A. & Merzlyak, M.N. (1994). Spectral reflectance changes associated with autymn senescence of Aescules Hippocastanum L. and Acer Platanoides L. leaves. Spectral features and relation to chlorophyll estimation. Journal of Plant Physiology, 143, 286-292.

Gitelson, A.A. & Merzlyak, M.N. (1996). Signature analysis of leaf reflectance spectra: Algorithm development for remote sensing of chlorophyll. Journal of Plant Physiology 148. 494-500.

Gitelson, A.A., Merzlyak, M.N. Chivkunova, O.B. (2001). Optical properties and non-destructive estimation of anthocyan content in plant leaves. Photochemistry and Photobiology71. 38-45.

Gitselon, A.A. Zur, Y., Chivkunova, O.B. & Merzlyak, M.N. (2002). Assessing carotenoid content in plant leaves with reflectance spectroscopy. Photochemistry and Photobyiology 75, 272-281.

Hendriks, Paul, Peter Paul Schollema, Roelf Pot, Henk Jan Ottens, Erik Querner, Ralf Verdonschot, 2016. Ruimte voor natuur bij onderhoud aan watergangen. H2O Online, 15 februari 2016.

Huete, A.R., Liu, H., Batchily, K.m & Van Leeuwen, W. (1997). A comparison of vegetation indices over a globasl set of TM images from EOS-MODIS. Remote Sensing of Environment, 59(3), 440-451.

Huthoff, F., 2007. Modeling hydraulic resistance of floodplain vegetation. PhD Thesis, University of Twente, Enschede, The Netherlands.

Huthoff, F., 2012. Theory for flow resistance caused by submersed roughness elements. Journal of Hydraulic Research, 50:1, 10-17.

John, C. M, and Kavya Nath, 2014. INTEGRATION OF MULTISPECTRAL SATELLITE AND SPECTRAL FIELD DATA FOR AQUATIC MACROPHYTE STUDIES. The International Archives of the Photogrammetry, Remote Sensing and Spatial Information Sciences, Volume XL-8, 2014. ISPRS Technical Commission VIII Symposium, 09 – 12 December 2014, Hyderabad, India.

Meijer, D.G. and E.H. Van Velzen, 1999. Prototype scale flume experiments on hydraulic roughness of submersed vegetation. Proceedings of the 28th International IAHR Conference, Graz, Austria.

Mitchell, J.J., Shrestha, R., Spaete L. P. and Glenn, N.F. (2015) Combining airborne spectral and LiDAR data across local sites for upscaling shrubland structural information: Lessons for HyspIRI. Remote Sensing of Environment, http://dx.doi.org/10.1016/j.rse.2015.04.015

Peñuelas, J. Pinol, J., Ogaya, R. & Filella, R. (1997). Estimation of plant wáter concentration by the reflectance wáter index WI (R900/R970) (In Mitchell et al., 2015).

Pitlo, R.H., and C.J.H. Griffioen, 1991. Stromingsmodel voor begroeide waterlopen. Waterschapsbelangen 1991, nummer 10. In Dutch.

Rouse, J.W., Haas, R.H., Schell, J.A. & Deering, D. W. (1973). Monitoring vegetation systems in the Great Pleains with ERTS. Thrist ERTS Symposium, NASA SP-351-NASA, Washington DC, Vol. 1. (pp309-317)

Schoelynck, Jonas, Kris Bal, Veerle Verschoren, Ellis Penning, Eric Struyf, Tjeerd Bouma, Dieter Meire, Patrick Meire, and Stijn Temmerman, 2014. Different morphology of Nuphar lutea in two contrasting aquatic environments and its effect on ecosystem engineering. Earth Surf. Process. Landforms 39, 2100–2108 (2014).

Tucker, C.J. (1979) 'Red and Photographic Infrared Linear Combinations for Monitoring Vegetation', *Remote Sensing of Environment*, **8(2)**,127-150.

Vargas-Luna, Andrés, Alessandra Crosato, and Wim S.J. Uijttewaal, 2015. Effects of vegetation on flow and sediment transport: comparative analyses and validation of predicting models. Earth Surf. Process. Landforms 40, 157–176 (2015).

Vogelmann, J.F., Rock, B.N., &Moss, D.M. (1993). Red edge spectral measurements from sugar maple leaves. *International Journal of Remote Sensing, 14 1563-1575*

Zong, Lijun, and Heidi Nepf, 2010. Flow and deposition in and around a finite patch of vegetation. Geomorphology 116 (2010) 363–372.

Literature references - miscellaneous

Unie van Waterschappen (2012). Gedragscode Flora- en faunawet voor waterschappen. Den Haag: Unie van Waterschappen.

Strykstra, R., Vegter, U. (2013). Veldgids buitendienst, beheer en onderhoud volgens natuurwetgeving. Waterschap Hunze en Aa's, Veendam: Studio Rob Pentinga, De Bondt Grafimedia.

Querner E.P. (1995). Vaststellen maaionderhoud in waterlopen: hydrologische benadering. Het Waterschap, 80 (4), 170-175.

Peeters, E.T.H.M., Veraart, A.J., Verdonschot, R.C.M., Zuidam, J.P. van, Klein, J.J.M. & P.F.M. de, Verdonschot, P.F.M. (2014). Sloten; ecologisch functioneren en beheer. Zeist: KNNV Uitgeverij.

Verdonschot, R.C.M. (2012). Drainage ditches, biodiversity hotspots for aquatic invertebrates. Defining and assessing the ecological status of a man-made ecosystem based on macroinvertebrates. Wageningen: Alterra Scientific Contributions 40.

Crombaghs, B.H.J.M., Akkermans, R.W., Gubbels, R.E.M.B. & Hoogerwerf, G. (2000). Vissen in Limburgse beken. De verspreiding en ecologie van vissen in stromende wateren in Limburg. Maastricht: Stichting natuurpublicaties Limburg.

Nijboer, R. (2000). Natuurlijke levensgemeenschappen van de Nederlandse binnenwateren deel 6, sloten. Achtergronddocument bij het Handboek Natuurdoeltypen in Nederland. Wageningen: Rapport EC-LNV nr. A-06.

Painter, D. (1998). Effects of ditch management patterns on Odonata at Wicken Fen, Cambridgeshire, UK. Biological Conservation (84), 189-195.

Schoelynck, J., Groote, T. de, Bal, K., Van den Bruwaene, W., Meire, P. & Timmerman, S. (2012). Self-organised patchiness and scale-dependent bio-geomorphic feedbacks in aquatic river vegetation. Ecography, 35 (8), 760-768.

Gurnell, A.M. & Grabowski, R.C. (2015). Vegetation–Hydrogeomorphology Interactions in a Low-Energy, Human-Impacted River. River Research and Applications. DOI: 10.1002/rra.2922

Verdonschot, P.F.M. (red.). (1995). Beken stromen. Leidraad voor ecologisch beekherstel. Amersfoort: STOWA rapport 95-03.

Wiersma P., Ottens, H.J., Kuiper, M.W., Schlaich, A. E., Klaassen, R.H.G., Vlaanderen, O., Postma, M. & Koks, B.J. (2014). Analyse effectiviteit van het akkervogelbeheer in provincie Groningen. Scheemda: Stichting Werkgroep Grauwe Kiekendief.

Kuiper M.W. (2015). The value of field margins for farmland birds. PhD thesis. Wageningen: Wageningen University, The Netherlands.

Ottens H.J., Kuiper, M.W., Scharenburg, C.W.M. van & Koks, B.J. (2013b). Akkerrandenbeheer niet de sleutel tot succes voor de Veldleeuwerik *Alauda arvensis* in Oost-Groningen. Limosa (86), 140-152.

Groot, P. de (2014). Airborne LiDAR [pdf]. Ontvangen via email van AHAB/Leica.

Brochure Leica Ahap ChiropteraII, Topographic and Bathymetric Lidar System.

Stigermark, C.J. 2014. AHAB-Leica SUPERB 2014. Skåne Projektet [pdf]. Beschikbaar op: http://www.google.nl/url?sa=t&rct=j&q=&esrc=s&source=web&cd=1&ved=0ahUKEwjv4Zy4yovMAhVGkQ8KHdV5BQkQFggkMAA&url=http%3A%2F%2Fwww.ultra-superb.eu%2Findex.php%2Fladda-ner%2Fpresentationer%2Fcategory%2F20-superbs-slutkonferens-3-442014%3Fdownload%3D77%3Asuperbs-slutkonferens&usg=AFQjCNEuUPvHqyTExkRt6p8Yun-amI4j8Q, geraadpleegd 13 april 2016.

Guenther, G.C., (1985). Airborne Laser Hydrography. System Design and Performance Factors. Rockville: National Oceanic and Atmospheric Administration, 396 p.

Pfennigbauer, M., Ullrich, A. (2011). Multi-Wavelength Airborne Scanning. In: *International LiDAR Mapping Forum.* [online] New Orleans, 10p. Beschikbaar op http://www.riegl.com/uploads/tx_pxpriegldownloads/Paper_ILMF_2011_RIEGL_Multiwavelength_ALS.pdf, geraadpleegd 1 april 2016.

Vegt, J. v.d., Chatillon, J., (2015). Pilotproject: Meten ondiepe sloten in de polder Groot Wilnis Vinkeveen met laser bathymetry.

Piel, S., Populus, J., Chust, G., Galparsoro, I. (2012). Mesh + MeshAtlantic. Recommended Operating Guidelines for Lidar Surveys. [online] European Union, p.8. Beschikbaar op: http://www.emodnet-seabedhabitats.eu/pdf/MeshA_ROG_ Lidar_Survey_v4.0.pdf, geraadpleegd 21 December 2015

Aarrestad, S.M. (2014). Use of Underwater Spectral Imagery for Geological Characterization of the Seabed. MSc Thesis. Norwegian University of Science and Technology.

Bukata, R.P., Jerome, J.H., Kondratyev, K.Y., Pozdnyakov, D.V. (1995). Optical Properties and Remote Sensing of Inland and Coastal Waters. United States: CRC Press, 363 p.

Bartholomeus, H.M., Schaepma, M.E., Kooistra, L., Stevens, A., Hoogmoed, W.B., Spaargaren, O.S.P. (2008). Spectral Reflectance Based Indices for Soil Organic Carbon Quantification. *Geoderma* [online] 145, 8p. Beschikbaar op: http://www.sciencedirect.com, geraadpleegd 12 januari 2016 10 H2O-Online 14 april 2016.

He, M., Liu, Z., Du, K., Li, L., Chen, R., Carder, K., and Lee, Z. (2000) Retrieval of Chlorophyll from Remote Sensing Reflectance in the China Seas. *Applied Optics* [online] 39 (15), 8p. Beschikbaar op: http://www.osapublishing.org, geraadpleegd 2 februari 2016.

APPENDIX A - TECHNICAL SPECIFICATIONS FULL SPECTRUM CAMERA

The Cubert full spectrum camera UHD 185 – 'Firefly' consists of the camera body, the mini pc (controlling unit) and three cables (2x network, 1x power). WIFI is used to operate the camera from ground. The setup needs about 20W at 12V. This is typically available from the battery of the drone itself, but if this is not the case a separate battery has to be carried as well. Only the camera has to be mounted to a gimbal, the pc (and battery) can be fixed to the drone directly. The controlling pc can also be connected to the GPS of the drone (via a RS232 communication port). Using the GPS unit on the drone allows for geo-referencing.

The typical Setup of the UHD 185 consists of one UHD 185, one controlling unit and optional one battery pack.

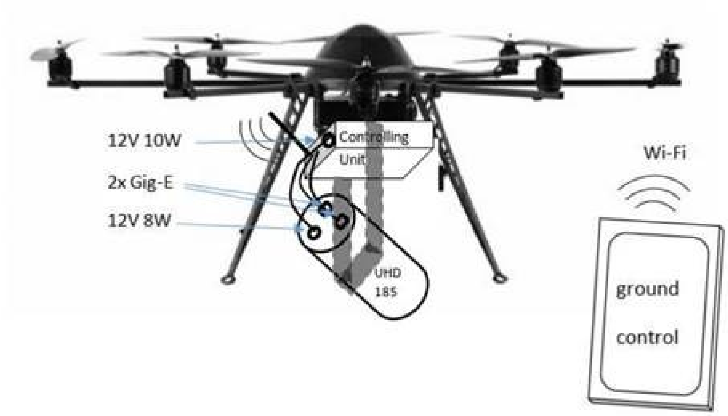

Technical specifications UHD 185 „Dragonfly“

1 UHD 185 Dragonfly

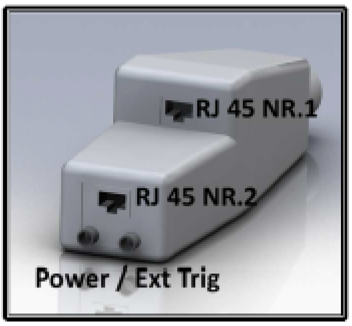

2 Electronic wiring

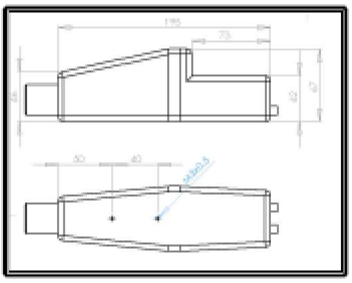

3 Overall

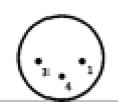

1(bn)	Power V_{DC}
3(bu)	GND
4(bk)	NC

4 Interface power supply

Real-Time Spectral Imagine Frame Camera

Data quality:

Wavelength range	450 nm-950 nm
Detector	Silicon Sony ICX285
Spectral resolution	8 nm (@532 nm)
Spectral sampling	4 nm (125 channels)
Spectral sampling (physical)	1,05 nm/Pix@450 nm; 4,54 nm/Pix@650 nm; 8,13 nm/Pix@900 nm
Wavelength accuracy Δλ @ 532nm / 808nm	±2,5nm / ±4,5nm
Spatial resolution	1000*1000 Pixel²
SNR @ 25ms	58dB

Sensor data:

Type	Silicon
Cooling system	air-cooled
Digitalization	12 bit
Integration time	0.1 ms up to 10 000 ms
Measure frequency (UAV)	5 Hz

Mechanical data:

Weight	470 g
Size	appr. 195 mm*67 mm* 60 mm

Operating data:

Dust protection	Yes
Splash guard	Yes
Environmental conditions	Not condensing
Operating temperature	0°C up to +40°C

Optical data:

Focal length	e.g. 12 mm, 17 mm, 23 mm, 35mm
Aperture (angle)	e.g. 27°, 20°, 15°, 10°

Electronic data:

Voltage	DC 12 V
Power	15 W

APPENDIX B – DETAILS OF LINGE EXPERIMENT

The locations where vegetation recordings were made are given in below pictures

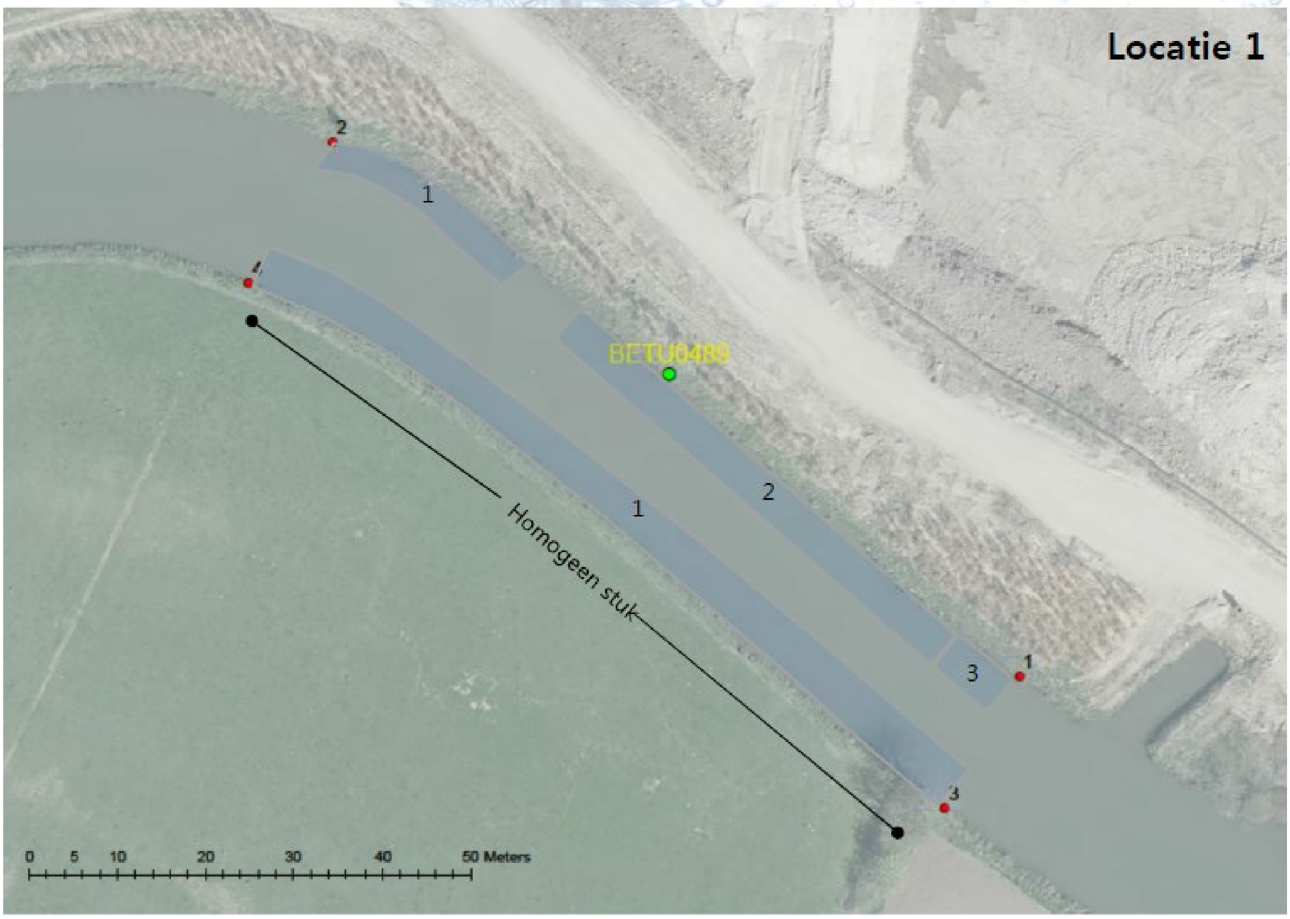

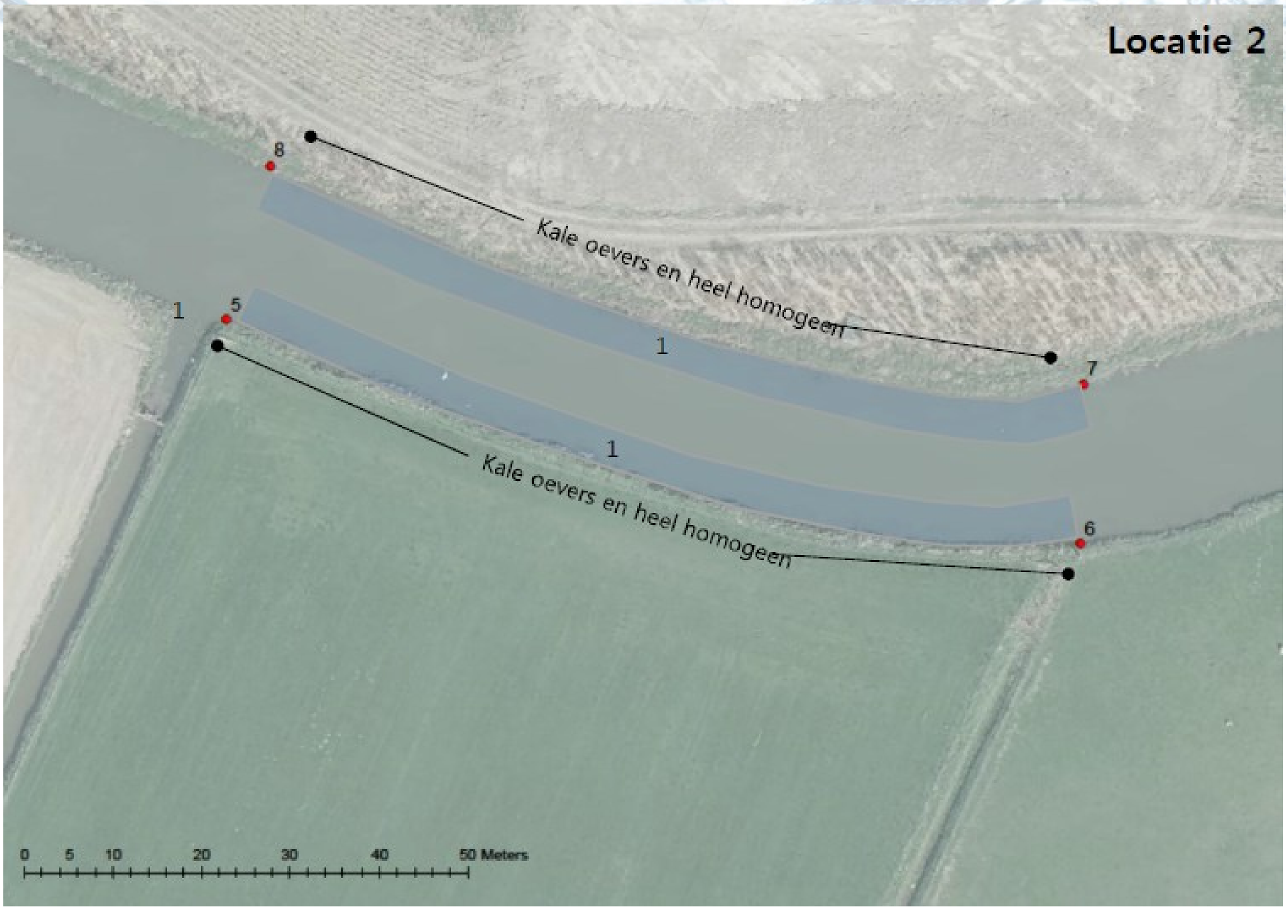
Locatie 2
8
Kale oevers en heel homogeen
1
5
1
7
1
Kale oevers en heel homogeen
6
0 5 10 20 30 40 50 Meters

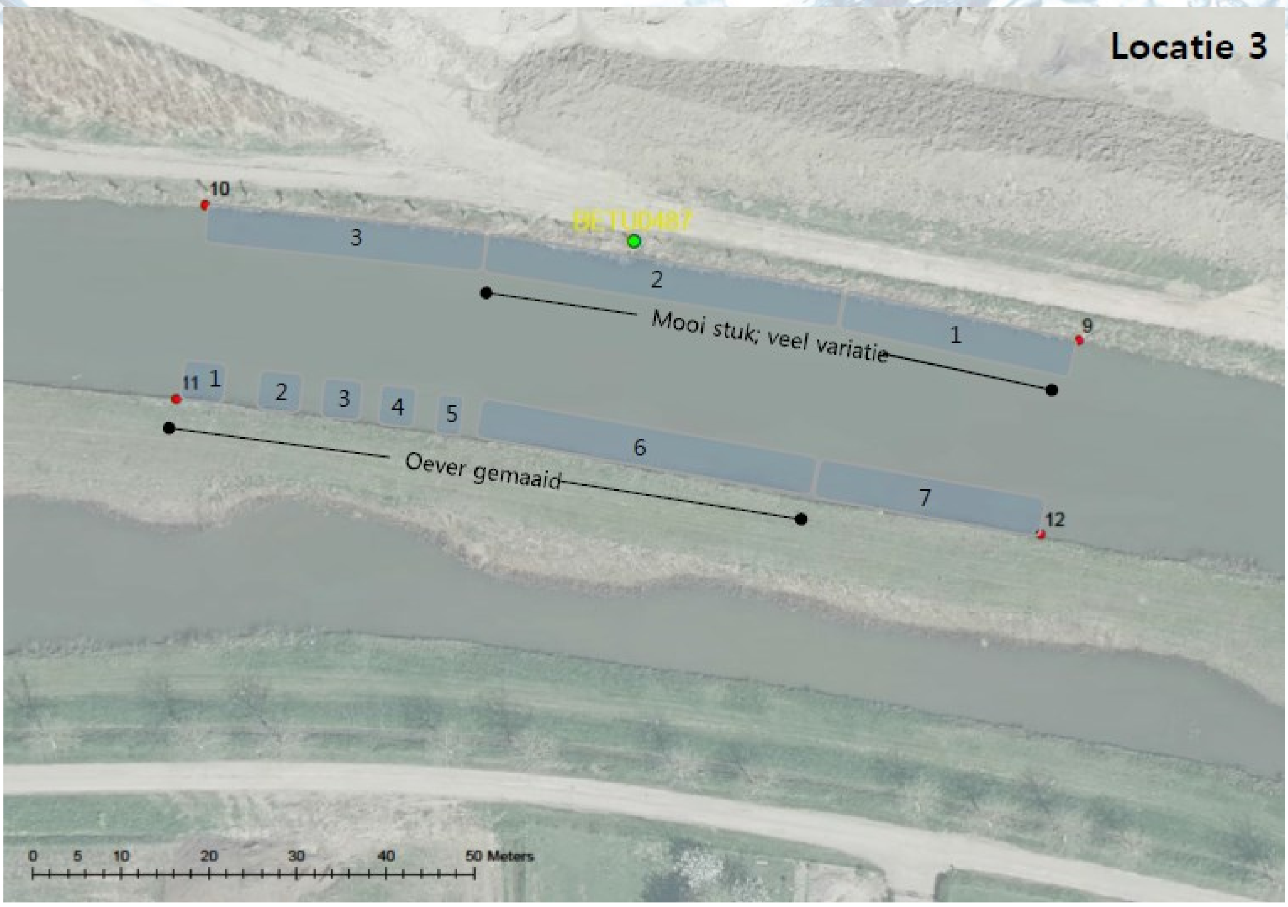

Locatie 3
10
BETU0487
3
2
1
9
Mooi stuk; veel variatie
11
1
2
3
4
5
6
7
12
Oever gemaaid
0 5 10 20 30 40 50 Meters


Locatie 4
13
14
15
16
5
1
1
2
2
3
3
4
5
0 5 10 20 30 40 50 Meters

APPENDIX C – DETAILS OF LAGE RAAM EXPERIMENT – FLOW MEASUREMENTS

Below Dutch text is the full memo of the hydraulic measurements on the Lage Raam as carried out in November 2016, together with the Dutch text on the WFD assessment carried out in sept. 2016.

An English summary of this text is found in the main text (chapter 4).

ACHTERGROND

Het doel van het dotterproject is het efficiënt beheren van watergangen, het mogelijk maken van een goede aan- en afvoer van water en het vergroten van natuurwaarden in water.

In beken van waterschappen zorgt de groei van waterplanten voor obstakels in de stroming wat kan leiden tot problematiek in het waterbeheer. Het beheersen van de hoeveelheid vegetatie wordt gedaan met behulp het maaien van de vegetatie. De exacte bepaling van het te maaien traject gebeurd op basis van visuele inspectie en lokale kennis. Als gevolg van deze methode wordt gezorgd voor een goed doorstroomoppervlak maar gaan veel financiële middelen en natuurwaarden verloren.

In het dotterproject wordt met behulp van full spectrum beelden een efficiëntieslag behaald in het hele proces. Hiervoor is het noodzakelijk om enige hydraulische condities achter de hand te hebben om modellen op basis van spectrale beelden te valideren. Daarnaast geven metingen van een begroeid traject de mogelijkheid om de ruwheid te bepalen en hydraulische condities te begrijpen.

In deze memo worden de resultaten kort besproken en de belangrijkste conclusies naar aanleiding van observaties gegeven en wat er mogelijk is met deze data set.

Op de velddag zijn 2 locaties bezocht op de Lage Raam, te noemen IJzerbroekse stuw (site #2) en Kwekerijweg (site #3). De velddag vond plaats op 22 november 2016 in licht zonnige condities tussen 9 en 3 uur. Tijdens de velddag zijn op 4 trajecten afvoermetingen gedaan met behulp van een StreamPro. 1 profiel is gemeten met een puntsnelheidsmeter. Op 10 locaties verspreid over 3 profielen zijn er langdurige snelheidsmetingen gedaan. Daarnaast is de afvoer bepaald over de stuw bovenstrooms van de metingen en zijn er verscheidene schetsen en foto's gemaakt. Andere leden van het team hebben samples verzameld van de vegetatie en spectrale beelden gemaakt.

BEELDMATERIAAL

Er zijn van beide locaties (Figuur 0.1, Figuur 0.2) foto's gemaakt, in een zip file worden deze allemaal samengevoegd (1221455-000-ZWS-0005_Foto.zip). In Figuur 0.3 wordt een overzicht gegeven van de verschillende locaties (bron Chanjoo Lee/KICT).

In Figuur 0.4 is te zien dat de rechteroever redelijk begroeid is en dat de linkeroever glad gemaaid. Het talud van de linkeroever is een stuk steiler dan de rechteroever.

In Figuur 0.5 is te zien dat hier veel vegetatie is gegroeid vanaf beide oevers. De geul is vrij klein in breedte door de vegetatie.

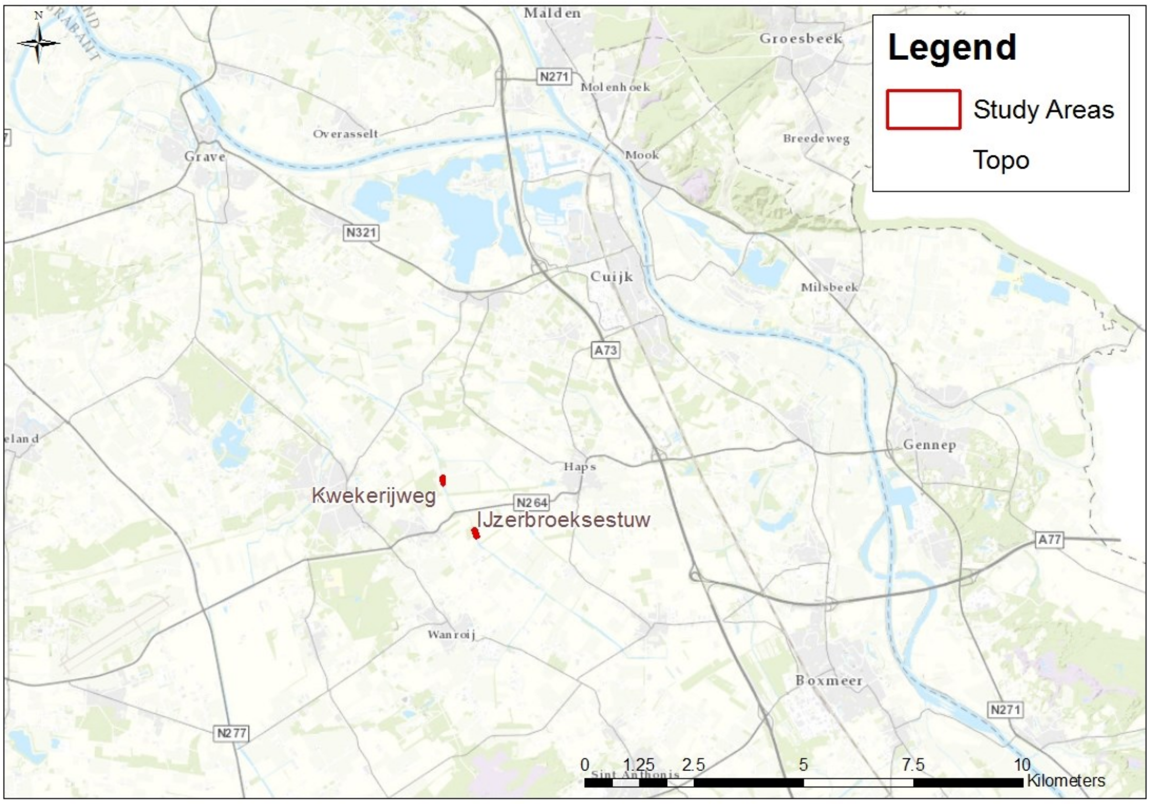

Figuur 0.1 Overzichtskaart van de twee veldwerklocaties

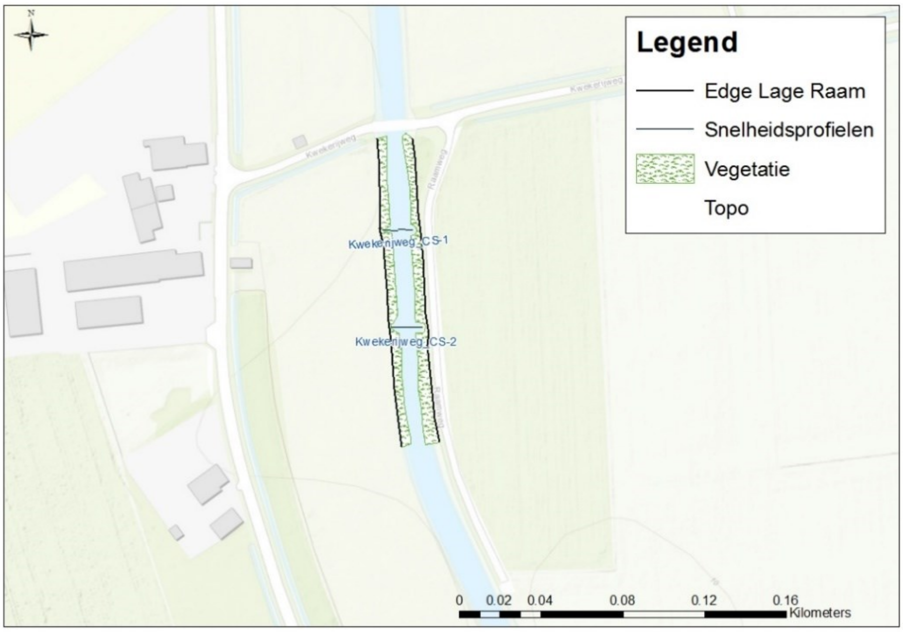

Figuur 0.2 Detailkaarten van de twee veldwerklocaties


Site #2-downstream of weirs (N51.676498, E5.827559) Site #3-upstream of the bridge (N51.688578, E5.816463)


Site #2 (looking downstream) *Site #3 (looking upstream)*

Figuur 0.3 Overzicht van locaties, beeldmateriaal van Chanjoo Lee/KICT.

Figuur 0.4 Site #2 genomen vanaf de stuw stroomafwaarts gericht.

Figuur 0.5 Site #3 genomen vanaf de brug stroomopwaarts gericht.

ADCP METINGEN

Voor de metingen plaatsvonden is een traject vrijgemaakt in de vegetatie zodat de StreamPro zo dicht mogelijk tegen de oever was te brengen. De locatie van het uiteinde van het transect werd bepaald door te kijken wanneer metingen niet meer mogelijk waren. De afstand tot de oever is opgenomen in de software. Daarnaast is op elke locatie handmatig de breedte van de beek gemeten.

Per profiel is er 6 keer heen en weer gevaren tussen de oevers. De meting is 10 seconden uitgevoerd bij het uiteinde van het transect. Daartussen is de StreamPro met een constante snelheid over de beek getrokken. Op verscheidene locaties van het transect is vervolgens een snelheidsmeting gedaan door de StreamPro op 1 locatie stil te laten liggen.

Figuur 0.6 Site #3, profiel 1, voorbeeld van het uitzetten van een traject voor de StreamPro.

Afvoeren

Tussen de transects is een grote spreiding te zien in de resultaten (Figuur 0.7). De spreiding is tussen de 5-10% wat in lijn is met onnauwkeurigheid van de StreamPro. Door middel van nabewerking is het mogelijk om de onnauwkeurigheid te verkleinen, maar een spreiding van 5% is niet te vermijden in de resultaten.

Tussen de verschillende locaties is een spreiding van meer dan 10% te zien. Dit komt door de eerste locatie die een veel grotere afvoer laat zien dan de andere locaties (Tabel 0.1). Dit komt waarschijnlijk door de hoge afvoer door de bovenste laag en de onderste laag (Profiles.xlsx). Tevens is de gemeten breedte breder dan de breedte uit het profiel wat onwaarschijnlijk is. Het verschil tussen de afvoer in de bovenste laag tussen de IJzerbroekseweg-1 en de andere locaties is ongeveer de afwijking in afvoer tussen deze locatie en de anderen. De onnauwkeurigheid in de eerste locatie kan komen door de nabije ligging van de stuw waardoor de stroming turbulenter is.

Al met al valt op dat in het midden van de geul bijna al het water stroomt. Praktisch gezien stroomt er niets door de vegetatie zelf wat overeen komt met de observaties van de dag zelf. Daarbij wordt de stroming door de vegetatie waarschijnlijk overschat doordat voor de meting een transect is vrijgemaakt in de vegetatie wat niet representatief is over de lengte van de rivier.

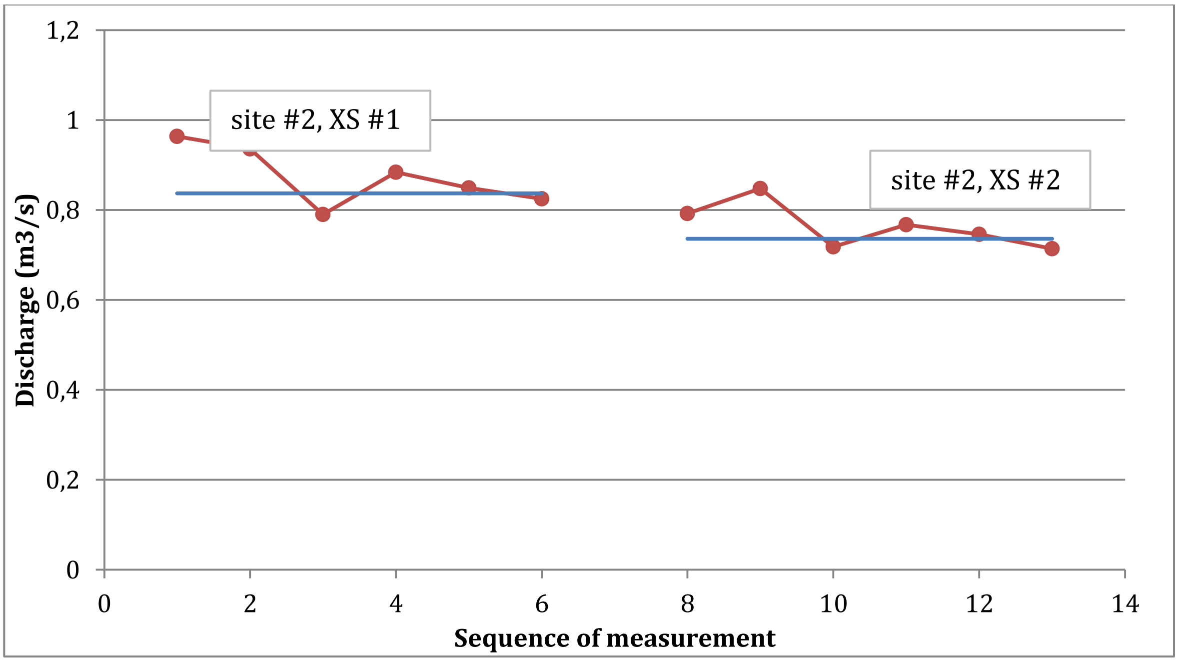

Figuur 0.7. Scatter in de transects binnen 1 profiel voor locatie IJzerbroekseweg, bron Chanjoo Lee/KICT.

Tabel 0.1. Gemiddelde afvoer van de 6 transects van elk van de profielen, Kwekerijweg-2 is op basis van puntmetingen en stuw IJzerbroek op basis van de waterdiepte op de stuw gecombineerd met de breedte van de stuw.

	Total Flow [m3/s]	Flow through center [m3/s]	Flow in vegetation [m3/s]	Width [m]	Area [m2]	Flow velocity [m/s]	Max. Flow Velocity [m/s]	Channel velocity [m/s]
Ijzerbroekseweg-1	0.87	0.87	0.01	10.85	5.53	0.15	0.75	0.28
Ijzerbroekseweg-2	0.76	0.76	0.00	11.30	6.46	0.11	0.72	0.25
Kwekerijweg-1	0.82	0.83	0.00	12.50	5.32	0.14	0.85	0.35
Kwekerijweg-2	0.79	0.80	-0.01	11.80	5.43	0.17	0.84	0.32
Weir	0.8							

Snelheidsmetingen

In de metingen (Figuur 0.8) is zichtbaar dat er een grote spreiding zit in de gemeten snelheden en dat dichter bij de vegetatie er meer ontbrekende waarnemingen zijn. Dit komt doordat de beams van de StreamPro worden geblokkeerd door de vegetatie. Deze metingen van de StreamPro zijn dus onbetrouwbaarder. Dit is ook zichtbaar in een procentile plot (Figuur 0.9).

Op basis van de puntmetingen in profiel 2 van site #3 is een iets waarschijnlijker snelheidsverdeling zichtbaar. De metingen zijn gedaan aan de rand van de vegetatie en in het midden van de geul (Figuur 0.10). Het verloop in snelheid over kleine laterale afstand is goed zichtbaar. Daarnaast is de afname in snelheid nabij het wateroppervlak dichtbij de vegetatie erg opvallend. De toppen van de vegetatie remt de stroming mogelijk meer af dan de stelen in het water zelf. Verder is er een sterk logaritmisch snelheidsprofiel zichtbaar in de verticale richting met zeer snel afnemende stroomsnelheden vanaf de bodem.

De stroomsnelheid (Tabel 3.1) over de complete breedte van de Lage Raam is om en nabij 0,15 m/s. De gemiddelde stroomsnelheid in de geul in het midden van de Lage Raam is tussen de 0,25 en 0,35 m/s met maximale waarden tot 0,85 m/s. De stroomsnelheid door de vegetatie is moeilijk te bepalen maar zal in ieder geval minder zijn dan 0,10 m/s als er al stroming is tussen de vegetatie. Op basis van de observaties gedurende de velddag is het waarschijnlijker dat er geen noemenswaardige stroomsnelheid is te vinden in de vegetatie zelf.

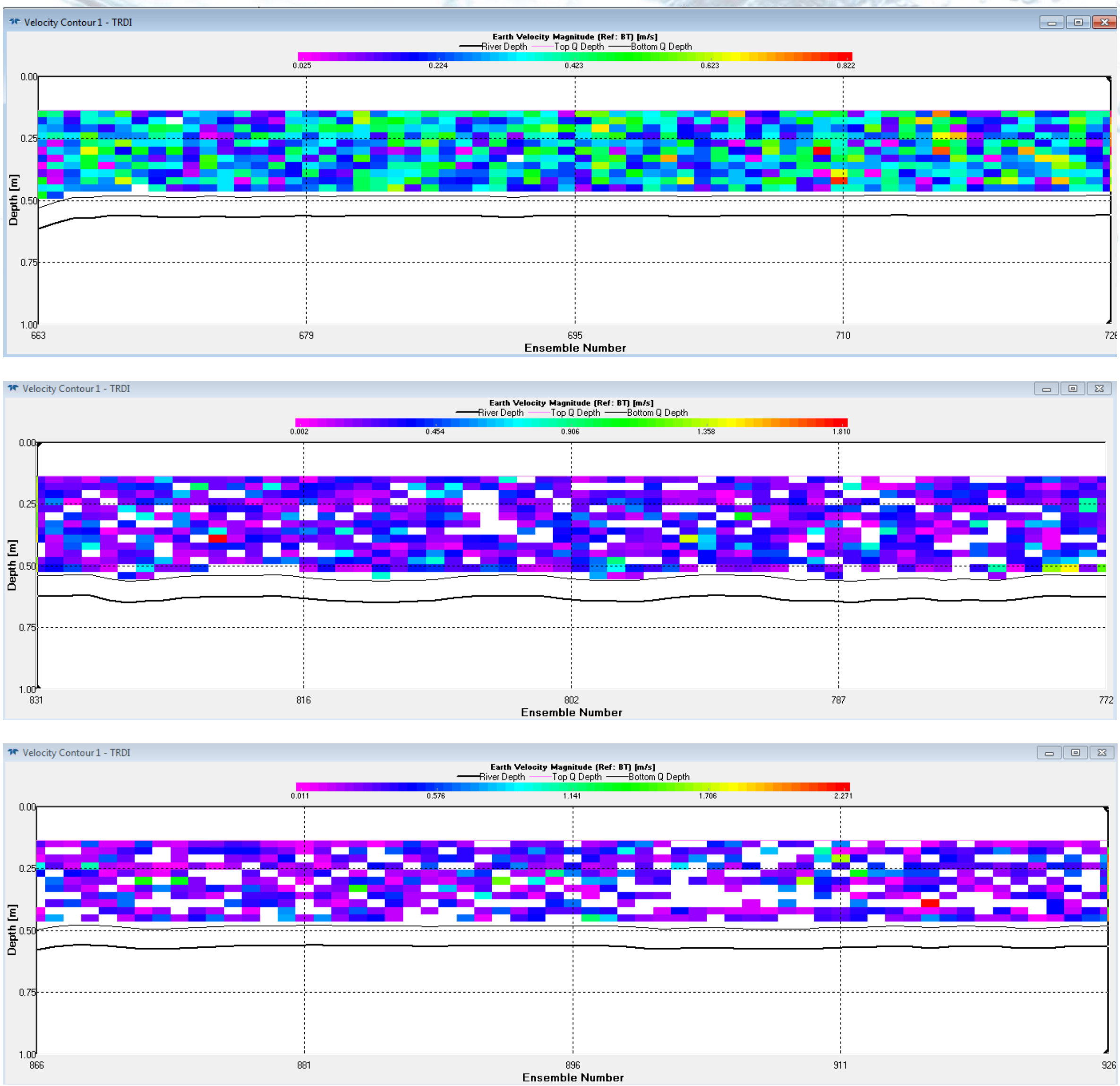

Figuur 0.8 Drie snelheidsprofielen van locatie 2 op site #2, bovenste grafiek is in de geul, middelste rand van de vegetatie en de laatste in de vegetatie.

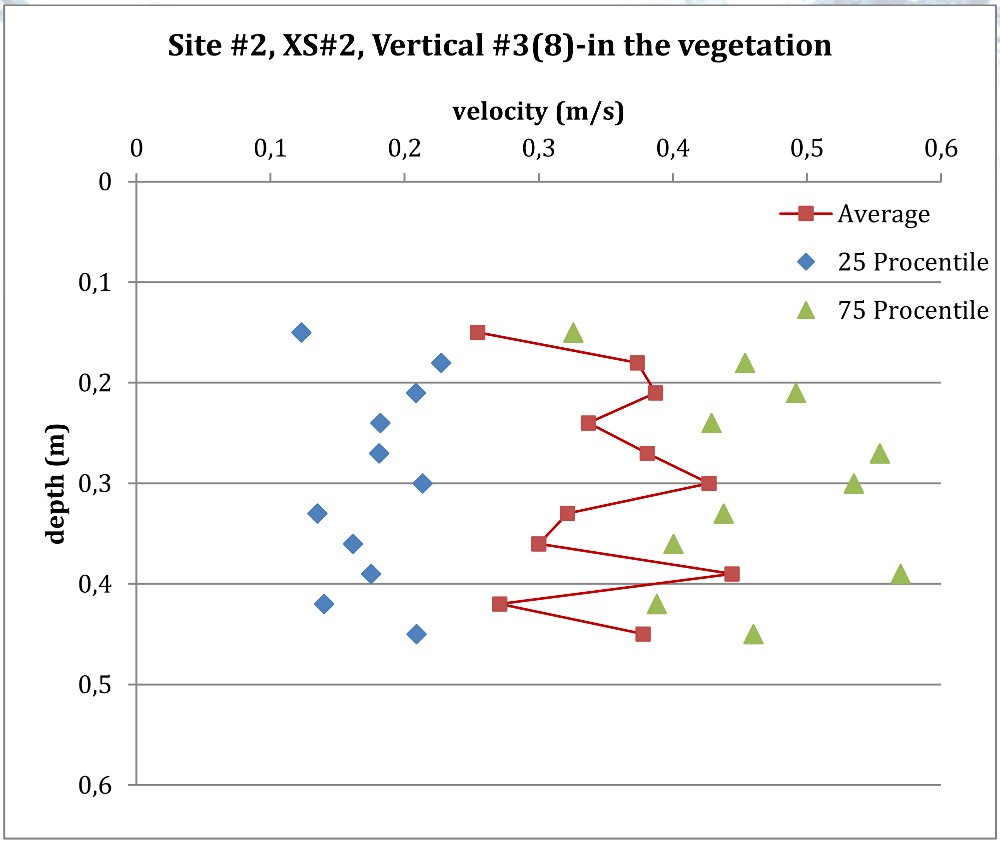

Figuur 0.9. Percentiles in de vegetatie (Bron: Chanjoo Lee/KICT).

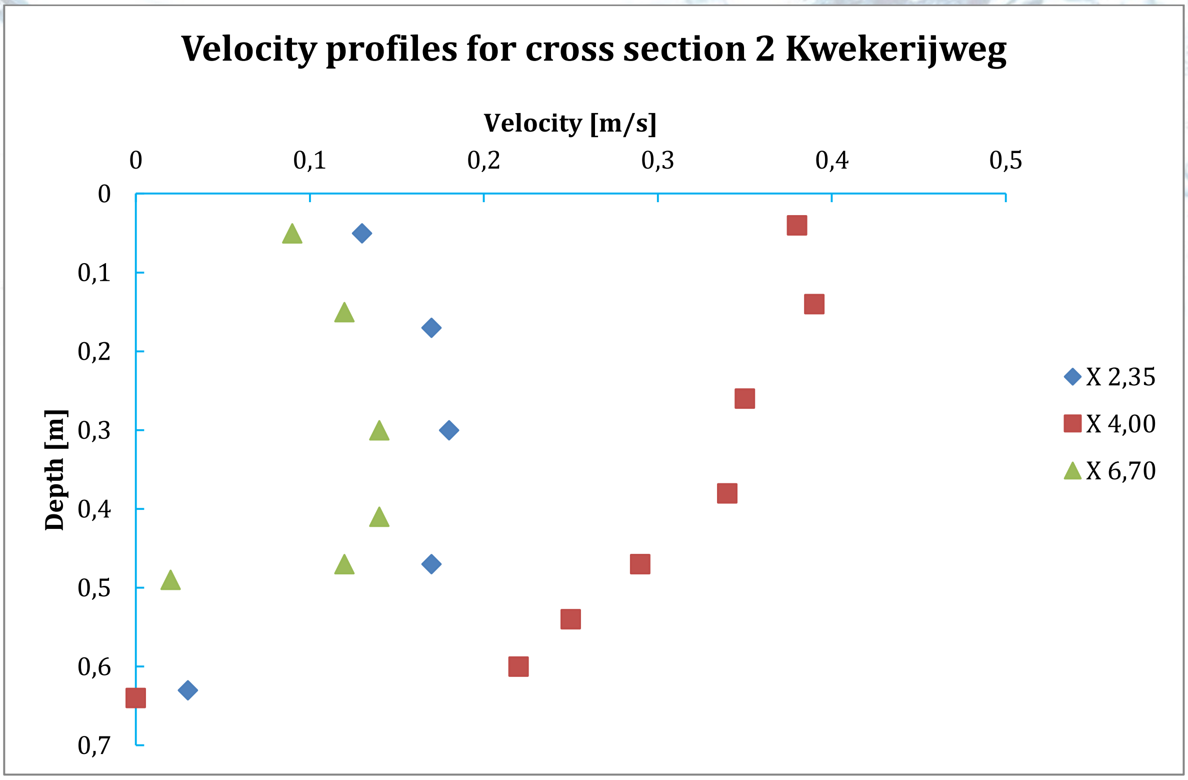

Figuur 0.10 Snelheidsprofiel voor profiel 2 bij site #3. X 2,35 en 6,70 zijn de randen van de vegetatie en X 4,00 is het midden van de geul.

CONCLUSIES EN AANBEVELINGEN

- Op basis van de gedane metingen is een vrij compleet beeld te schetsen van de hydraulica van de Lage Raam in deze gebieden;
- De nauwkeurigheid in de metingen is in de orde grootte 5-10%, dit is in lijn met de nauwkeurigheid van de StreamPro;
- De snelheidsprofielen in de nabijheid van de vegetatie zijn onbetrouwbaar, dit komt mede door het blokkeren van de beams door de vegetatie;
- De metingen zijn te gebruiken om een inschatting te maken van de ruwheid tussen twee transecten;
- De metingen zijn te gebruiken om modellen te valideren op afvoeren, de puntmetingen kunnen gebruikt worden de kwaliteit van de stroomsnelheid in modellen te beoordelen;
- Er heeft nu nog geen nabewerking op de data plaatsgevonden, dit kan de kwaliteit bevorderen van de gegevens;

- Voor toekomstige meetcampagnes kan het raadzaam zijn om meer puntmetingen te doen in en rondom de vegetatie, de verwachting is wel dat er weinig tot geen water stroomt door de vegetatie.

Beoordeling vegetatie-opnames Lage Raam van 15-9-2016

Op locatie 1 en 2 zijn vegetatie-opnames uitgevoerd volgens de protocollen volgens de KRW; op locatie 3 is een 'snelle' opname uitgevoerd van de watervegetatie, die een redelijke (maar niet volledige) indruk geeft van de vegetatiesamenstelling.

De vegetatie-opnames zijn beoordeeld met behulp van het programma QBWat (versie met KRW-maatlatten van 2012). De water- en oevervegetatie zijn hierbij elk afzonderlijk beoordeeld. Voor de Lage Raam is uitgegaan van het KRW-type R5 (Langzaam stromende middenloop/benedenloop op zand).

Referentiebeeld vegetatiesamenstelling R5

Onder optimale condities worden R5-beken sterk gevoed door schoon, vrij zacht kwelwater. Een aantal waterplanten scoort hoog voor dit type; voorbeelden van dergelijke soorten zijn Grote waterranonkel (*Ranunculus peltatus*), Haaksterrenkroos (*Callitriche brutia*), Dotterbloem (*Caltha palustris*), Bittere veldkers (*Cardamine armara*), Bronmos (*Fontinalis antipyretica*), Waterviolier (*Hottonia palustris*), Drijvende waterweegbree (*Luronium natans*), Teer vederkruid (*Myriophyllum alterniflorum*), Rossig fonteinkruid (*Potamogeton alpinus*) en Duizendknoopfonteinkruid (*P. polygonifolius*).

Onderstaand zijn de KRW-beoordelingen besproken.

Beoordeling locatie 1 Lage Raam

- Score deelmaatlat water groeivormen: 0,62 (water)
- Score deelmaatlat water soorten: 0,11 (water)

- Score deelmaatlat oever groeivormen: 0,14 (oever)
- Score deelmaatlat oever soorten: 0,00 (oever)

Opname water

De deelmaatlatscore voor de abundantie van de water-opname scoort goed (0,62). De deelmaatlat van de soortensamenstelling scoort daarentegen slecht (0,11). Geen van de bovengenoemde goed scorende soorten zijn tijdens de bemonstering aangetroffen. Verder valt op dat Drijvend fonteinkruid en Schedefonteinkruid een negatieve score krijgen, met andere woorden: zij verlagen de EKR-score. Dit is vermoedelijk het gevolg van de verstuwing in combinatie met de eutrofiering.

Hierbij moet opgemerkt worden dat Mirja Kits (Waterschap Aa en Maas) in mei 2016 lage bedekkingen van bloeiende Waterranonkels had gezien. Zeer waarschijnlijk is dit Grote waterranonkel (*R. peltatus*);

als deze soort in een opname groeit, dan krijgt deze een hoge score (zie opname locatie 2). Een opname in de juiste tijd van het jaar (eind mei/juni) levert op deze locatie waarschijnlijk een duidelijk hogere EKR-score op de soortenmaatlat.

Opname oever

De deelmaatlat van de groeivormen op de oever levert een lage EKR-score; er groeit geen bos op de oever en de bedekking van helofyten is waarschijnlijk te hoog. De EKR-score van de oever is 0, dit komt ook door een negatieve score van eutrafente soorten als Liesgras en Rietgras.

Beoordeling locatie 2 Lage Raam

- Score deelmaatlat water groeivormen: 0,72 (water)
- Score deelmaatlat water soorten: 0,53 (water)
- Score deelmaatlat oever groeivormen: 0,34 (oever)
- Score deelmaatlat oever soorten: 0,55 (oever)

In dit traject was de bodem zandiger in vergelijking met locatie 1, en groeide de vegetatie meer 'patchy'. Deze structuurvariatie zorgde ook voor een meer gevarieerde soortensamenstelling, met een hoger aandeel van kenmerkende soorten voor R5. Zo werd er onder meer enkele planten van Grote waterranonkel (*Ranunculus peltatus*) gevonden, een indicator van betere kwaliteit. Deze betere kwaliteit gold ook voor de oevervegetatie.

Beoordeling locatie 3 Lage Raam

- Score deelmaatlat water groeivormen: 0,60 (water)
- Score deelmaatlat water soorten: 0,26 (water)

Dit traject van de beek was zeer rijk aan ijzer; het water has een sterke roestkleur. De deelmaatlatscore van de groeivormen is goed; die van de soortensamenstelling ontoereikend. Gezien de slechte bereikbaarheid van deze locatie (en de geringe hoeveelheid tijd) zijn vermoedelijk niet alle soorten aangetroffen.

Sediment and water depth measurements in the Lage Raam Sept. measurement campaign

Red line: hard bed

Blue line: top of the soft sediment layer deposited on the original bed

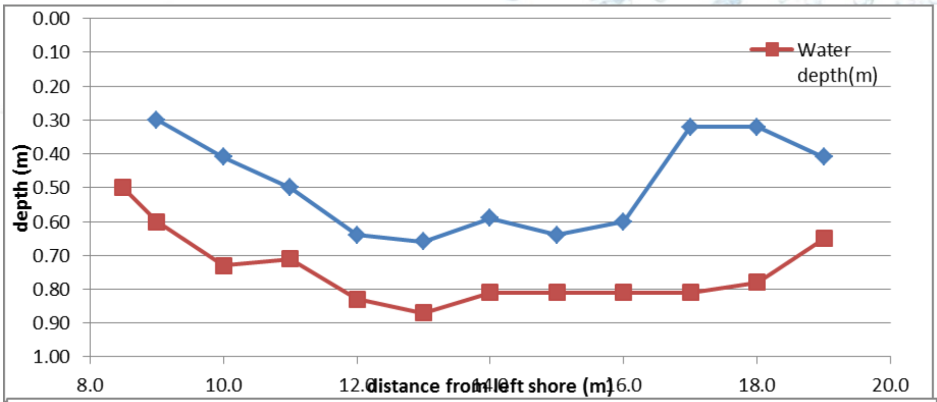

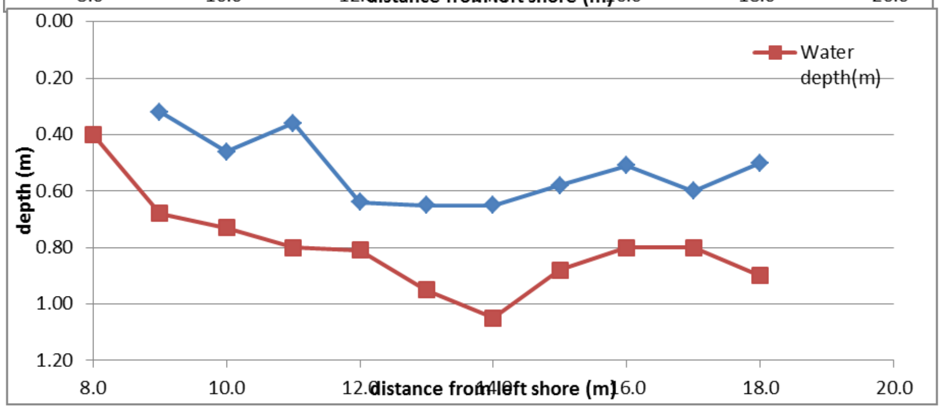

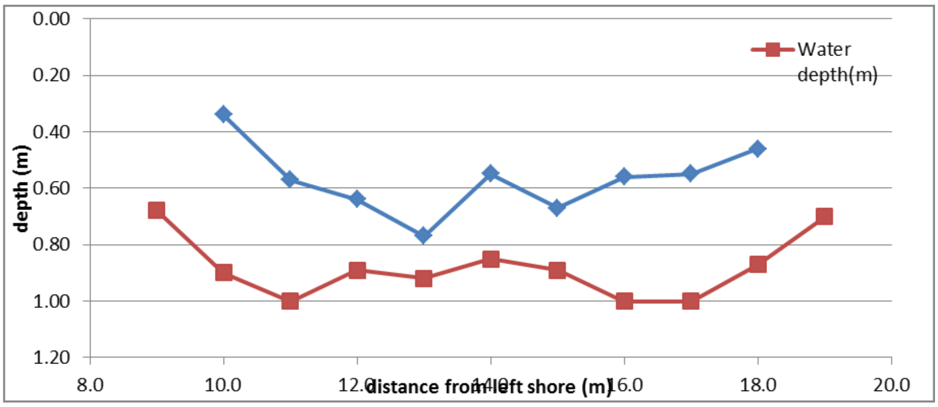

www.knowh2o.nl Watertorenweg 12 6571 CB BERG EN DAL t +31 (0)6 23 22 49 68
e info@knowh2o.nl Bank NL83 INGB 0006 2713 22 KvK 59020229

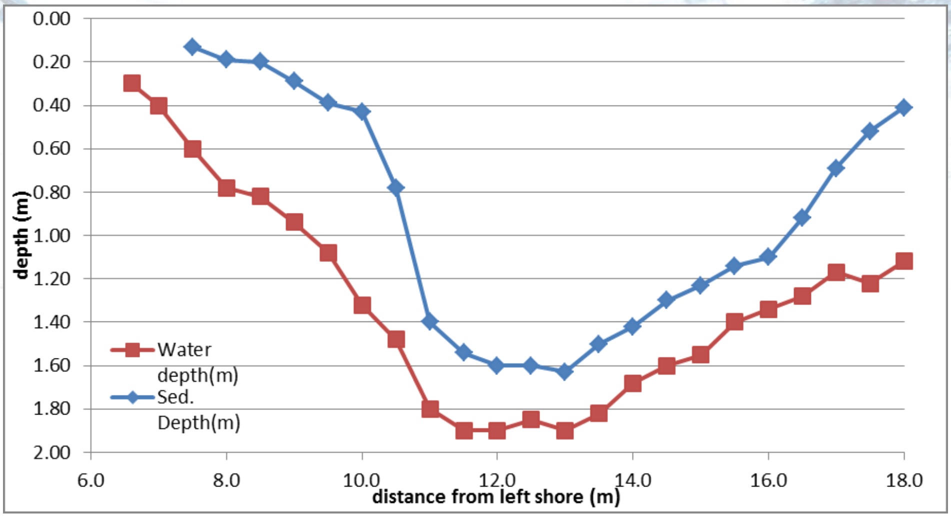
0.00
0.20
0.40
0.60
0.80
1.00
1.20
1.40
1.60
1.80
2.00
depth (m)
Water depth(m)
Sed. Depth(m)
6.0
8.0
10.0
12.0
14.0
16.0
18.0
distance from left shore (m)

APPENDIX D - DETAILS OF REC EXPERIMENTS (KOREA)

REC EXPERIMENTS OF VEGETATED FLOWS IN 2016

In the REC, vegetated flow measurements were carried out over the alternating (A1), cross-sectional (A2) and island (A2) patches. For the alternating patches, 3 patches were selected for comparative approaches on flows with different upstream flow conditions and different vegetation density. The cross-sectional and island patches were set to study flows over symmetric patches in a channel. The symmetric patches have the same densities as the alternating patches (i.e. dense and sparse). 3 sets of measurement for the alternating patches were conducted in 2016 while only 1 set of measurement for the cross-sectional & island patches was done due to unsuccessful vegetation growth. For experiments, flow velocity, water level and water depth were measured for submersed and emersed flow conditions.

Experimental setup

1. Alternating type (in A1)

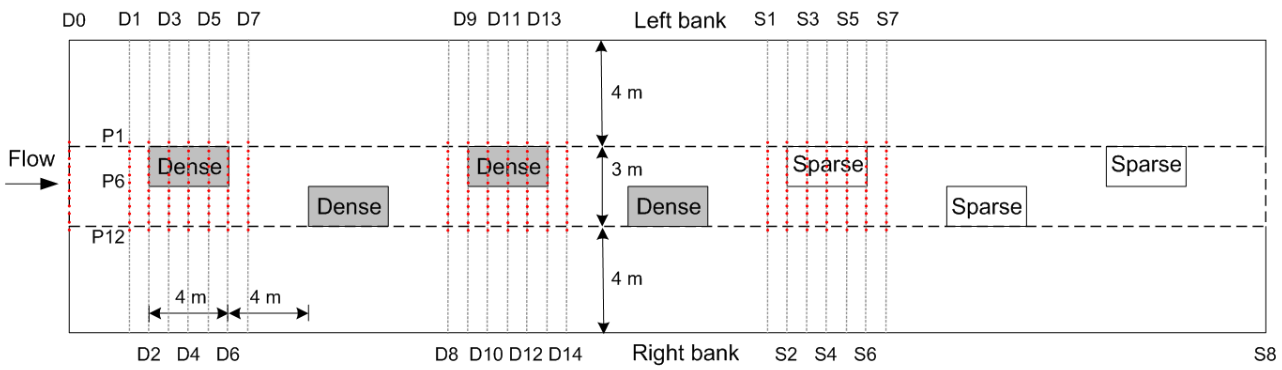

Target patches

Dense patch (DP) 1 & 3, Spare patch (SP) 1 (patches with measurement points marked in red dots in the figure)

Purpose of the selected patches

to compare flows between:

(1) 2 dense patches (DP 1 & 3) with different upstream flow conditions
(2) dense patch & sparse patch (DP 3 & SP 1)

Experimentation: Jun 27, Aug 01, Oct 24

Experimental conditions
Flows: Emergent (water depth of 0.6 m) & Submersed (water depth of 1.1 m)
Vegetation: based on vegetation parameters (height, stem thickness, number of leaves, leaf length)

Measurements
Velocity: ADV for: 7 cross sections in the longitudinal dir. (x); 15-18 locations in the cross-sectional dir. (y): every 10 cm points for non-vegetated flows and every 5 cm points over vegetated flows in the vertical dir. (z)
Water depth: manual ruler-bar measurements at identical x-y locations before & after an experiment
Water level: manual ruler-bar measurements at identical x-y locations

Others:
Sediment supply: sands (for bedload) were supplied from about 50 m upstream

2. Cross-sectional type (in A2)

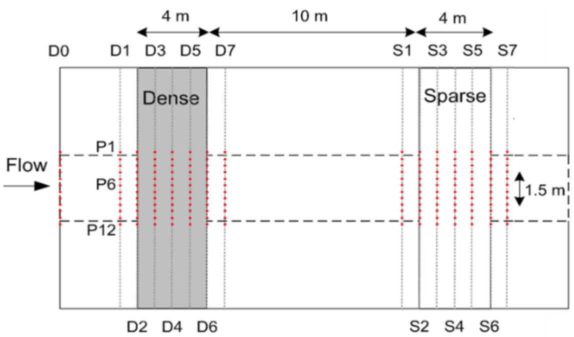

Target patches
Cross-sectional patches: DP 1 & SP 1

Experimentation: Jun 27

Experimental conditions & measurements
Identical to the alternating patches measurements

Others

There were some problems in measurements. Firstly, willows did not grow uniformly over the patches, which is different from the patch design purpose. The non-uniform vegetation density caused concentrated flows through some less dense spaces. Secondly, due to debris of floated mowed grass, the water flow looked like being blocked around free surface, which led to the flow moving downward causing the significant scour.

3. Island type (in A2)

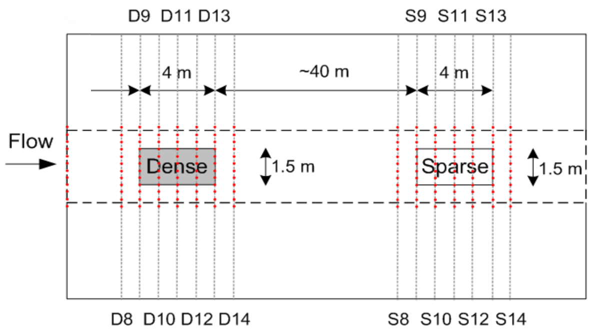

Target patches

Island patches: DP 1 & SP 1

Experimentation: Jun 27

Experimental conditions & measurements

Identical to the alternating patches measurements

Others

There were similar problems in measurements like the cross-sectional patches. Firstly, willows did not grow uniformly over the patches too. Secondly, there were also debris of floated mowed grass accumulating on the stems and leaves. However, it did not cause significant scour.

Preliminary results

Patch 01 (DP 1) of the alternating type: Emersed condition

Vertical distribution of the horizontal velocity (in the longitudinal diretion) over the vegetation patch along: the left edge; centerline; right edge; centerline of the channel section (green lines in the following figure)

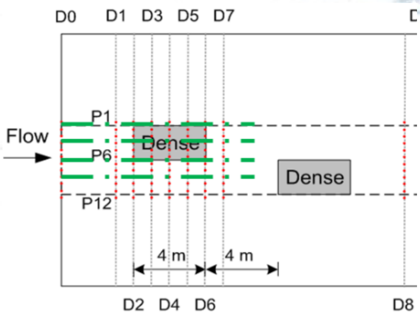

** Note that the left & right sides are determined on the direction from the upstream. The z-axis has z = 0 at – 5 cm from the free surface due to the ADV probe size. In the figures, the cross sections of D00 (black filled) and D06 (black empty) are located 1 m upstream and 1 m downstream of the patch respectively. The cross sections of D01~05 (red, orange, yellow, yellow-green, green) are located from the front edge to the rear edge with the distance of 1 m.

Over the vegetation patch

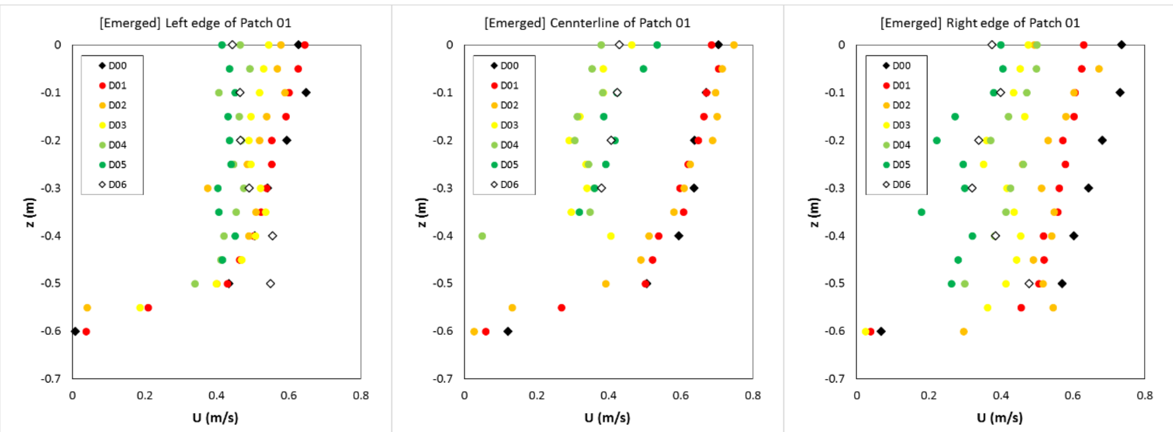

Along the channel section

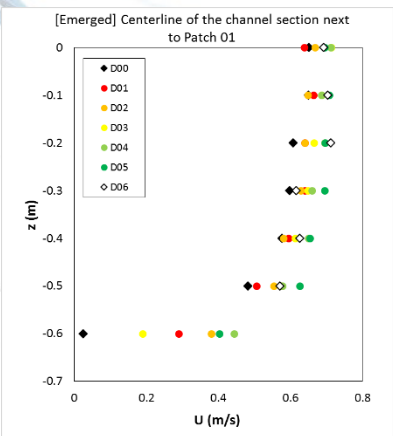

Patch 01 (DP 1) of the alternating type: Submersed condition

Vertical distribution of the horizontal velocity at the same locations as the emersed case

Over the vegetation patch

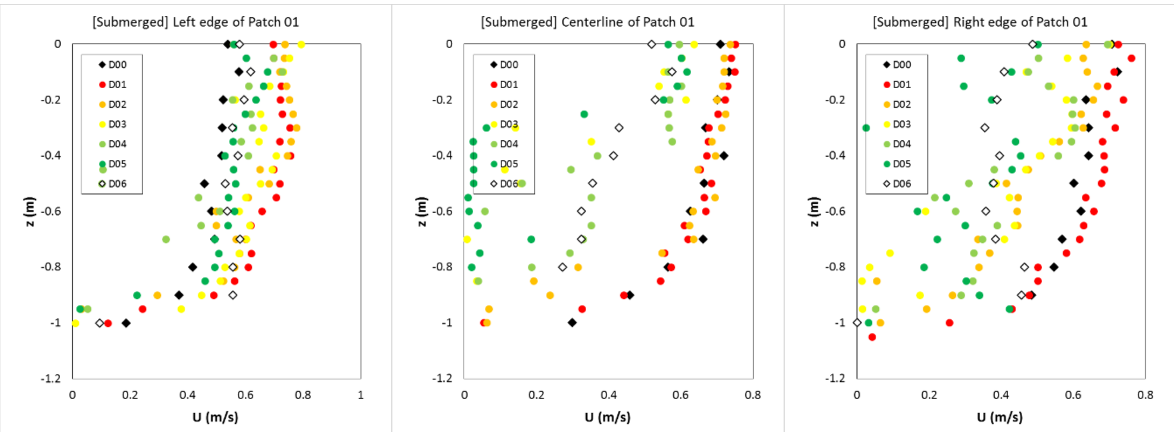

Along the channel section

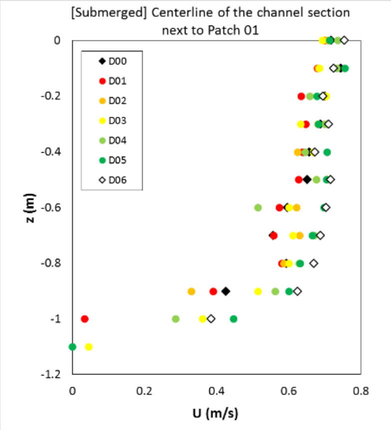
[Submerged] Centerline of the channel section
next to Patch 01
D00
D01
D02
D03
D04
D05
D06
z (m)
U (m/s)
0
-0.2
-0.4
-0.6
-0.8
-1
-1.2
0
0.2
0.4
0.6
0.8

ALL FIGURES - WATER LEVEL HEIGHT SPECTRA

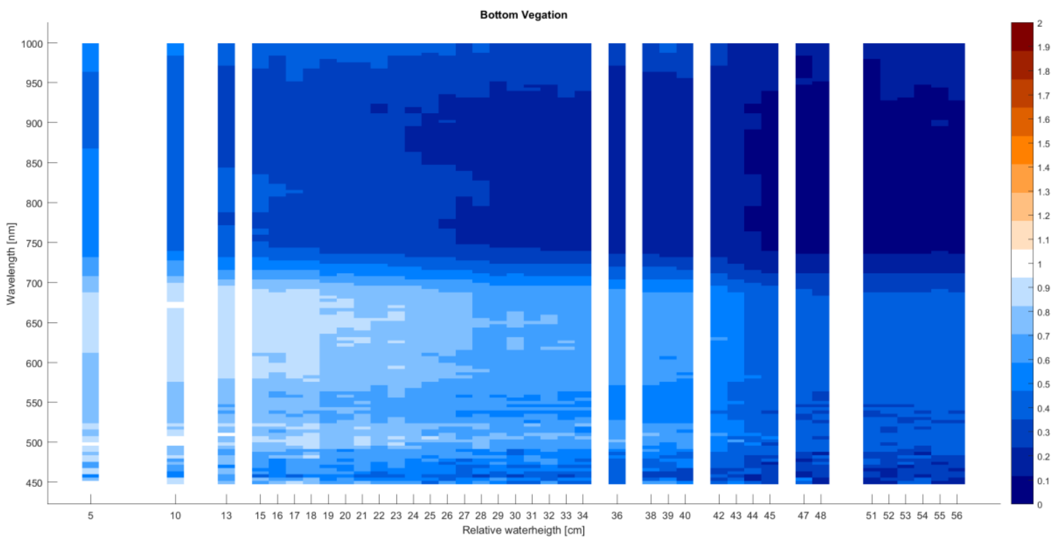

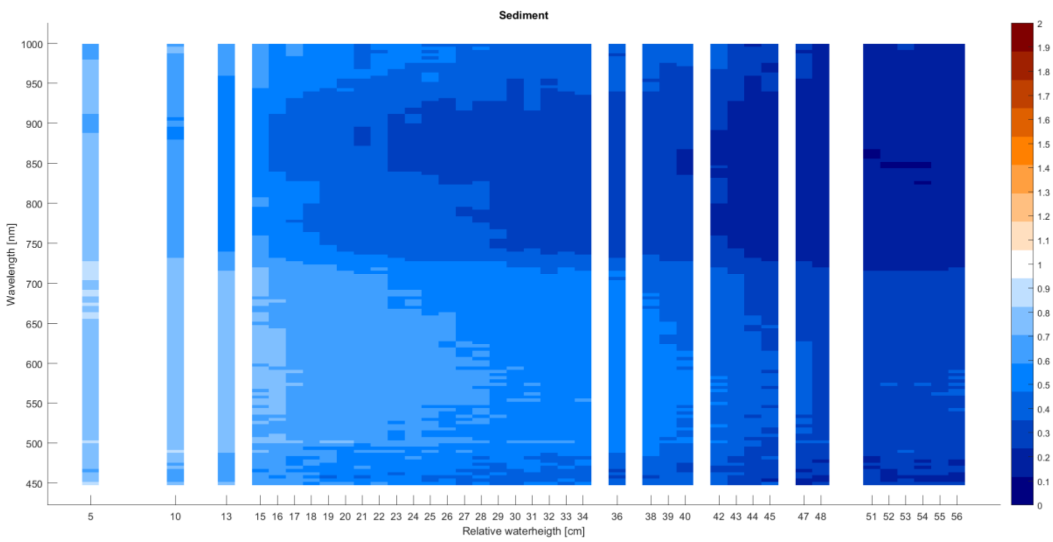

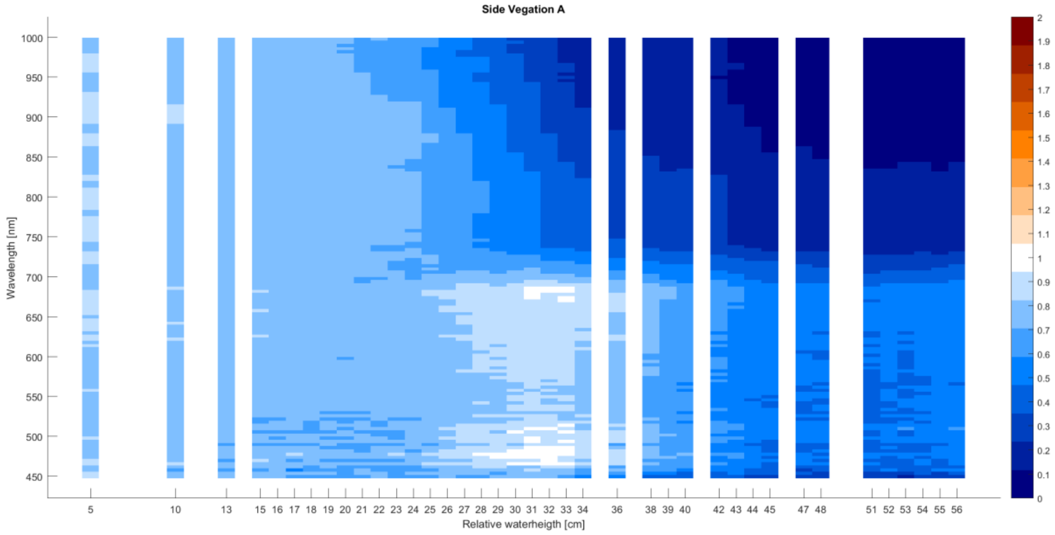
Side Vegation A
Wavelength [nm]
Relative waterheigth [cm]

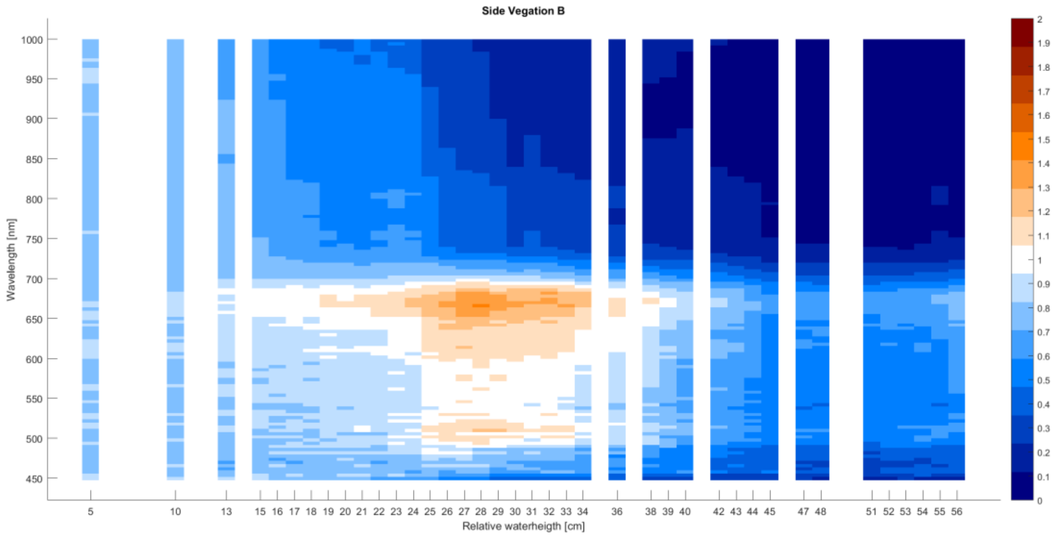
Side Vegation B
Wavelength [nm]
Relative waterheigth [cm]

Advies, Innovatie en Verbinding in Water

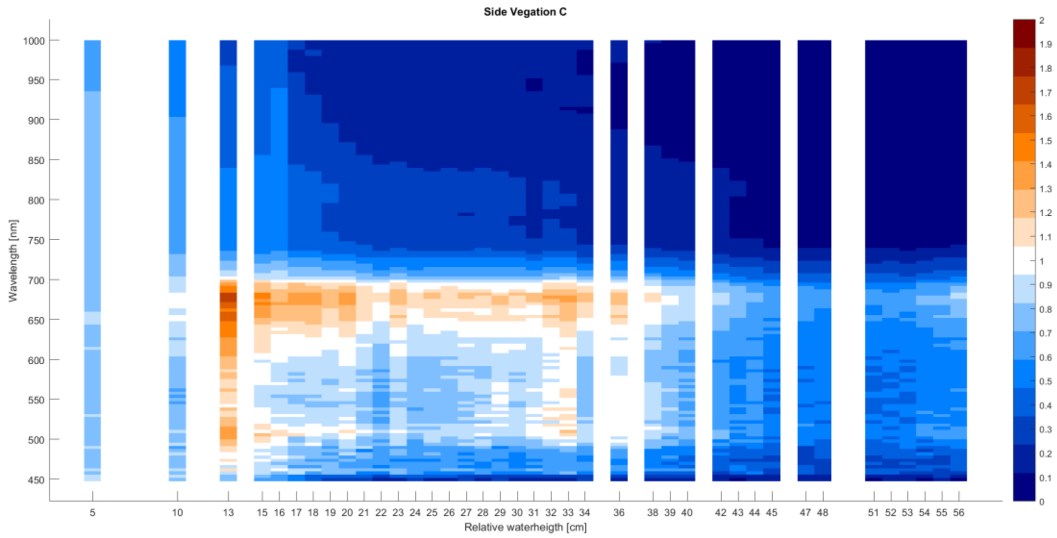

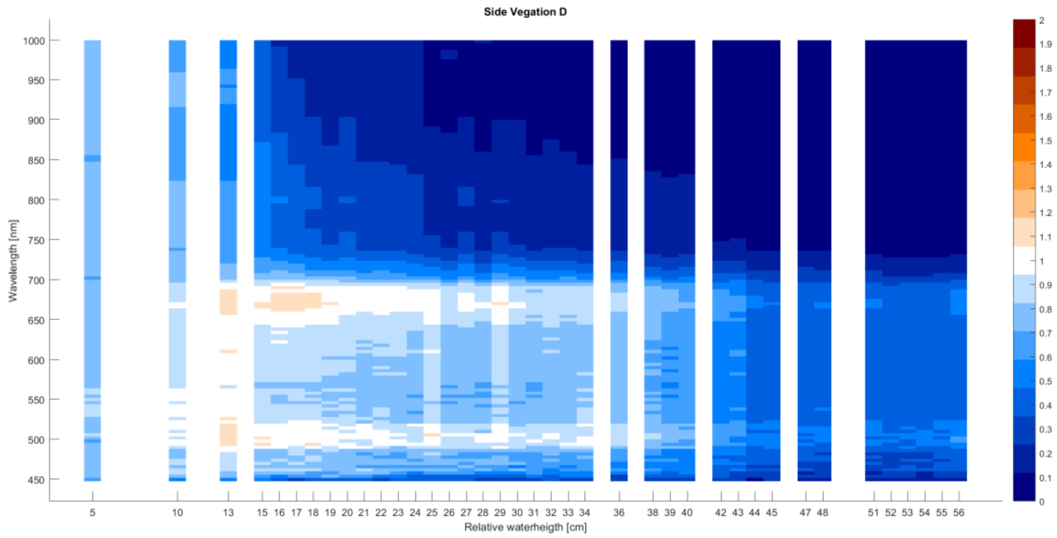

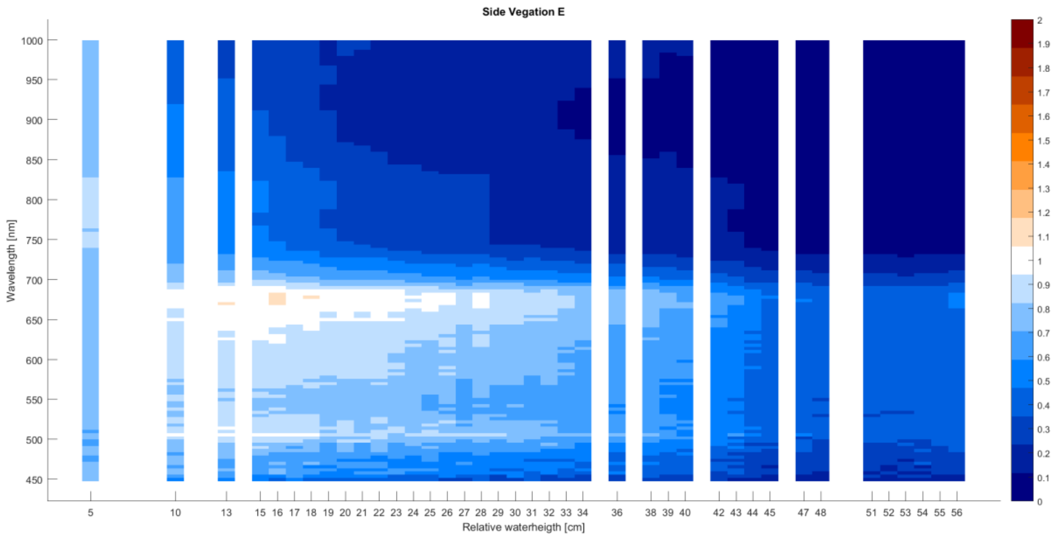
Side Vegation E
Wavelength [nm]
Relative waterheigth [cm]

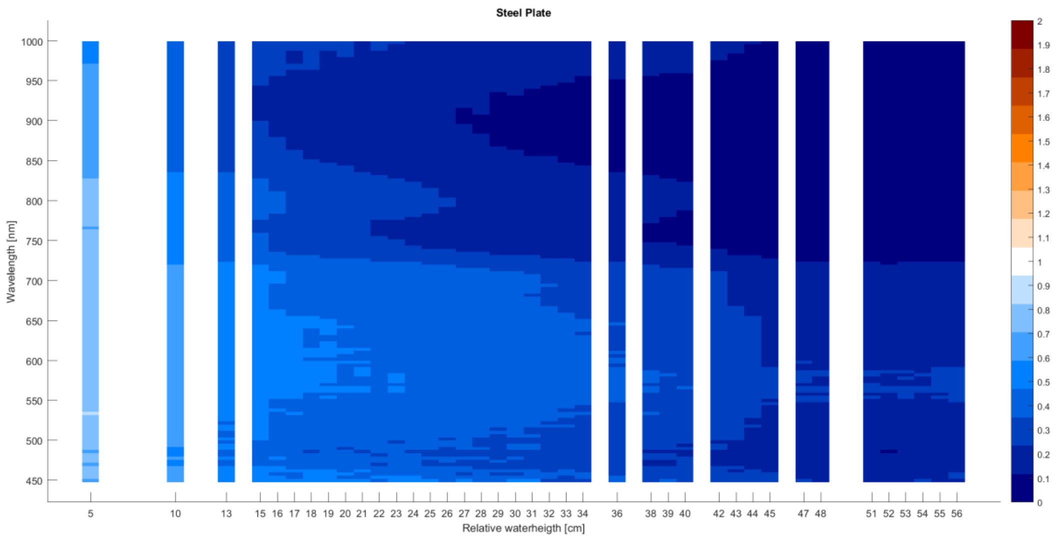
Steel Plate
Wavelength [nm]
Relative waterheigth [cm]

ALL FIGURES - WATER LEVEL HEIGHT AND CHANGES IN INDICES

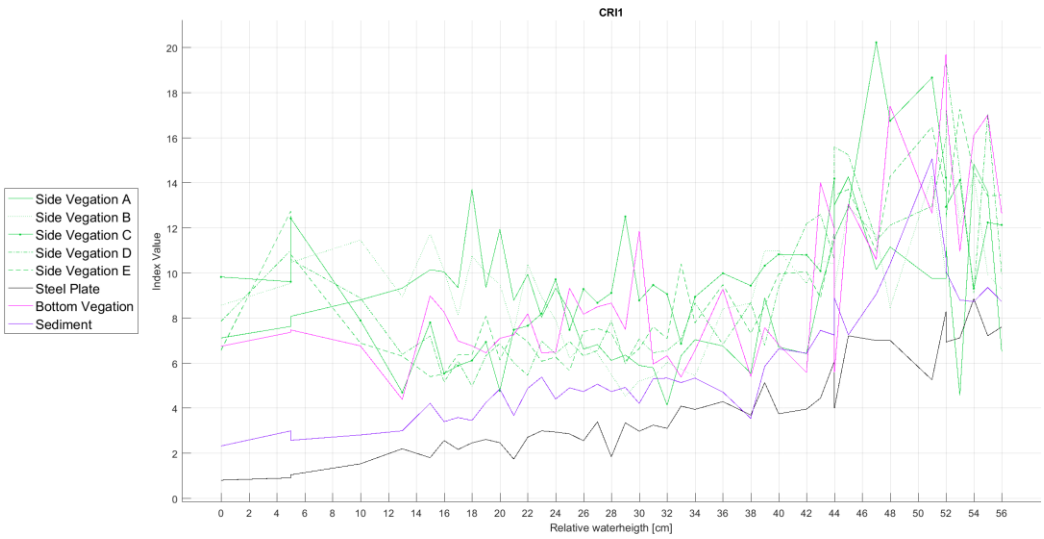

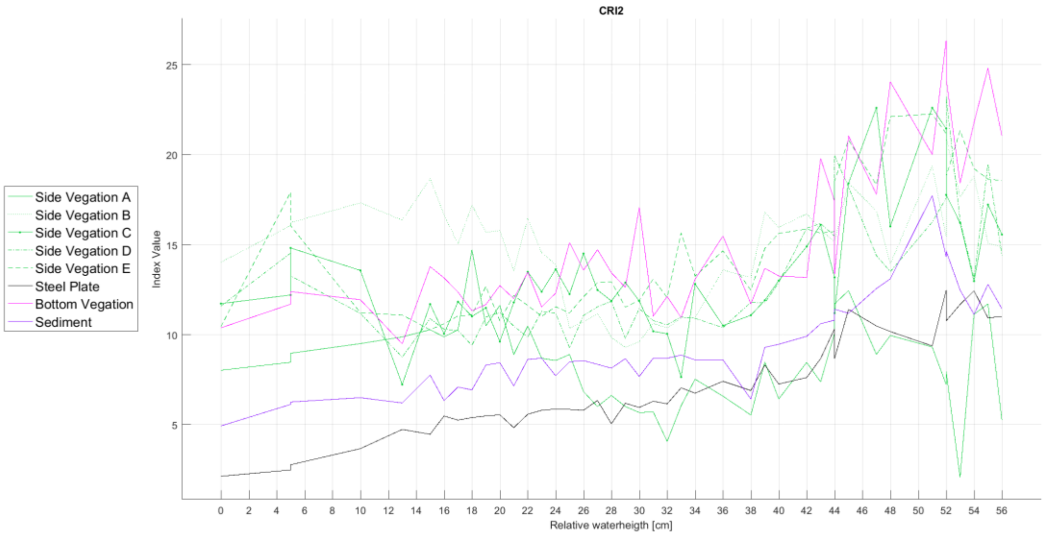
CRI2
Side Vegation A
Side Vegation B
Side Vegation C
Side Vegation D
Side Vegation E
Steel Plate
Bottom Vegation
Sediment
Index Value
Relative waterheigth [cm]

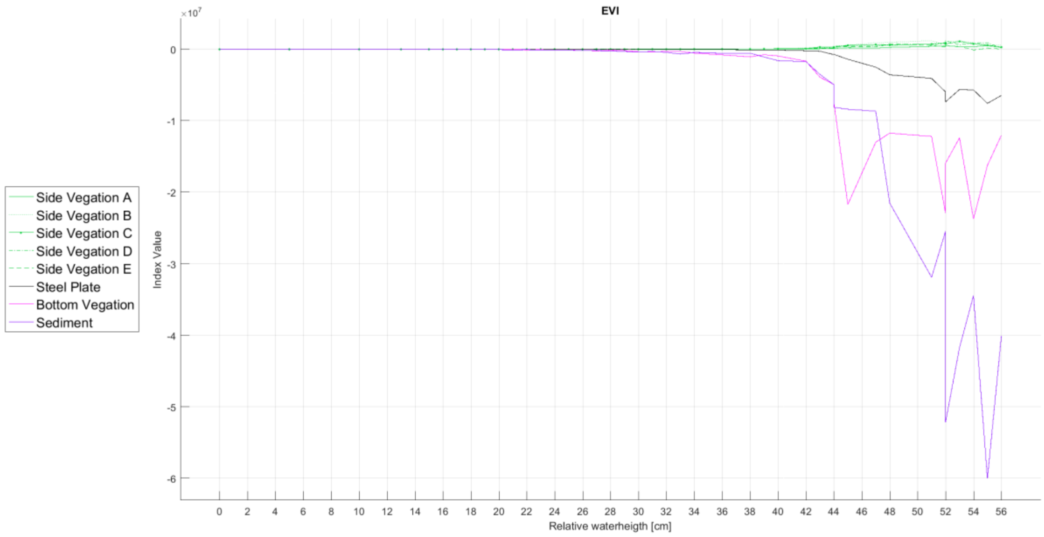
EVI
×10^7
Side Vegation A
Side Vegation B
Side Vegation C
Side Vegation D
Side Vegation E
Steel Plate
Bottom Vegation
Sediment
Index Value
Relative waterheigth [cm]


GNDVI
Index Value
Relative waterheigth [cm]
Side Vegation A
Side Vegation B
Side Vegation C
Side Vegation D
Side Vegation E
Steel Plate
Bottom Vegation
Sediment

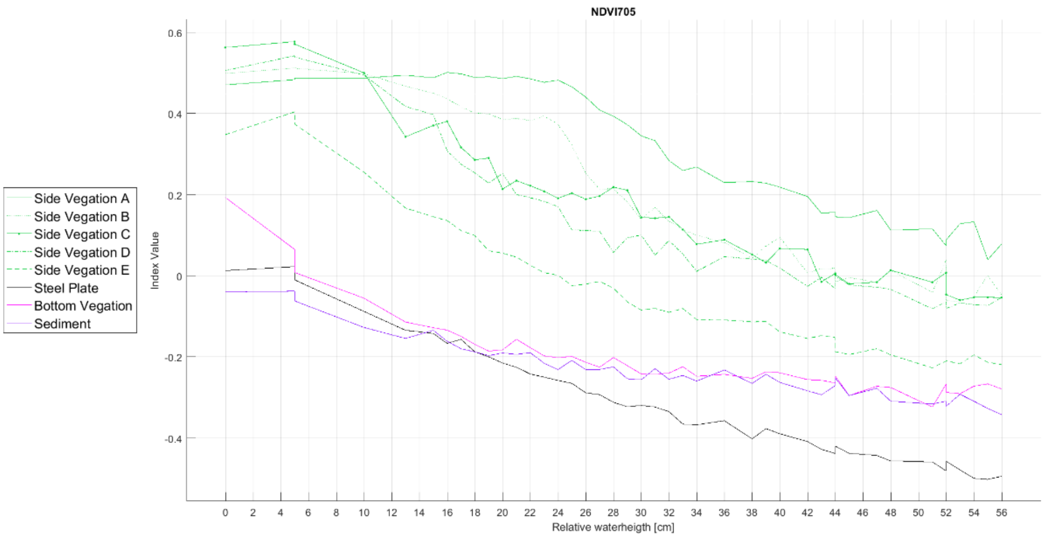
NDVI705
Index Value
Relative waterheigth [cm]
Side Vegation A
Side Vegation B
Side Vegation C
Side Vegation D
Side Vegation E
Steel Plate
Bottom Vegation
Sediment

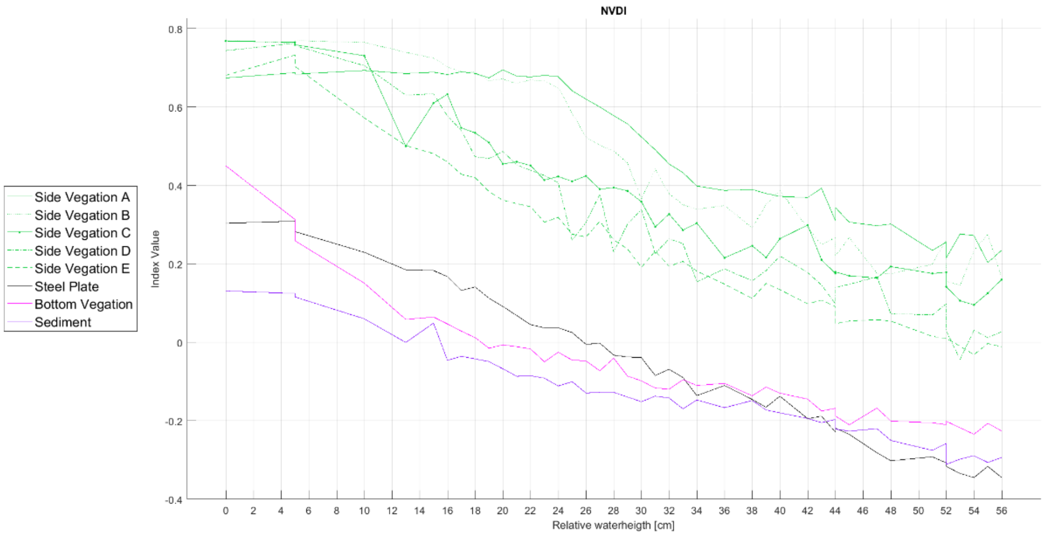
NVDI
Side Vegation A
Side Vegation B
Side Vegation C
Side Vegation D
Side Vegation E
Steel Plate
Bottom Vegation
Sediment
Index Value
Relative waterheigth [cm]

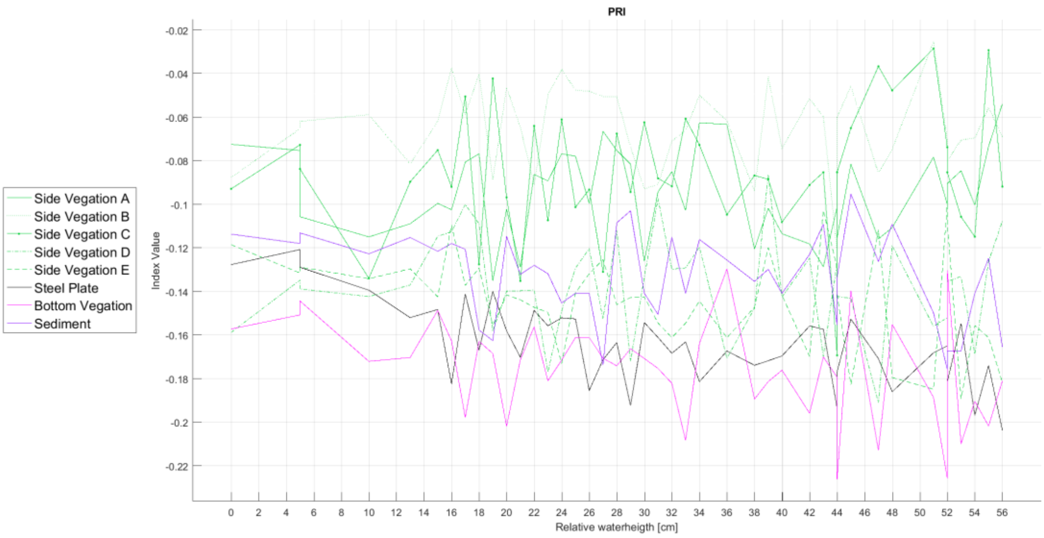
PRI
Side Vegation A
Side Vegation B
Side Vegation C
Side Vegation D
Side Vegation E
Steel Plate
Bottom Vegation
Sediment
Index Value
Relative waterheigth [cm]


PSRI
Side Vegation A
Side Vegation B
Side Vegation C
Side Vegation D
Side Vegation E
Steel Plate
Bottom Vegation
Sediment
Index Value
Relative waterheigth [cm]

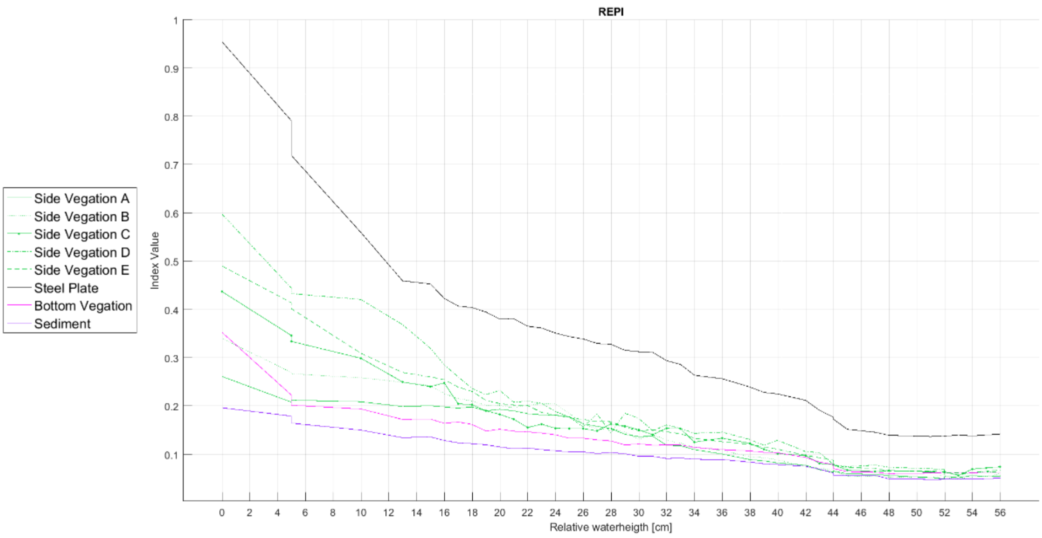
REPI
Side Vegation A
Side Vegation B
Side Vegation C
Side Vegation D
Side Vegation E
Steel Plate
Bottom Vegation
Sediment
Index Value
Relative waterheigth [cm]

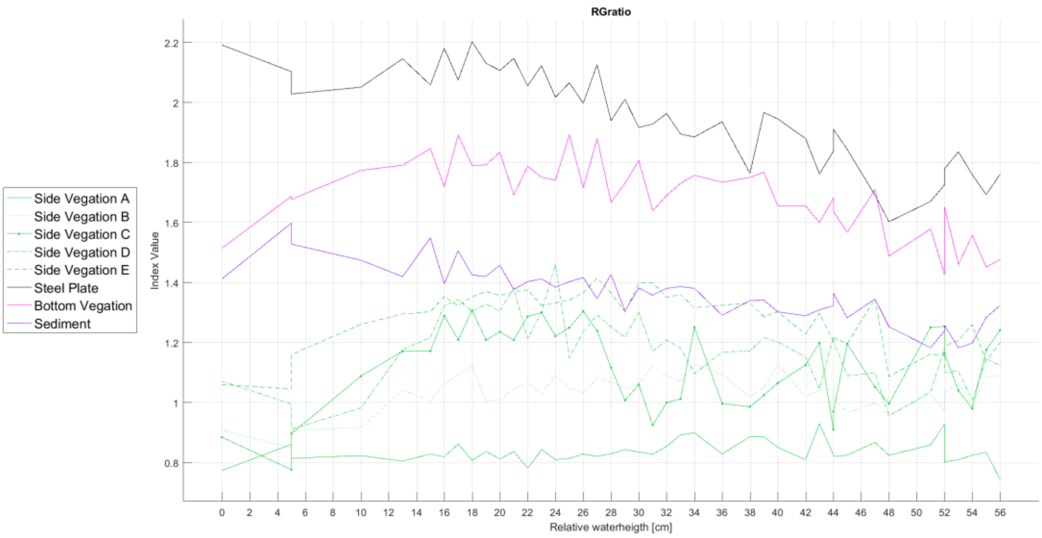
RGratio
Index Value
Relative waterheigth [cm]
Side Vegation A
Side Vegation B
Side Vegation C
Side Vegation D
Side Vegation E
Steel Plate
Bottom Vegation
Sediment

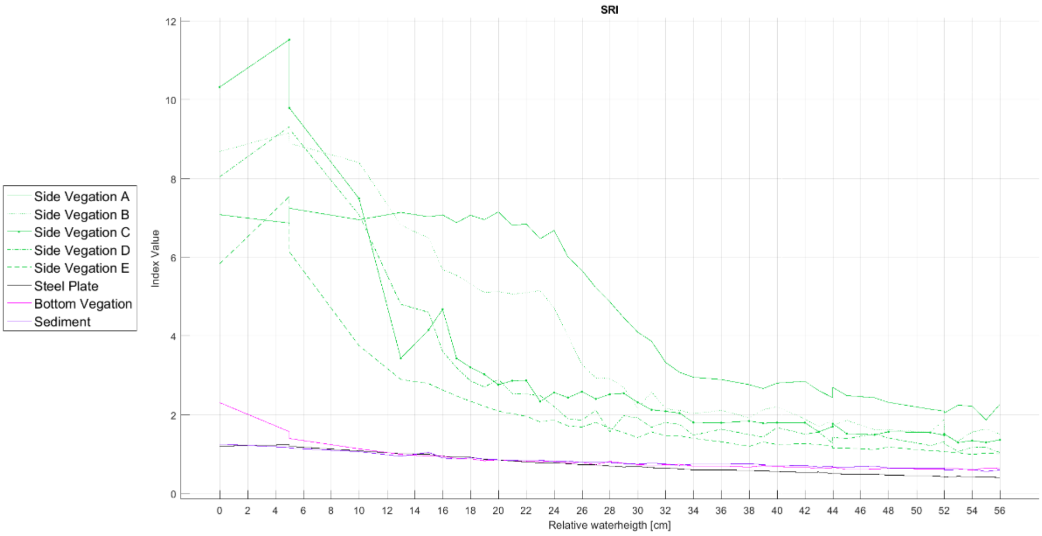
SRI
Index Value
Relative waterheigth [cm]
Side Vegation A
Side Vegation B
Side Vegation C
Side Vegation D
Side Vegation E
Steel Plate
Bottom Vegation
Sediment


VOG1
Side Vegation A
Side Vegation B
Side Vegation C
Side Vegation D
Side Vegation E
Steel Plate
Bottom Vegation
Sediment
Index Value
Relative waterheigth [cm]

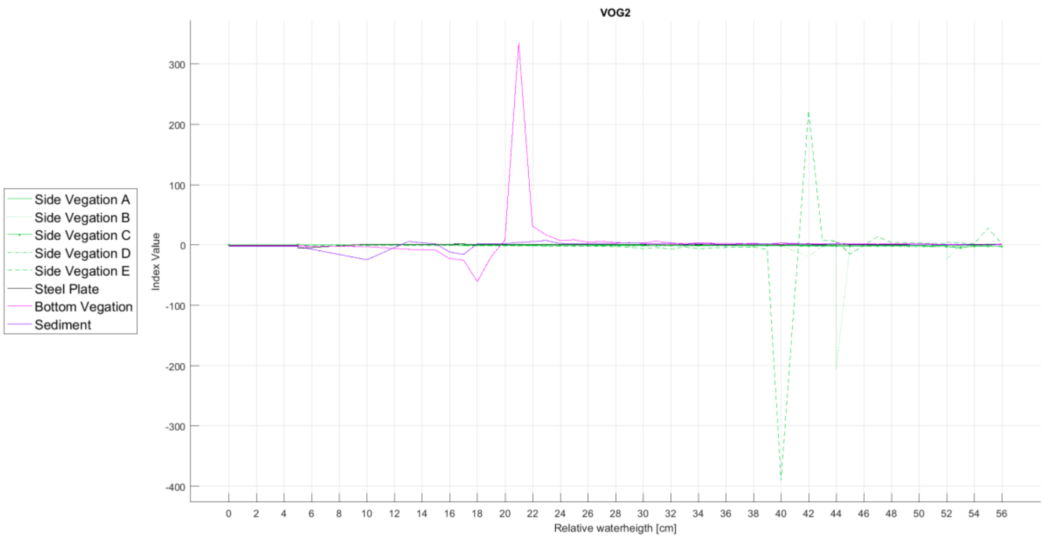
VOG2
Side Vegation A
Side Vegation B
Side Vegation C
Side Vegation D
Side Vegation E
Steel Plate
Bottom Vegation
Sediment
Index Value
Relative waterheigth [cm]

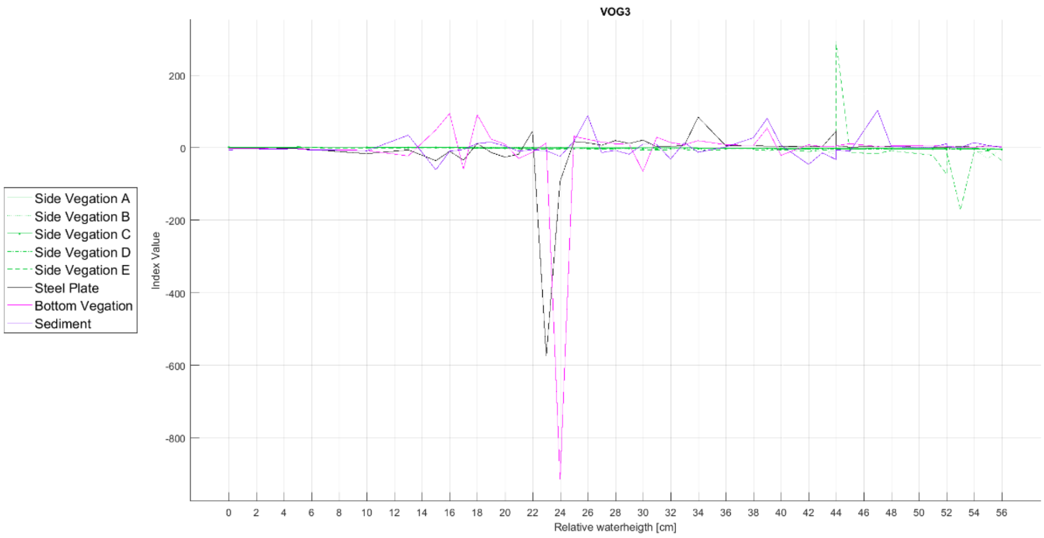
VOG3
Side Vegation A
Side Vegation B
Side Vegation C
Side Vegation D
Side Vegation E
Steel Plate
Bottom Vegation
Sediment
Index Value
200
0
-200
-400
-600
-800
0 2 4 6 8 10 12 14 16 18 20 22 24 26 28 30 32 34 36 38 40 42 44 46 48 50 52 54 56
Relative waterheigth [cm]

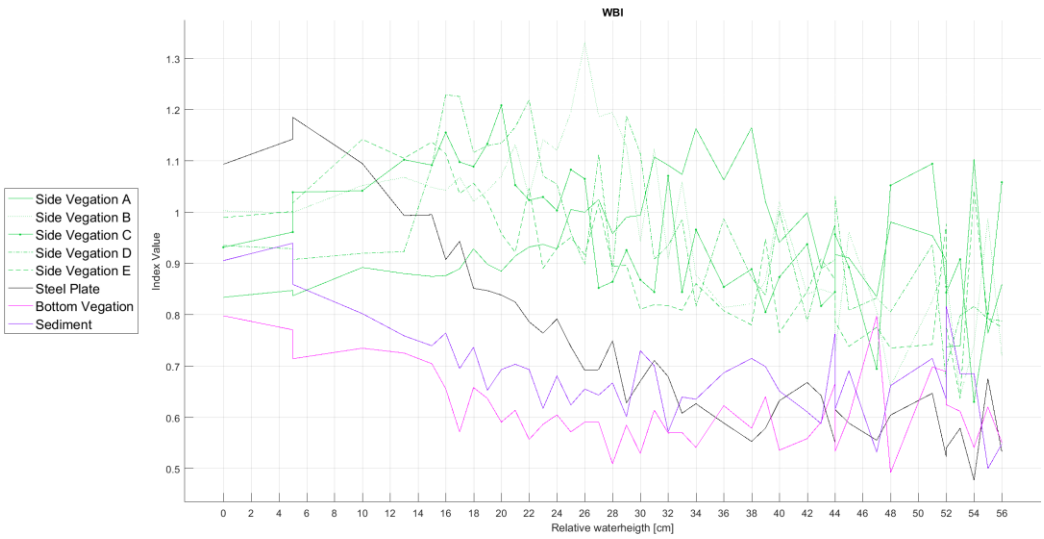
WBI
Side Vegation A
Side Vegation B
Side Vegation C
Side Vegation D
Side Vegation E
Steel Plate
Bottom Vegation
Sediment
Index Value
1.3
1.2
1.1
1
0.9
0.8
0.7
0.6
0.5
0 2 4 6 8 10 12 14 16 18 20 22 24 26 28 30 32 34 36 38 40 42 44 46 48 50 52 54 56
Relative waterheigth [cm]

ALL FIGURES - EFFECTS OF TURBIDITY

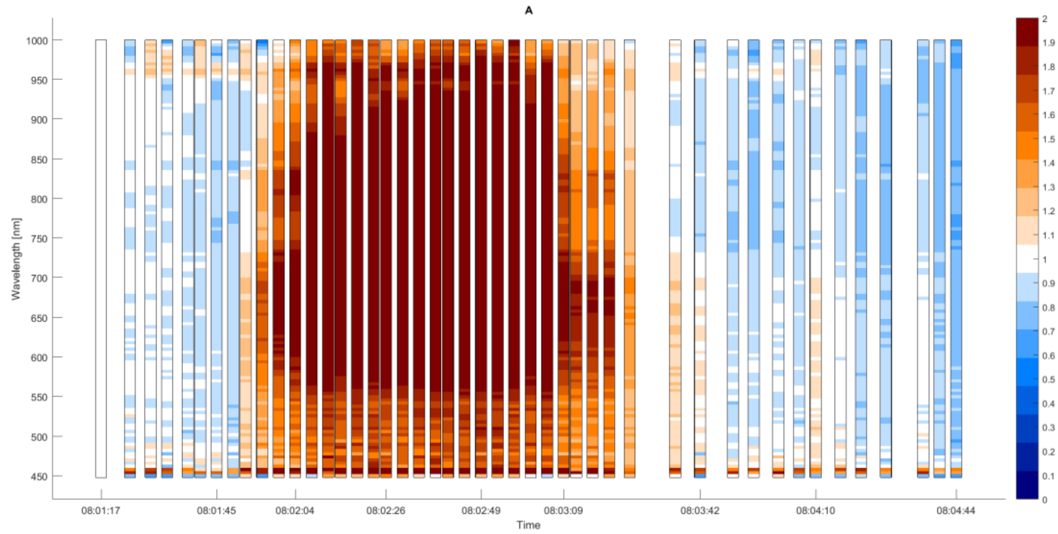

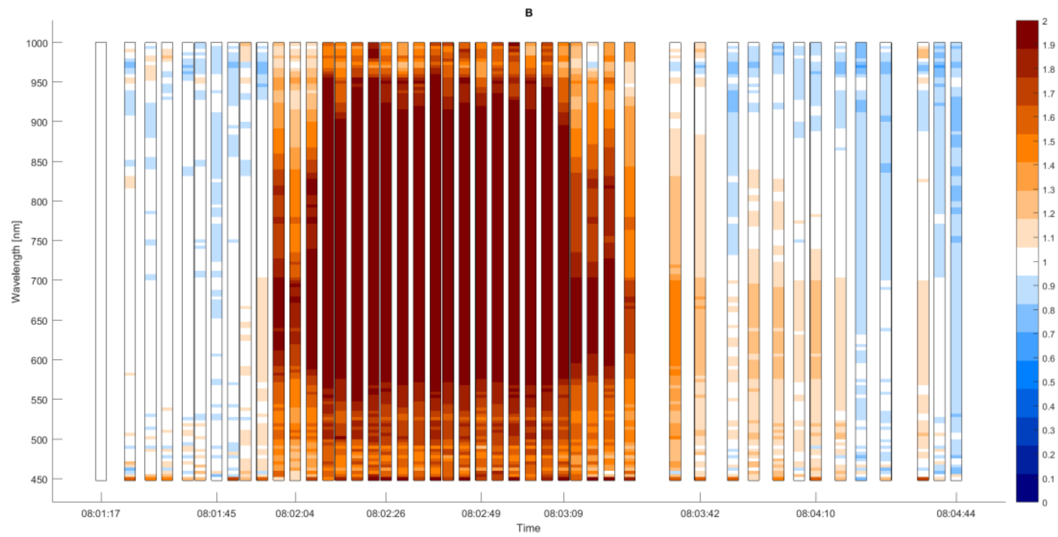

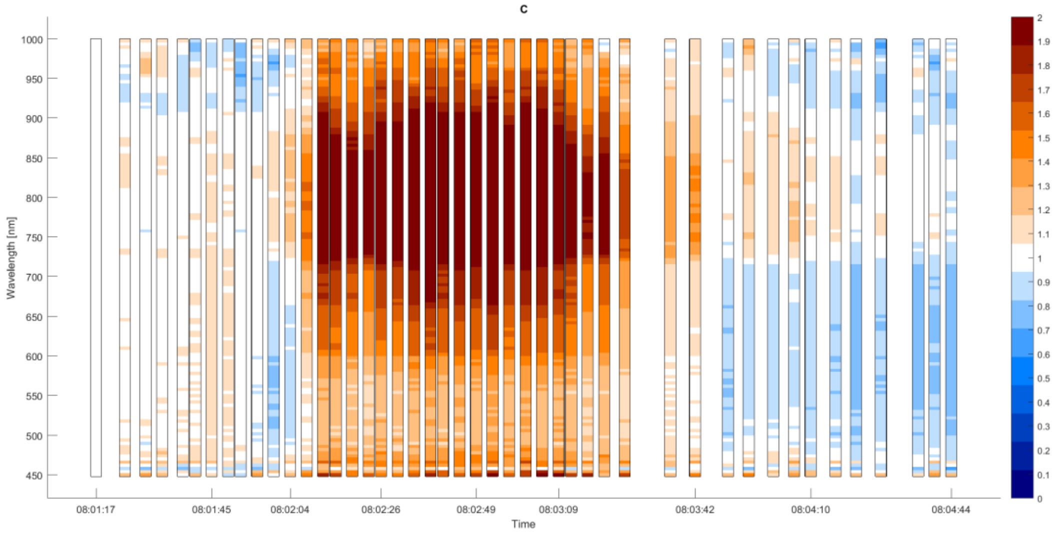
C
Wavelength [nm]
Time
08:01:17
08:01:45
08:02:04
08:02:26
08:02:49
08:03:09
08:03:42
08:04:10
08:04:44

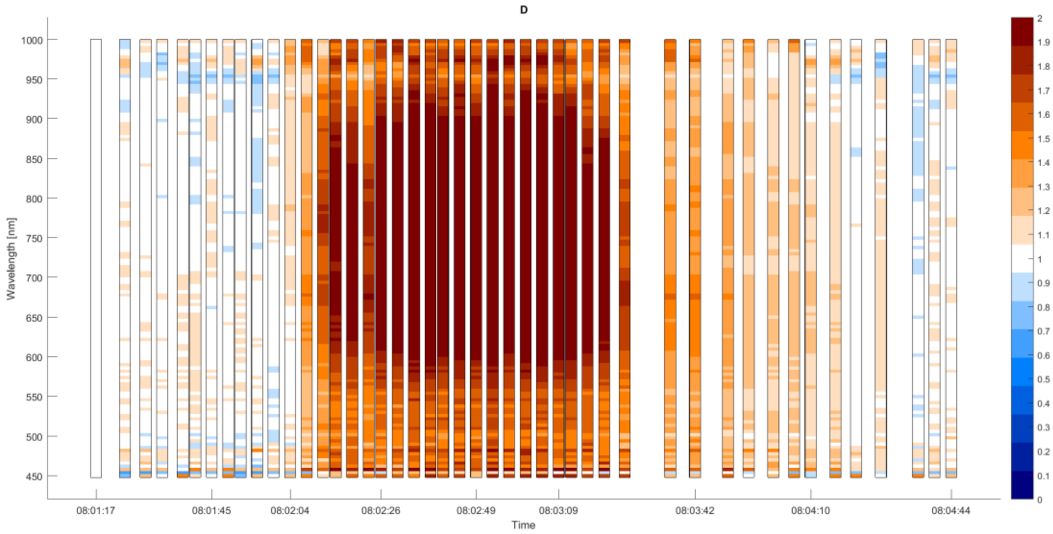
D
Wavelength [nm]
Time
08:01:17
08:01:45
08:02:04
08:02:26
08:02:49
08:03:09
08:03:42
08:04:10
08:04:44

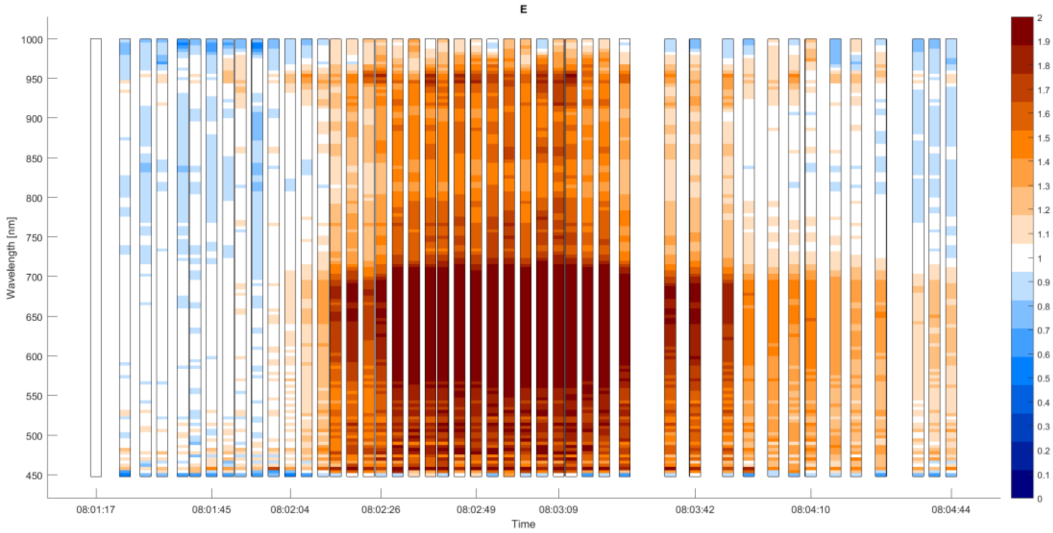
E
Wavelength [nm]
1000
950
900
850
800
750
700
650
600
550
500
450
08:01:17
08:01:45
08:02:04
08:02:26
08:02:49
08:03:09
08:03:42
08:04:10
08:04:44
Time
2
1.9
1.8
1.7
1.6
1.5
1.4
1.3
1.2
1.1
1
0.9
0.8
0.7
0.6
0.5
0.4
0.3
0.2
0.1
0

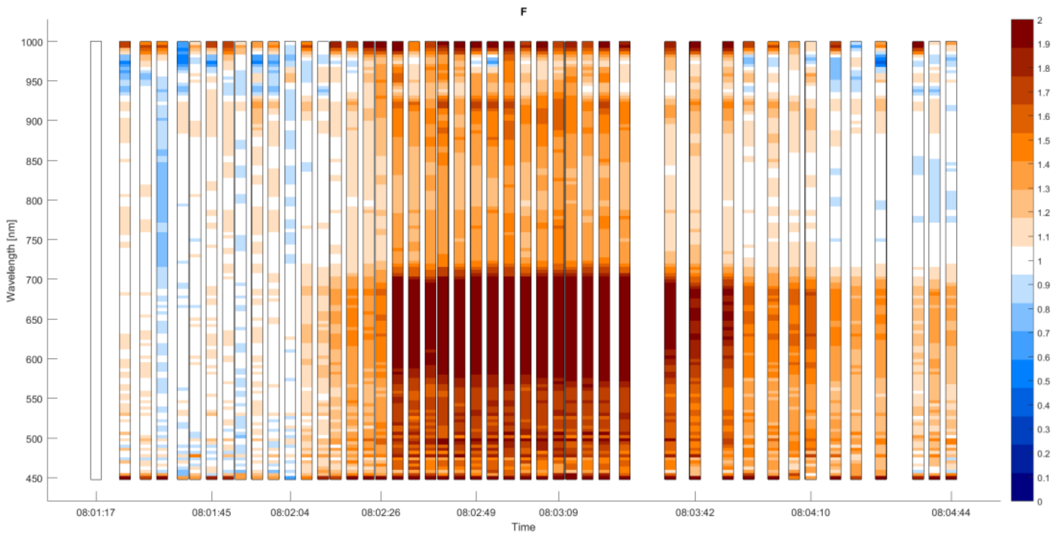
F
Wavelength [nm]
1000
950
900
850
800
750
700
650
600
550
500
450
08:01:17
08:01:45
08:02:04
08:02:26
08:02:49
08:03:09
08:03:42
08:04:10
08:04:44
Time
2
1.9
1.8
1.7
1.6
1.5
1.4
1.3
1.2
1.1
1
0.9
0.8
0.7
0.6
0.5
0.4
0.3
0.2
0.1
0

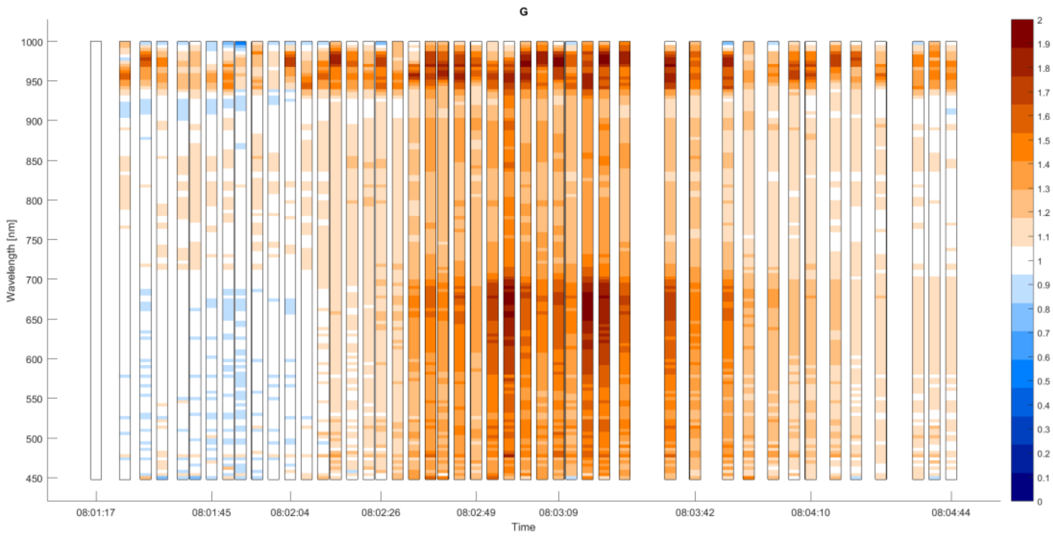
G
1000
950
900
850
800
750
700
650
600
550
500
450
Wavelength [nm]
08:01:17
08:01:45
08:02:04
08:02:26
08:02:49
08:03:09
08:03:42
08:04:10
08:04:44
Time
2
1.9
1.8
1.7
1.6
1.5
1.4
1.3
1.2
1.1
1
0.9
0.8
0.7
0.6
0.5
0.4
0.3
0.2
0.1
0

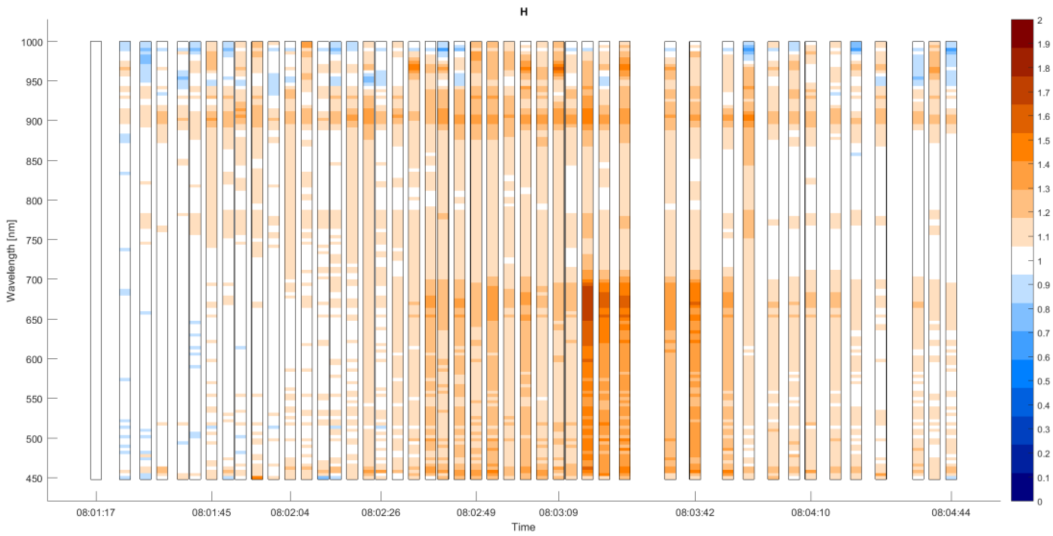
H
1000
950
900
850
800
750
700
650
600
550
500
450
Wavelength [nm]
08:01:17
08:01:45
08:02:04
08:02:26
08:02:49
08:03:09
08:03:42
08:04:10
08:04:44
Time
2
1.9
1.8
1.7
1.6
1.5
1.4
1.3
1.2
1.1
1
0.9
0.8
0.7
0.6
0.5
0.4
0.3
0.2
0.1
0

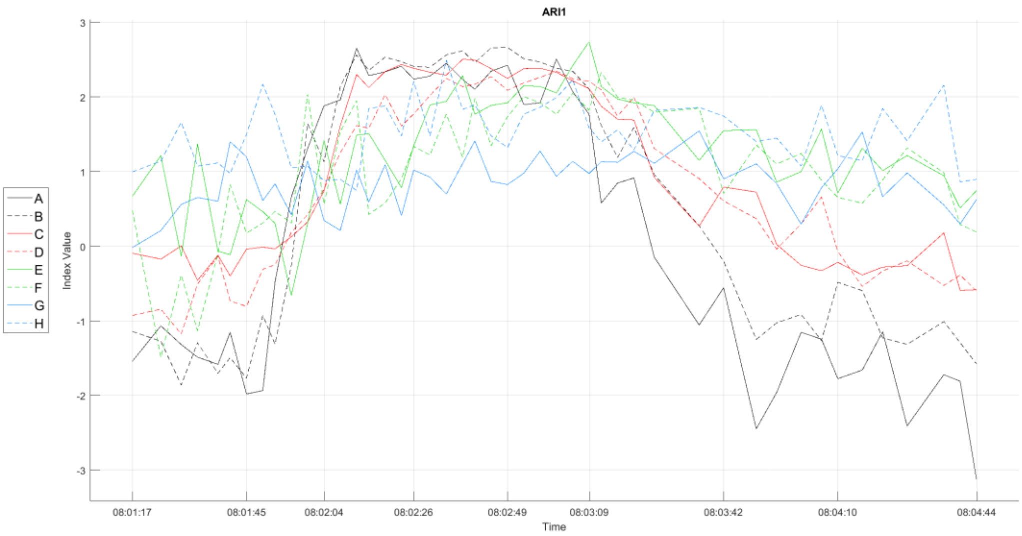
ARI1
Index Value
Time
A
B
C
D
E
F
G
H
3
2
1
0
-1
-2
-3
08:01:17
08:01:45
08:02:04
08:02:26
08:02:49
08:03:09
08:03:42
08:04:10
08:04:44

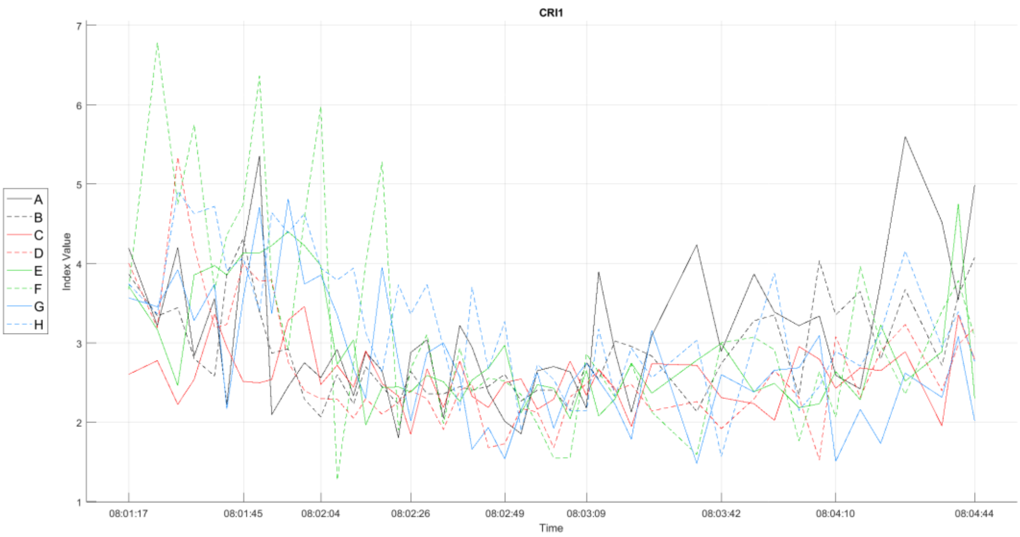
CRI1
Index Value
Time
A
B
C
D
E
F
G
H
7
6
5
4
3
2
1
08:01:17
08:01:45
08:02:04
08:02:26
08:02:49
08:03:09
08:03:42
08:04:10
08:04:44

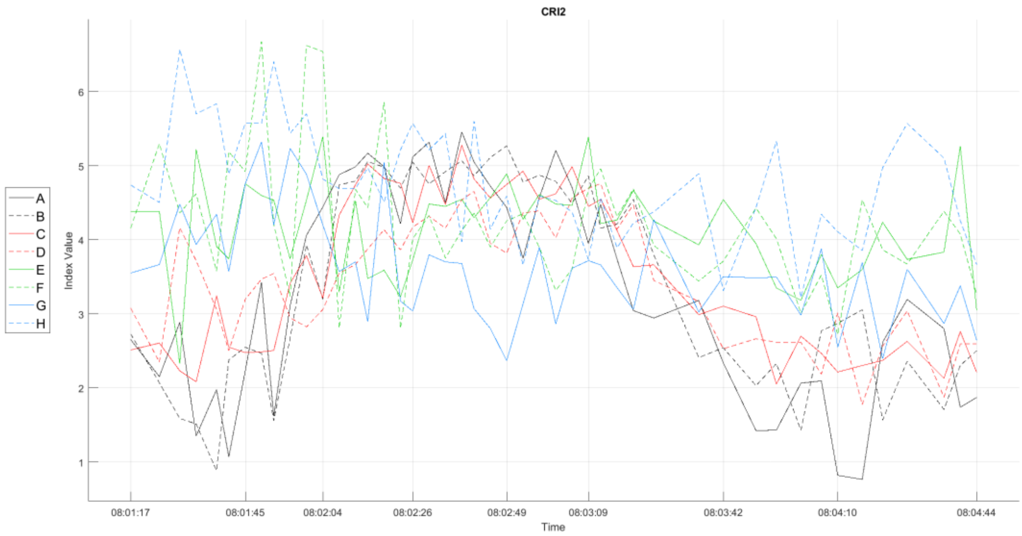
CRI2
Index Value
Time
08:01:17
08:01:45
08:02:04
08:02:26
08:02:49
08:03:09
08:03:42
08:04:10
08:04:44
A
B
C
D
E
F
G
H

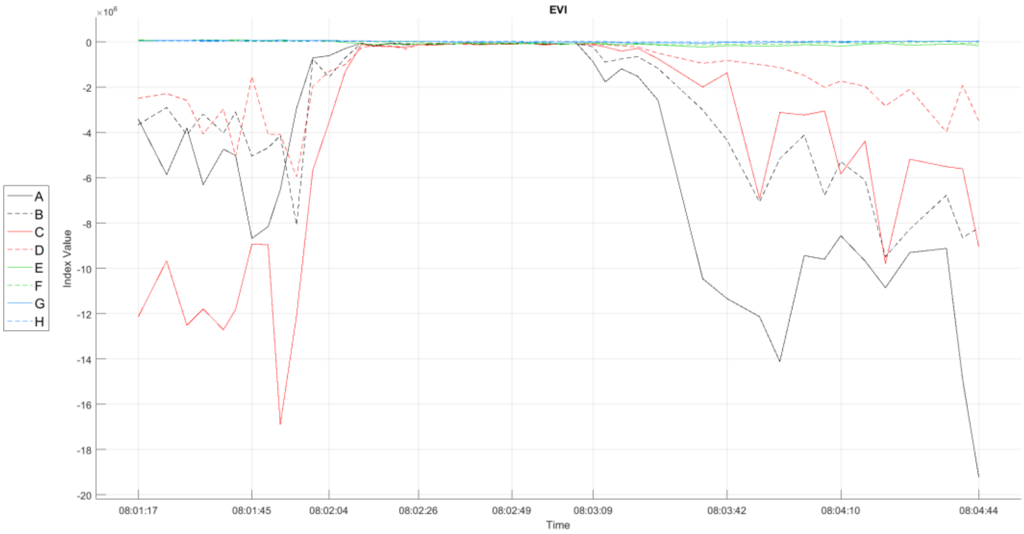
EVI
Index Value
Time
08:01:17
08:01:45
08:02:04
08:02:26
08:02:49
08:03:09
08:03:42
08:04:10
08:04:44
A
B
C
D
E
F
G
H

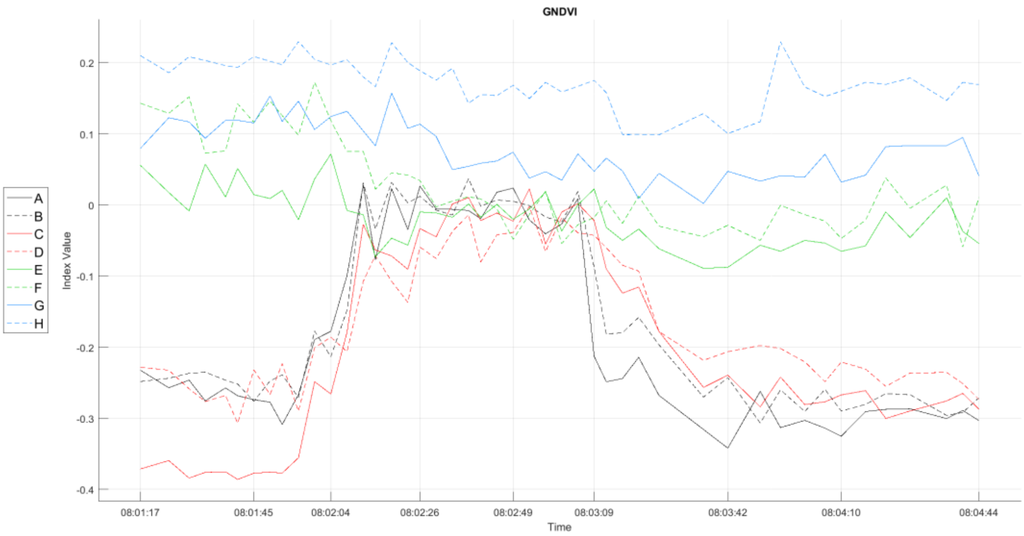
GNDVI
Index Value
Time
A
B
C
D
E
F
G
H
08:01:17
08:01:45
08:02:04
08:02:26
08:02:49
08:03:09
08:03:42
08:04:10
08:04:44

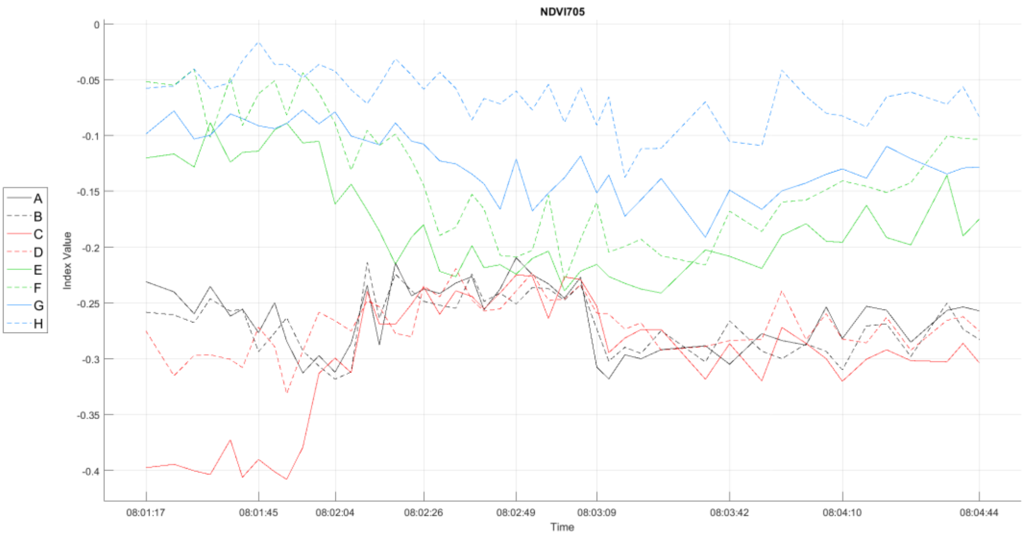
NDVI705
Index Value
Time
A
B
C
D
E
F
G
H
08:01:17
08:01:45
08:02:04
08:02:26
08:02:49
08:03:09
08:03:42
08:04:10
08:04:44

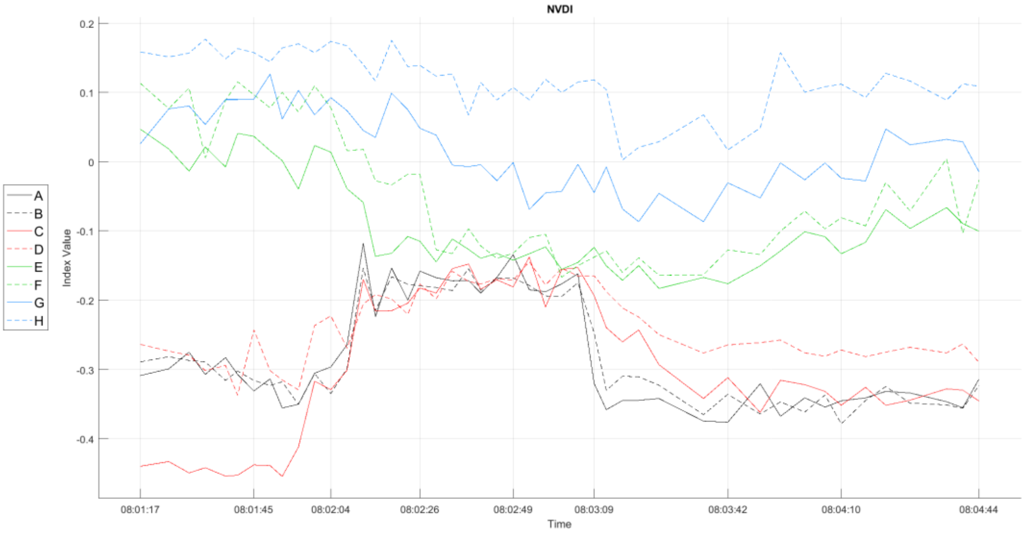
NVDI
Index Value
Time
A
B
C
D
E
F
G
H
0.2
0.1
0
-0.1
-0.2
-0.3
-0.4
08:01:17
08:01:45
08:02:04
08:02:26
08:02:49
08:03:09
08:03:42
08:04:10
08:04:44

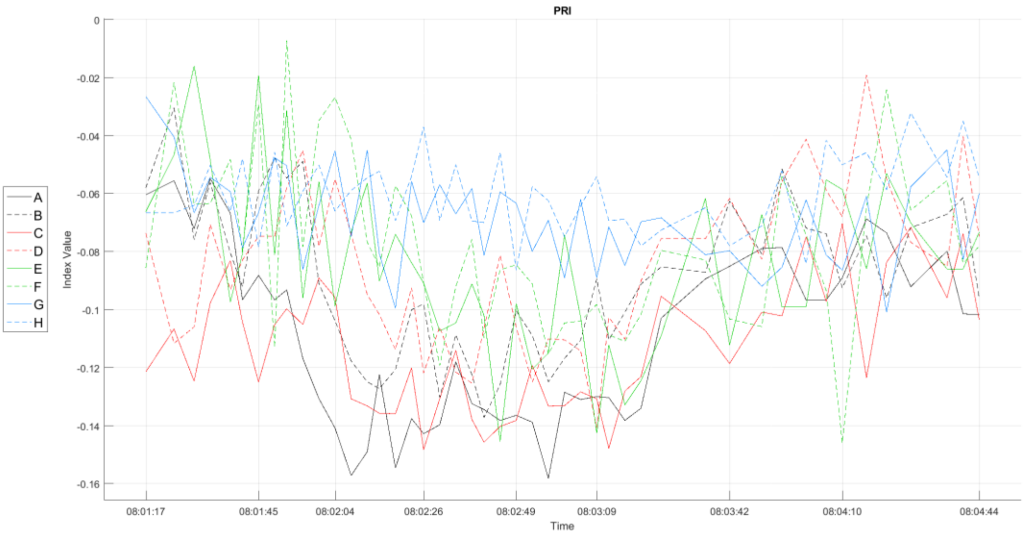
PRI
Index Value
Time
A
B
C
D
E
F
G
H
0
-0.02
-0.04
-0.06
-0.08
-0.1
-0.12
-0.14
-0.16
08:01:17
08:01:45
08:02:04
08:02:26
08:02:49
08:03:09
08:03:42
08:04:10
08:04:44

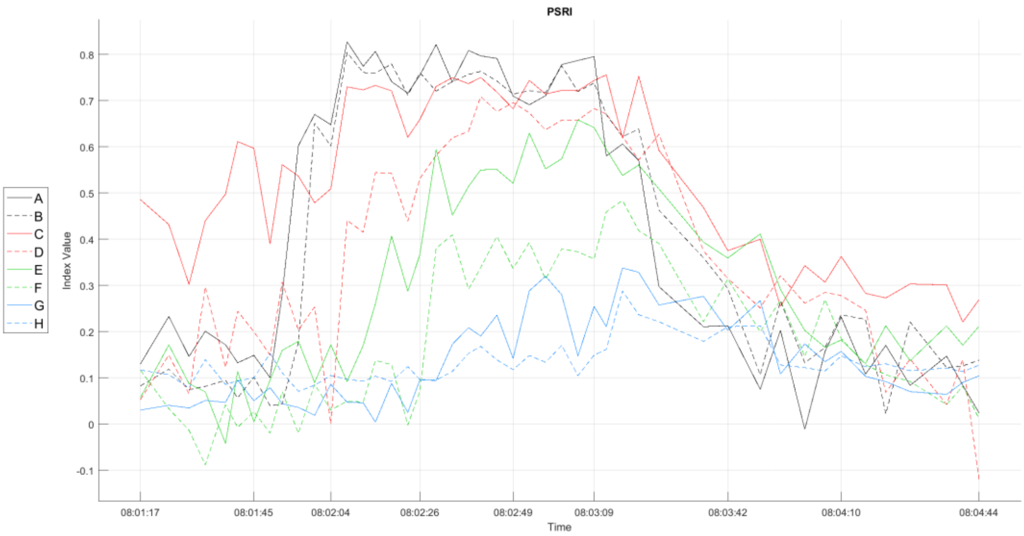
PSRI
A
B
C
D
E
F
G
H
Index Value
Time
08:01:17
08:01:45
08:02:04
08:02:26
08:02:49
08:03:09
08:03:42
08:04:10
08:04:44

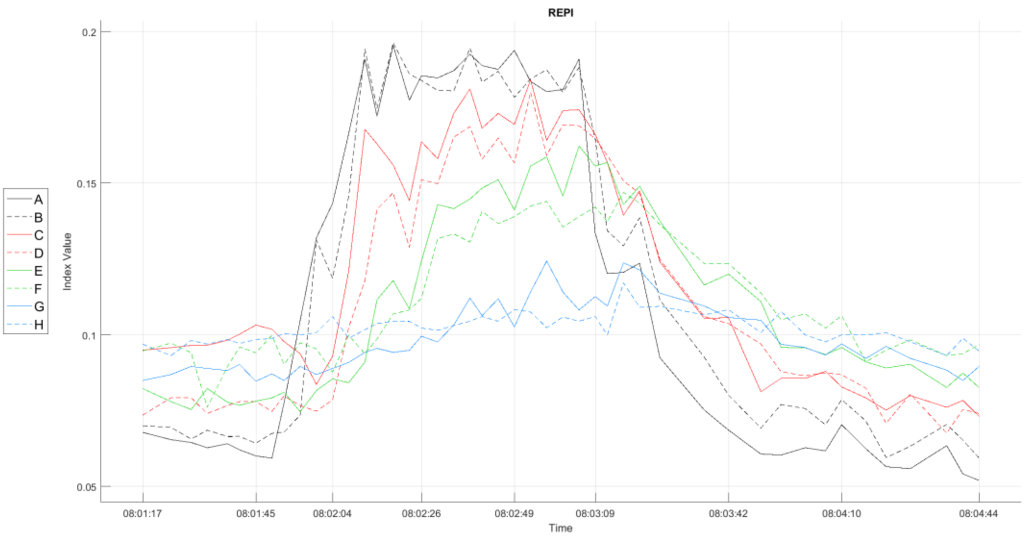
REPI
A
B
C
D
E
F
G
H
Index Value
Time
08:01:17
08:01:45
08:02:04
08:02:26
08:02:49
08:03:09
08:03:42
08:04:10
08:04:44

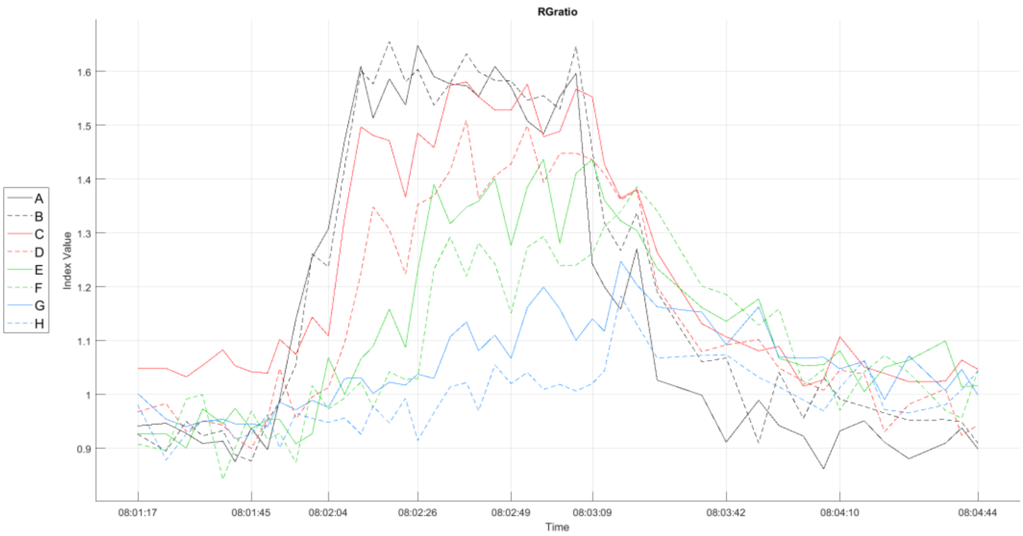
RGratio
Index Value
Time
A
B
C
D
E
F
G
H


SRI
Index Value
Time
A
B
C
D
E
F
G
H

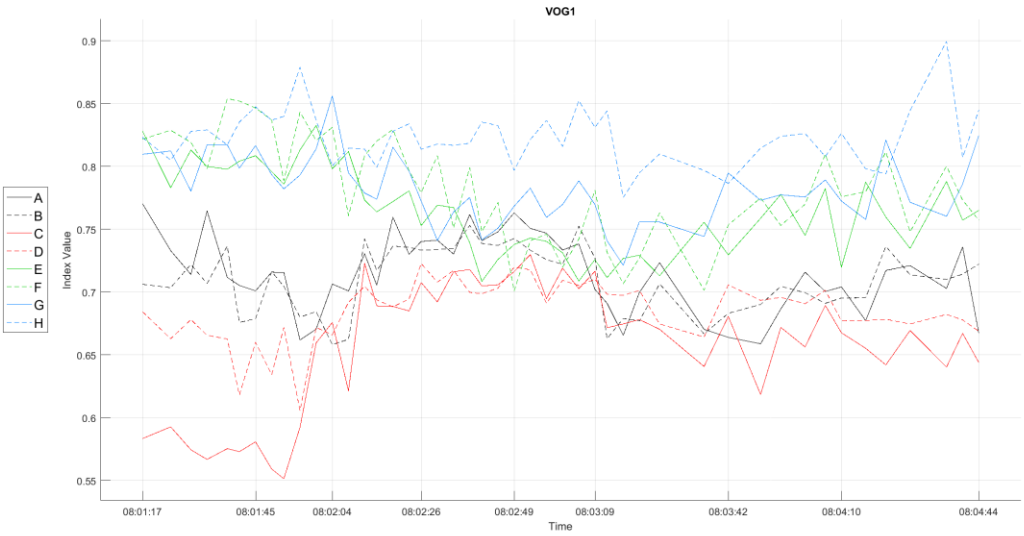
VOG1
A
B
C
D
E
F
G
H
Index Value
0.9
0.85
0.8
0.75
0.7
0.65
0.6
0.55
08:01:17
08:01:45
08:02:04
08:02:26
08:02:49
08:03:09
08:03:42
08:04:10
08:04:44
Time

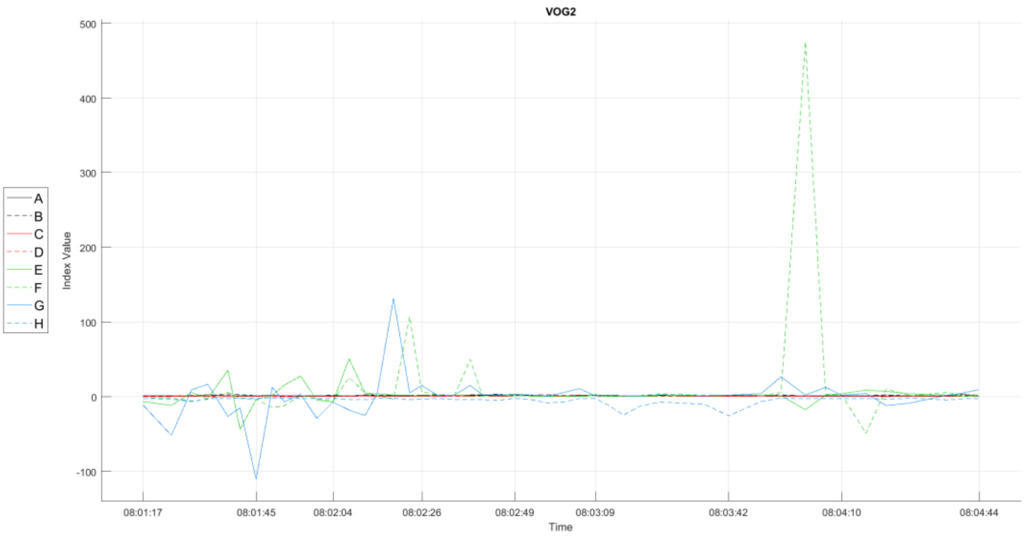
VOG2
A
B
C
D
E
F
G
H
Index Value
500
400
300
200
100
0
-100
08:01:17
08:01:45
08:02:04
08:02:26
08:02:49
08:03:09
08:03:42
08:04:10
08:04:44
Time

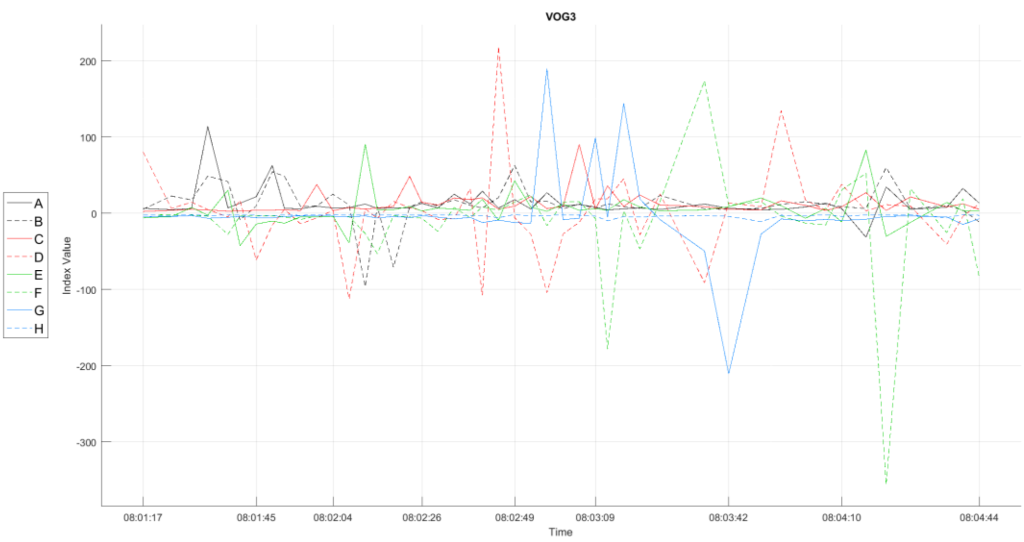
VOG3
Index Value
200
100
0
-100
-200
-300
A
B
C
D
E
F
G
H
08:01:17
08:01:45
08:02:04
08:02:26
08:02:49
08:03:09
08:03:42
08:04:10
08:04:44
Time


WBI
Index Value
Time
A
B
C
D
E
F
G
H
1.6
1.5
1.4
1.3
1.2
1.1
1
0.9
0.8
0.7
0.6
08:01:17
08:01:45
08:02:04
08:02:26
08:02:49
08:03:09
08:03:42
08:04:10
08:04:44

APPENDIX E - VEGETATION RECORDING PROTOCOL

VEGETATION RECORDINGS REC SEPT 2016

Location name:
Surveyors:
General remarks (incl. date, time of recording, time of photo's etc.)
Vegetation type ***Wet weight total monster*** ***Wet volume of total monster***

Plot size (cm*cm)
Local water depth **Local organic layer sediment thickness**

	Length	Diameter	Number of stems
Layer 1 (from bottom)			
Layer 2			

Layer 3 (or leave properties including width, length and thickness))			

APPENDIX F - ADDITIONAL ACTIVITIES AND MEETINGS

As part of the Dotter Project there has been an exchange of KICT-Staff and Deltares/TU Delft students between the two institutes. From KICT the following visits to Deltares and v.v. have been taking place:

- March 2016: KICT/KICT-Joint Venture team consisting of dr. Yong Uk Ryu, prof. dr. Un Ji, dr. Sang Hwa Jung, dr. Joon Go Kang and dr. Dong Sop Rhee visited 1 week for starting the 2016 cooperation.
- August 2016 – prof. dr. Un Ji – 1 month visit to work on the hydro-morphological modelling of the REC channel data
- Sept-December – dr. Chan Joo Lee – 3 month visit to cooperate on the image analyses from the full spectrum camera.
- October-December – dr. Sang Hwa Jung – 2 month visit to explore future work in relation to ecohydraulic research using Delft Software and more in depth discussions on the management of large scale facilities
- October 2016 – 2 day visit of dr. Yong Uk Ryu and prof. dr. Un Ji to Deltares for progress meeting.
- September 2016 Deltares/KnowH2O staff (dr. Ellis Penning, dr. Rik Noorlandt, Mike van der Werf, dr. Gé van den Eertwegh and dr. Bas van Vossen) visited KICT REC for 2 weeks
- August-November 2016 : TUDelft student Florian Laurens has carried out an internship at KICT-Rec to assist with measurements of various sorts. (final report available).

The Dotter Project has had various moments in which it shared its developments with the research and water management community both in the Netherlands, Korea and the USA. Below is a list of attended meetings:

- Attending meetings from the ‘stroombaanmaaien-platform’ in June 2016 and October 2016
- A presentation of the project during the River Flow conference (St. Louis USA) in July 2016
- A seminar at KICT headquarters (Ilsan Campus) in September 2016
- A presentation of the Dotter Project at the CoP Beheer en Onderhoud (STOWA) on 15th of November 2016
- A presentation of the project at the innovation market of Water Board Delfland in November 2016
- A visit to the Center for Ecohydraulic Research of the University of Idaho (Boise USA) December 2016 to discuss future cooperation

Various press releases were made during the year, including the making of a website on both the KnowH2O website (www.knowh2o.nl), and at the TKI-website-wikipedia. The project has been selected to feature in the annual report of Deltares and in the R&D highlights of Deltares.

Advies, Innovatie en Verbinding in Water

www.knowh2o.nl Watertorenweg 12 6571 CB BERG EN DAL t +31 (0)6 23 22 49 68
e info@knowh2o.nl Bank NL83 INGB 0006 2713 22 KvK 59020229